University of Bradford eThesis

Towards the Development of an Efficient Integrated 3D Face Recognition System

Subtitle: Enhanced Face Recognition Based on Techniques Relating to Curvature Analysis, Gender Classification and Facial Expressions

By

Xia Han

Submitted to

The University of Bradford

In Partial Fulfilment of the Requirements

For the Degree of

Doctor of Philosophy

Department of Electronic Imaging and Media Communication

School of Computing, Informatics and Media

2011

Abstract

Towards the Development of an Efficient Integrated 3D Face Recognition
System

Subtitle: Enhanced Face Recognition Based on Techniques Relating to Curvature
Analysis, Gender Classification and Facial Expressions

By

X. Han

Keywords: *2D/3D face recognition, curvature estimation, gender classification, facial
profile, facial expressions, geometric descriptors*

The purpose of this research was to enhance the methods towards the development of an
efficient three dimensional face recognition system. More specifically, one of our aims
was to investigate how the use of curvature of the diagonal profiles, extracted from 3D
facial geometry models can help the neutral face recognition processes. Another aim
was to use a gender classifier employed on 3D facial geometry in order to reduce the
search space of the database on which facial recognition is performed. 3D facial
geometry with facial expression possesses considerable challenges when it comes face
recognition as identified by the communities involved in face recognition research. Thus,
one aim of this study was to investigate the effects of the curvature-based method in
face recognition under expression variations. Another aim was to develop techniques
that can discriminate both expression-sensitive and expression-insensitive regions for

face recognition based on non-neutral face geometry models.

In the case of neutral face recognition, we developed a gender classification method using support vector machines based on the measurements of area and volume of selected regions of the face. This method reduced the search range of a database initially for a given image and hence reduces the computational time. Subsequently, in the characterisation of the face images, a minimum feature set of diagonal profiles, which we call T shape profiles, containing diacritic information were determined and extracted to characterise face models. We then used a method based on computing curvatures of selected facial regions to describe this feature set. In addition to the neutral face recognition, to solve the problem arising from data with facial expressions, initially, the curvature-based T shape profiles were employed and investigated for this purpose. For this purpose, the feature sets of the expression-invariant and expression-variant regions were determined respectively and described by geodesic distances and Euclidean distances. By using regression models the correlations between expressions and neutral feature sets were identified. This enabled us to discriminate expression-variant features and there was a gain in face recognition rate.

The results of the study have indicated that our proposed curvature-based recognition, 3D gender classification of facial geometry and analysis of facial expressions, was capable of undertaking face recognition using a minimum set of features improving efficiency and computation.

Publications

I. X. Han, H. Ugail, I. Palmer, "3D face recognition using symmetry profile comparison based on mean curvature," in the Proceedings of the 8th Informatics Workshop for Research Students, pp. 153-155, ISBN 978 1 85143 2462, University of Bradford, Bradford, UK, 2007.

II. X. Han, H. Ugail, I. Palmer, "Gender classification based on 3D face geometry features with SVM," *International Conference on CyberWorlds*, pp. 114-118, 2009.

III. X. Han, H. Ugail, I. Palmer, "Method of Characterising 3D Faces Using Gaussian Curvature," *Chinese Conference on Pattern Recognition*, Nanjing, vol. 2, pp. 528-532, 2009.

To

My mother and father for their unconditional love and support

Acknowledgement

First of all, I would like to express my gratitude to my supervisor Professor Hassan Ugail for his guidance and support throughout this research. His encouragement and assistance are very valuable to me. He guides me towards the promising direction of my research.

Special thanks to Dr. Moi Hoon Yap for her very valuable help and suggestions during this research and writing up of this thesis. Her supervision and support to my academic research and living life are valuable to me by all means.

A special word of appreciation is passed to Dr. Ian Palmer for his helpful encouragement and discussions.

Finally, I would like to thank my parents who provide unconditional support and love to me throughout my entire life. Without them, I would not have finished this research work. And I would also like to thank my love, Alex Cui, for all the happiness he has shared with me and encouragement he has given.

Table of Contents

Appendix

Implementation code on CD

List of Figures

List of Tables

Acronyms

2D	Two-dimensional
3D	Three-dimensional
AAM	Active Appearance Model
AU	Action Unit
DCT	Discrete Cosine Transform
EGI	extended Gaussian image
FACS	Facial Action Coding System
FLD	Fisher Linear Discriminant
GA	Genetic Algorithm
GDA	Generalised Discriminant analysis
HMM	Hidden Markov Model
ICA	Independent Component Analysis
ICP	Iterative Closest Point
KNN	K-nearest neighbor classifier
KSR	Kernel Spectral Regression
LDA	Linear Discriminant analysis
MLR	Multiple Linear Regression
MPEG	Moving Picture Experts Group
NN	Nearest Neighbor classifier
NN	Neural Network
OBJ	Objective file
PCA	Principal Component Analysis
PIE	Poses, illumination and expressions

PLS	Partial Least Square
RBF	Radial Basis Function
SVM	Support Vector Machines
VRML	Virtual Reality Modelling Language

Chapter 1 Introduction

The area of person identification or recognition has drawn interest from researchers in the last few decades. The reliable identification or recognition systems [2, 16-21] for the military, industry, airports and anywhere that requires secured access are in a great demand. The traditional techniques, such as passwords and cards, have to rely on people's memory. The passwords are easy to crack or forget and the cards may be stolen or lost. Biometrics provides the information that does not rely on the user to maintain its security [22]. Biometric systems efficiently support the user since they do not need the user to carry cards or remember complex passwords. Thus, biometric techniques have received a lot of attention and become a very popular research area.

1.1 Biometric Identification Techniques

More and more people are focusing on the area of biometrics for person identification. Biometrics can be categorised into two groups, as shown in Fig. 1-1, which are: physiological biometrics, such as hand and face geometry, iris and fingerprints patterns; by contrast, behavioural biometrics comprise standardised measurements on voice recognition, signature matching, keystroke identification [23] and gait matching [1]. Nowadays, a large number of commercial biometrics systems mainly use physiological biometrics, since behavioural biometrics are unstable and influenced by many factors such as emotion and posture. The popular commercial biometrics techniques are shown in Fig. 1-2. The most widely used biometrics technique is fingerprint patterns. It is believed that the face technique is commonly used and accepted by researchers and users, as it ranks third in all biometrics. Being one of the most important physiological

biometrics, face recognition is not only reliable and natural but also easily accepted by

users.
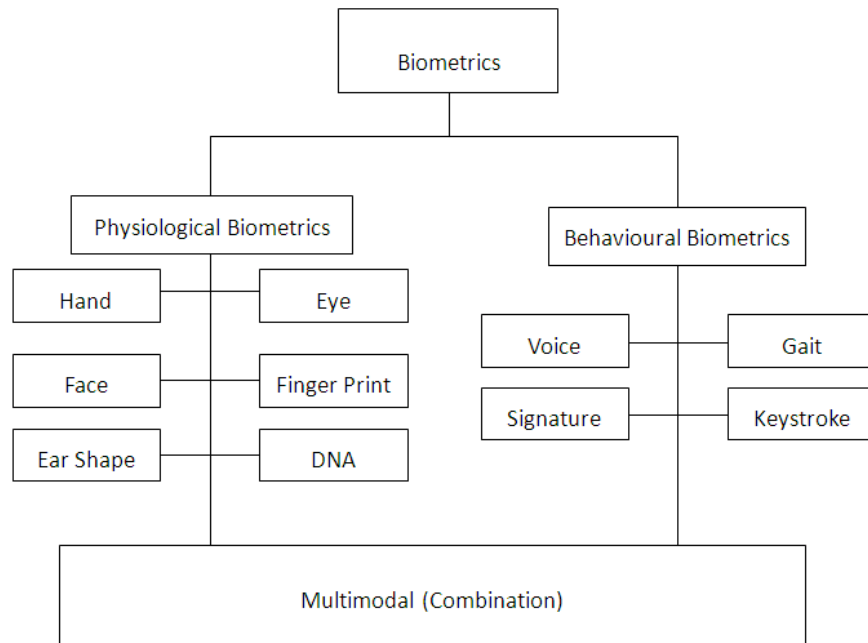
Fig. 1-1. Biometric modalities [1]
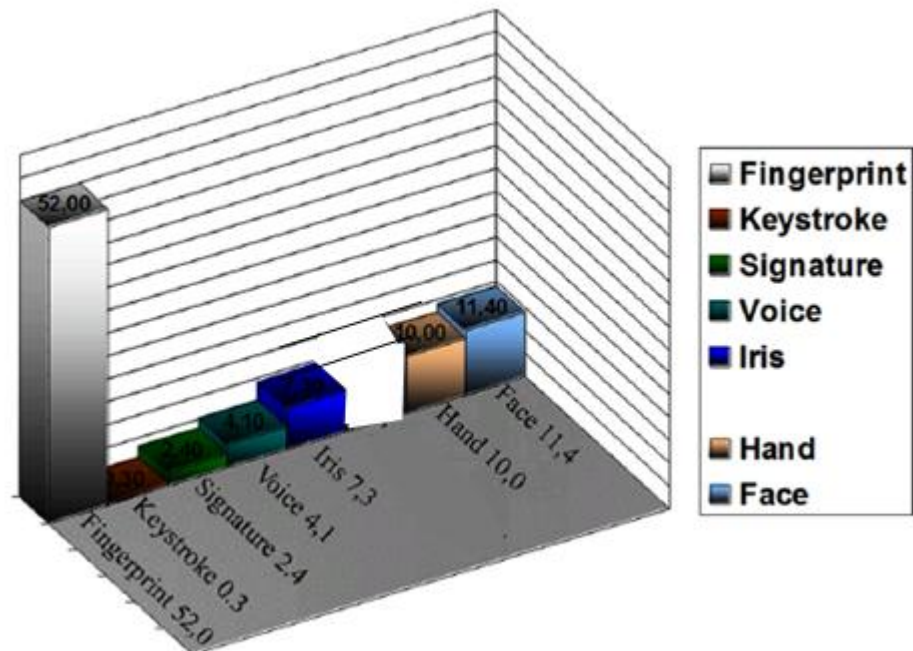
Fig. 1-2. The spreading of most popular biometrics [2]

1.2 Face Recognition

Face recognition has several advantages over the other biometrics:

- *Public acceptance.* This is the key factor for various organisations to determine the biometric techniques;

- *Non-intrusive.* Compared to the fingerprints and iris techniques, the face recognition technique can be simply implemented by looking at cameras from a distance. It is believed that this non-contact technique is like taking a photo of the users;

- *Database access.* There are a large number of facial images taken by an enormous number of facilities, such as cameras and CCTV, in all places.

Due to these advantages, face recognition technology has drawn interest from researchers and it has been used widely in the area of security, identity verification, surveillance tasks, such as the military, industrial or biometrics applications, airports and anywhere that requires secured access. Thus face recognition is a popular research area for its potential applications. Facial appearance is the crucial and unique key to identify a person, and it is a primary factor that people use to recognise each other. The applications of face recognition fall into two areas: face verification and face identification (henceforth, face recognition).

In general, face recognition applications are initialised with a set of databases that are composed of known face images. These databases are usually named as the gallery. In the recognition process, the given (query) image of a certain person is termed as the

probe, which is matched against the face images in the gallery.

Face verification is a one-to-one match that compares a query face image against a particular face image in the gallery, whose identity is being claimed. On the contrary, face recognition or identification is a one-to-many problem that compares a query face image against all the face images in the gallery to identify the best match. In the last few decades, major advances have occurred in face recognition or identification, with many systems capable of achieving recognition rates of greater than 90%. The face recognition techniques can be categorised into two major trends based on the dimensional images they utilise: 2D face recognition and 3D face recognition.

2D face recognition is the traditional modality technique of face recognition. There have been great successes made in this area, and some applications [2, 20]. Despite the significant process of 2D face recognition, there remain some issues, such as the well-known poses, illumination and expressions (PIE) problems, due to its nature and the multidimensionality of the problems. These problems affect the performance of methods applied in 2D face recognition by causing the error rates to increase. In an attempt to solve these problems, research has begun to focus on the use of 3D face models, motivated by four main aspects:

● 3D face recognition relies on the geometric shape information, rather than colour and texture information, and systems become invariant to lighting conditions.
● Face models rotation allows for compensation of variations in poses. It also aids those methods based on 3D face recognition requiring alignment prior to recognition.

- Third, the additional depth information in the facial surface structure, not directly available from 2D images, provides additional cues for recognition.

- The development of a 3D acquisition system and the capturing process has become cheaper and faster too.

For those advantages, as it has been widely required in various kinds of commercial and industrial applications for high accuracy rates, 3D face recognition has become a popular research area.

3D face recognition techniques have drawn people's attention. Many researchers have moved towards 3D human face recognition techniques. 3D face recognition is based on 3D images in which the shape (3D surface) of the human face is used either individually or in combination with the texture (2D intensity image) for the purpose of recognition. The 3D images are specifically captured and generated from a single shot by a 3D camera, which produces point clouds, triangulated meshes or polygonal meshes to represent 3D facial images, as shown in Fig. 1-3. The common representation applied in most 3D face recognition systems is the triangular mesh.

(a)   (b)   (c)
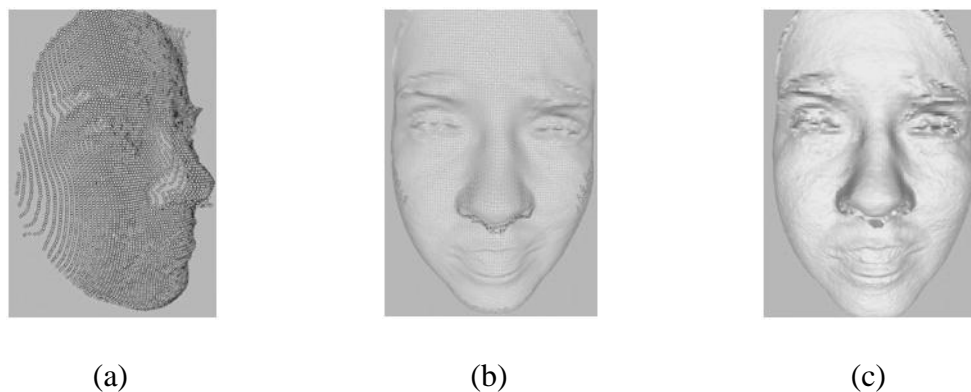
Fig. 1-3. 3D facial data (a) point cloud (b) triangular mesh (c) shaded triangular mesh [3]

In a face recognition system based on either 2D or 3D images, there are several procedures to be carried out. The initial step is the face detection. This involves the extraction of a face image from a larger scene, image or video sequence. The following procedure is for face alignment, which involves aligning the face image with a certain coordinate system and aids accurate results. These procedures can be accomplished by several key tasks:

- Model and representation of facial surfaces in a simplified multidimensional set. It aims to reduce the computational complexity and helps to achieve good performance in the recognition part.

- Extraction of 3D facial features. Feature extraction is to localise a set of feature points associated with the main facial characteristics, eyes, nose and mouth. At present the most popular methods for facial feature extraction are based on point clouds, facial profiles and surface curvature-based features etc [24].

- Matching algorithm and methodology used for 2D/3D facial surface data.

1.3 Research Objectives

This thesis aims to cover state-of-the-art 3D face recognition techniques, including the technical background, ideas, methodologies, and concepts. Our research work comprised several major components: reviewing 2D and 3D face recognition techniques; proposing novel methods for several specific purposes to enhance the existing methods in the development of face recognition systems. More specifically, there are a few issues we will address in the thesis:

- Explore the existing face recognition systems and relevant research as well as the current state-of-the-art in this area;

- Investigate the challenges in existing face recognition systems;

- Improve the existing face recognition algorithms by employing small feature sets;

- Identify the problems in the 3D face recognition including characterising faces and recognising faces in the presence of expressions;

- Determine specific aims-oriented methods and enhance them in the development of an effective face recognition system;

- Evaluate our proposed methods on multiple databases for comparison;

- Conclude limitations of the final face recognition system and propose further work to combat these limitations.

1.4 3D Face Databases

The development of face recognition systems relies on the availability of face image databases for the purpose of comparative evaluations of the systems. With the techniques of 3D face capture rapidly developing, currently more and more face databases on 3D have been built, oriented to different experimentation purposes: automatic face recognition, facial expression analysis, gender classification. In our face recognition integral system, two public databases will be utilised and compared for the purpose of our method's evaluation.

1.4.1 GavabDB Database

The 3D face database GavabDB [3] is one of the available public benchmark databases. It was developed for automatic face recognition experiments and other possible image applications, such as pose correction and 3D face model registration. It contains 427 3D facial surface images corresponding to 61 individuals (45 males and 16 females), and there are nine different images per person. In Table 1-1, in particular, there are two frontal (view number 1 and 2) and four rotated images (view number 3, 4, 5 and 6) without any facial expressions, and three frontal images in which the subject presents different facial expressions of smile, accentuated smile or laugh and random gesture (view number 7, 8 and 9).

Table 1-1. Nine views of the i-th individual of the database and their variation with respect to pose and facial expression [3].

View number	File name	Head orientation	Facial expression	Sample image
1	cara*i*_frontal1	Frontal	Neutral	
2	cara*i*_frontal2	Frontal	Neutral	
3	cara*i*_derecha	Right Profile: $\approx$ +90° of rotation around y axis.	Neutral	

4	cara*i*_izquierda	Left profile: ≈ -90° of rotation around *y* axis.	Neutral	
5	cara*i*_arriba	Looking up: ≈ +35° of rotation around *x* axis.	Neutral	
6	cara*i*_abajo	Looking down: ≈ -35° of rotation around *x* axis.	Neutral	
7	cara*i*_sonrisa	Frontal	Smile	
8	cara*i*_risa	Frontal	Accentuated laugh	
9	cara*i*_gesto	Frontal	Random gesture chosen by the subject.	

In this work, only the 3D geometry mesh without texture is regarded as the dataset. Every mesh is composed of points of the facial surface and their connectivity. The coordinates (x, y, z) of their points are referred to a coordinate origin placed in the scanner during the capture time. The meshes have been exported to a Virtual Reality Modeling Language (VRML) format file. VRML contains vertices, faces, normals, texture, etc. for describing 3D objects. Although restrictions have been introduced at the capture stage in order to minimise errors in the generated meshes, there are still

undesired noise in the images, as shown in Fig. 1-4 (a) and (b), and some individuals have beards and moustaches.

<table>
<tr><td align="center">(a)</td><td align="center">(b)</td></tr>
</table>

Fig. 1-4. Illustration of noise (a) a sample subject at the side view (b) a sample subject at the top view [3]

1.4.2 BU-3DFE Database

The other database we use in our proposed method for comparison is a 3D facial expression database, named BU-3DFE [4]. In brief, each one of 100 subjects (56 female, 44 male) is instructed to display seven universal expressions, i.e. *neutral*, *happiness*, *surprise*, *fear*, *sadness*, *disgust* and *anger*, as shown in Fig. 1-5. Along with the raw model data, additional semantic and surface feature data are also archived. In data processing, the unprocessed head-shoulder boundaries are truncated in order to generate a face model with the pure face region, as shown in Fig. 1-6. The facial data includes the 3D model, texture, as shown in Fig. 1-7, and enrollment information. The facial data contains about 13,000 – 21,000 polygons. In addition, 83 feature points on each facial model are located, as shown in Fig. 1-8. Given the set of feature points on the labelled face model, the feature regions on the face surface can easily be determined.
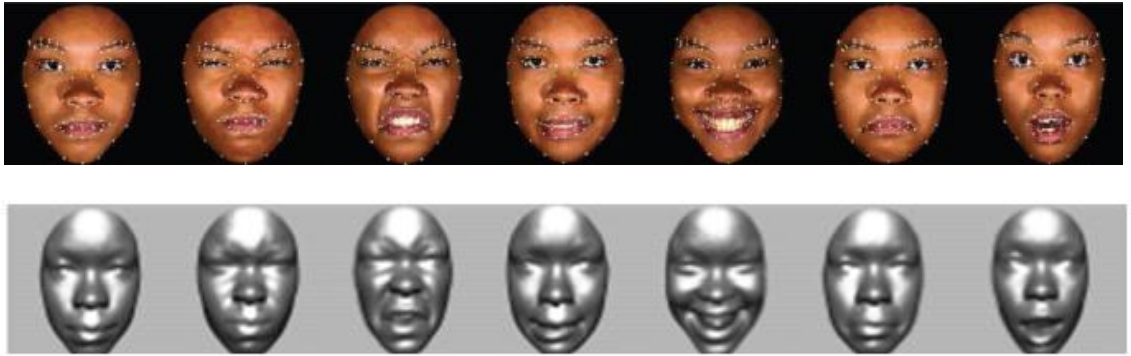
Fig. 1-5. One sample subject shows seven expressions (neutral, angry, disgust, fear, happiness, sadness, and surprise). The frontal-view texture models with the selected feature points (the top row) and facial shape models (the low row) are produced [4].
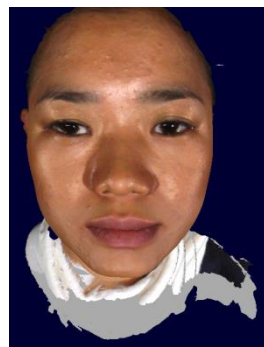
(a)   (b)

Fig. 1-6. A sample subject (a) before segmentation (b) after segmentation [4]
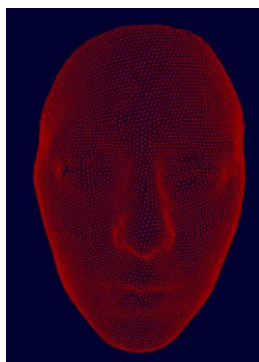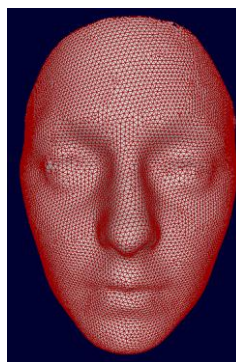
(a)   (b)   (c)

Fig. 1-7. 3D views of an individual (a) a triangular mesh (b) shaded face model (c) texture mapped face model [4]
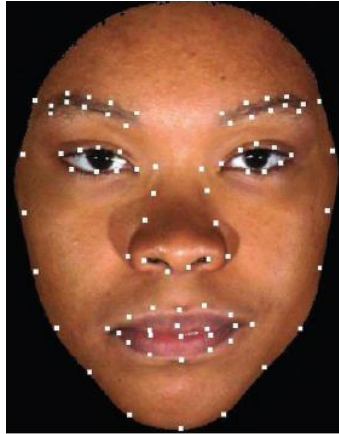
Fig. 1-8. Illustration of the 83 annotated feature points in BU-3DFE database [4]

There are a few reasons to encourage us to select the BU-3DFE facial expression database as the other experimental database for comparisons. Firstly, it has a larger sample size than the GavabDB database. 100 subjects participated in face scans, including undergraduates, graduates and faculty staff members from their department with a variety of racial ancestries. Secondly, female and male are not in the conditions of extraordinary disparity since 60 subjects are female and 40 subjects are male. This gender ratio is helpful to test our proposed method. Thirdly, denser geometric face models demonstrate more accurate faces in nature without losing much information. There is a difference of the range of $4000 - 8000$ vertices between BU-3DFE, which has around 12,000, and GavabDB, which has around 6000.

1.5 Thesis Contribution

To address the research objectives described earlier, we have enhanced the specific aims-oriented methods in the development of an efficient face recognition system. The

contribution of the thesis can be summarised as follows:

- Established a new and efficient method of characterising faces, using curvature on the T shape profiles. This contribution reduces the dimensions of feature sets and demonstrates that this method can characterise the face efficiently. Refer to Publications I and III for further information.

- Developed a gender classifier. Given a face image, a face recognition system can benefit by separating the database into two categories and reduce the search range by integrating this gender classifier. Refer to Publications II for further information.

- Constructed a framework associated with expression-invariants and expression-variants for the purpose of recognising faces in the presence of expressions. This framework allows for identifying the correlation between six significant expressions and neutral mutually.

- Enhanced the method of face recognition under expressions by incorporating the curvature-based method using the T shape profiles in the framework.

1.6 Thesis Structure

The structure of this thesis is directly based on the functional plug-ins dealing with the specific problem. Chapter 2 discusses the literature review of face recognition with emphasis on 3D face recognition, gender classification and expression-invariants recognition. Chapter 3 presents a curvature-based method using the T shape profiles to characterise faces for face recognition. Chapter 4 describes a method of gender classification using support vector machines (SVM). Chapter 5 discusses the

performance of the curvature-based method using the T shape profiles in dealing with expressions and the neutralization of the face models. Chapter 6 presents a framework of expression-invariants and expression-variants for the purpose of dealing with the expression problem, and investigates the correlation between expressions and neutral face. Finally, the incorporation of the curvature-based method using the T shape profiles is evaluated. Finally, Chapter 7 concludes this research work of the thesis and states the limitations and the future work related to this research work. The implementation code is provided in Appendix on a CD. The curvature code is in C++ and the rest in Matlab M files.

Chapter 2 Literature Review

With the development of multimedia and networks, higher quality human-like human-computer interfaces are required. As one of the most important parts of virtual human face synthesis technology, 3D human face recognition techniques have been greatly developed over the last few decades. Along with this technological evolution, face recognition technology has drawn interest from researchers and major strides have been made in 2D face recognition. Face recognition has long been a popular research area due to its potential applications [2, 20-21]. Although some aspects human face images can be affected by illumination, facial expression, makeup etc., they are non-intrusive in nature and easy to collect in environments where other biometrics, such as finger prints and iris, require the cooperation of the subjects. Therefore face recognition is both an attractive and a challenging area for research.

2.1 2D Face Recognition Techniques

As 2D face recognition techniques have been widely used in various kinds of commercial and industrial application [20, 25], it indicates the current status of 2D face recognition is well established and advanced. Various 2D face recognition methodologies can be categorized into two groups, appearance-based face recognition [26-27] and model-based face recognition [28-29].

2.1.1 Appearance-Based 2D Face Recognition

Appearance-based 2D face recognition techniques entirely rely on 2D intensity images rather than 3D facial images. In this section, three popular appearance-based statistical methods, namely Principal Component Analysis (PCA), Independent Component Analysis (ICA) and Linear Discriminant Analysis (LDA), are described.

PCA, ICA, and LDA play an important role in 2D image-based face recognition applications [2]. These methods produce a set of projecting vectors that best represent the sampling images and preserve most information of the original samples so that the set of projecting vectors can be used to perform recognition tasks in a lower dimension space named the feature or face space.

Turk et al [26] were the first to introduce the eigenfaces idea and employ PCA in face recognition. In a near-real-time environment, they detected faces and recognised them by projecting them onto a lower dimension space, namely face space which best represents the variation between the known testing images. The face space is defined by eigenfaces which represents facial features in a lower dimension. Based on the face space, they obtain the corresponding set of weights for each face. By comparing test image weights and their weights in the known faces database, they identify the test facial image. Their experiments showed 96% recognition over varied lighting, 85% over varied orientation and 64% over varied size.

Eigenfaces are characteristic features in face recognition domain, but generally it is called principal components. In face recognition and computer vision, PCA obtains a set

of projection vectors or principal components for feature extraction from given training patterns through maximising the variance of the projected patterns in order to represent original information as precisely as possible. However, for the purpose of classification, as an unsupervised method, PCA does not sufficiently use class information of given patterns and its maximisation to the variance of the projected patterns might not consider discrimination among classes. Thus for the purpose of classification either introducing class information into it or finding a substitute would be taken into consideration.

Due to drawbacks mentioned about the PCA method, further research has been developed. Some researchers show that ICA outperforms PCA in face recognition and feature extraction [30-32]. ICA searches for a linear transformation to express a set of random variables as linear combinations of statistically independent source variables. Basically PCA considers the 2nd order moments only and it formulates data uncorrelated, while ICA accounts for higher order statistics and it formulates data independent. ICA thus provides a more powerful data representation than PCA. However, it is worthy of pointing out that due to the higher order of statistics it utilises, the problem of time-consumption arises compared to PCA. Barlett [32] implements a fast ICA algorithm to reduce computational cost by extending Hyvarinen [33] work.

As another common method for classification and dimensionality reduction, LDA is reducing dimensionality of data while preserving as much of the class discriminatory information as possible by maximising the ratio of between-class variance to the within-class variance in data set in order to guarantee maximal separability. LDA doesn't change the location of the original facial images when transformed to a lower

dimension space but only tends to maximise the separability between classes and draw a decision region between the given classes. Belhumeur et al. [27] indicate that employing class information performs better recognition results.

2.1.2 Model-based 2D Face Recognition

Unlike appearance-based techniques, model-based approaches aim at constructing a model of the human face, which is able to capture the facial variations. The matching parameters, like distances, angles and relative position features, are derived from the placement of internal facial features, such as eyes, nose tip and mouth. To recognise faces, the matching parameters are utilised to match against the parameters of faces in the database. In general, model-based face recognition techniques contains three main stages to be accomplished: 1) Model construction 2) The model fitting to the given facial images 3) Using the parameters of the fitted model as the feature vector to calculate similarity between the query face and faces in the database to perform the recognition. Some main strategies of model-based face recognition will be discussed.

The earliest example of model-based techniques was implemented by Kanade [34]. By localising the corners of the eyes and nostrils, etc, he develops a system which computes distances and relative position features from feature points (eyes, nose). Comparing against those of known faces using Euclidean distance metric, the system automatically extract the variations to recognise faces. Wiskott [35] has generated a image graph by fiducial points, which maximise similarity between this graph and the original facial image. This graph can be translated, scaled, rotated and deformed during the matching process. By labelling edges with the distance information and labelling

nodes with wavelet coefficients in jets (explained further on page 28 section 2.3), he develops a labelled graph to generate image graph. To deal with the image transformations tending to happen, this model graph can be translated, scaled, rotated and deformed during the matching process. They apply the graph matching system for face recognition and achieve very high recognition rate 99% for frontal views. Cootes [36] develops a 2D morphable face model, Active Appearance Model (AAM), to learn the face variations by setting up model parameters on the shape and texture respectively for the purpose of recognising faces. AAM has been further developed and employed in other studies [37-39]. For example, AAM is used to generate synthetic images that are as realistic as possible. It also provides a basis for a broad range of applications by coding the appearance of a given image in terms of a compact set of parameters that are useful for higher-level interpretation of the scenes. In brief, a scene interpretation is a scene description in terms of instantiated aggregate concepts consistent with evidence and context information, for example traffic scene interpretation in driver assistance systems, criminal acts recognition, and other monitoring tasks such as airport activity recognition.

2.1.3 2D Face Recognition Evaluation

Face Recognition Vendor Test 2002 (Phillips et al., 2002) [40] shows that the vast majority of face recognition methods based on 2D image processing using intensity or color images has reached a recognition rate higher than 90% under lighting controlled conditions, and whenever subjects are consentient. Unfortunately in case of addressing pose, illumination and expression variations the system performances are insufficient, because 2D face recognition methods still encounter the same difficulties. In addition

the analysis states [40] that the performance of certain popular commercial 2D facial images based applications strongly depends on the intensity of facial images and the size of the database. The computational cost is required as a key factor in some face recognition applications, such as real-time systems.

2.2 3D Face Recognition Techniques

Despite significant advances in 2D face recognition technology, it has yet to achieve levels of accuracy required for some commercial and industrial applications. The inherent problems from 2D face recognition, such as changes in illumination, expression and pose, cause the error rates to increase.

In an attempt to solve the problems, research has begun to focus on the use of 3D face models, motivated by six main motivations.

● The use of geometric shape data, rather than colour and texture information, makes face recognition systems less sensitive to lighting conditions.

● The rotation of face models allows for compensation of variations in pose, and aids those methods requiring alignment prior to recognition.

● The use of the additional depth information in the facial surface structure, not directly available from 2D images, provides supplementary cues for recognition.

● The development of 3D acquisition system and the capturing process is becoming cheaper and faster.

● The use of in 2D face recognition techniques seems unable to solve problems, such as facial pose, expression and illumination variation. This aspect is supported by the

work of Xu et al [41]. They compare intensity images against depth images with respect to the discriminating power of recognising people. From their experiments, the authors conclude that depth maps perform more robust face representation because intensity images are very sensitive to changes in illumination.

Because of these strong factors, 3D face recognition approaches [2, 16, 42-48] have been developed and studied by more researchers and become more practical in applications. In general, 3D face recognition applications consist of two main roles, which are representation of 3D facial models and matching methods to recognise and identify between models. Within extensive research on the 3D face recognition techniques, the two roles are subjected to be two relatively individual targets. People tend to combine these two roles into an integral face recognition system nowadays. Based on the features used for recognition, the techniques can be grouped into two aspects, curvature-based and profiles-based face recognition.

Gordon et al. [49] implement a solution to 3D face recognition based on depth and curvature features. By establishing a high level face descriptor in terms of various measurements and curvatures, they generate a map of ridge lines or valley lines in a face and extract several face-specific features, such as eyelids, eyeballs, and noses, from the line maps. It is worth pointing out that the curvature-based descriptor has the potential for higher accuracy in describing surface based events and is better suited to describe characteristics of the face in areas such as cheeks, foreheads, and chins. In addition, it is viewpoint invariant. Their proposed method achieved recognition rate in the range of 80% to 100% for a small database.

Tosranon et al. [50] utilise curvature and mean curvature to compute a geometric invariant, the shape feature which is local and intrinsic. Therefore it could be used for shape matching. For the purpose of determining local geometrical features in terms of regions, Moreno et al. [5] labelled each point of 3D facial meshes as concave elliptical, convex elliptical, hyperbolical, concave cylindrical, convex cylindrical or planar by Hoshen-Kopelman (HK) algorithm. HK algorithm is to assign a label corresponding to the cluster to which the cell belongs. Based on the curvature analysis of various regions, they showed that the regions 4, 5 and 3, as shown in Fig. 2-1, possess the most power of discrimination. Their recognition rate of 90.16% is based on the seven segmented regions and two lines.

Region 4 (R4): concave elliptical points of the left eye cavity (from the threshold image).

Region 6 (R6): convex elliptical points of the left eye (from the not threshold image).

Line 1 (L1): points in which sign of median curvature (H) changes at left of nose (from the not-threshold image).

Region 1 (R1): convex elliptical points of the nose tip (from the threshold image).

Region 3 (R3): hyperbolic points in the upper bridge of the nose (from the threshold image).

Region 5 (R5): concave elliptical points of the right eye cavity (from the threshold image).

Region 7 (R7): convex elliptical points of the right eye (from the not-threshold image).

Line2 (L2): points in which median curvature sign changes at left of nose (from the not-threshold image).

Region 2 (R2): convex cylindrical points of the nose (from the threshold image).

Fig. 2-1. Illustration of the discriminating features in a variety of regions: the most discriminating features in segmented regions 3, 4 and 5 [5].

Mahoor et al. [6] develop a 3D binary image comprising ridge lines, as shown in Fig. 2-2. The face model is represented by ridge lines, which are around the important regions of the face for the purpose of face recognition. They achieved a recognition rate

of 93.5% by analysing principal curvature on the ridge lines.
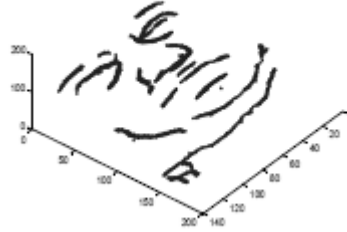
Fig. 2-2. A sample of the ridge lines extracted from one subject [6].

Li et al. [7] evaluate a variety of profiles, such as central vertical profile, central horizontal profile, two vertical profiles and two horizontal profiles, and a frontal face contour defined 30mm behind the nose tip for the purpose of face recognition and demonstrates the central vertical profile, as shown in Fig. 2-3, is the most discriminating profile to characterise the faces and the contour information significantly provides the additional information for face recognition. In addition, the significance of the central vertical profile has been evaluated in Nagamine et al. [51].
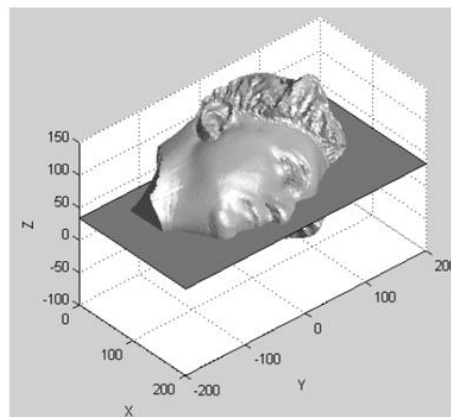
Fig. 2-3. A sample illustration of extraction of the central vertical profile [7].

In Lee and Milios [52], they create an extended Gaussian image (EGI) which corresponds to the convex regions based on the signs of the mean and Gaussian curvature from range images. By correlating the EGIs of a test image and an image in the database, the optimal correspondence is established for the recognition task.

Cartoux et al. [8] propose an iterative algorithm, which evaluates the similarity of the Gaussian curvature values of the facial surface, to extract the quasi-symmetric plane in the facial image for obtaining the profile, as shown in Fig. 2-4. The facial profiles are used to fit two faces based on the least square method for matching purpose.

(a)   (b)
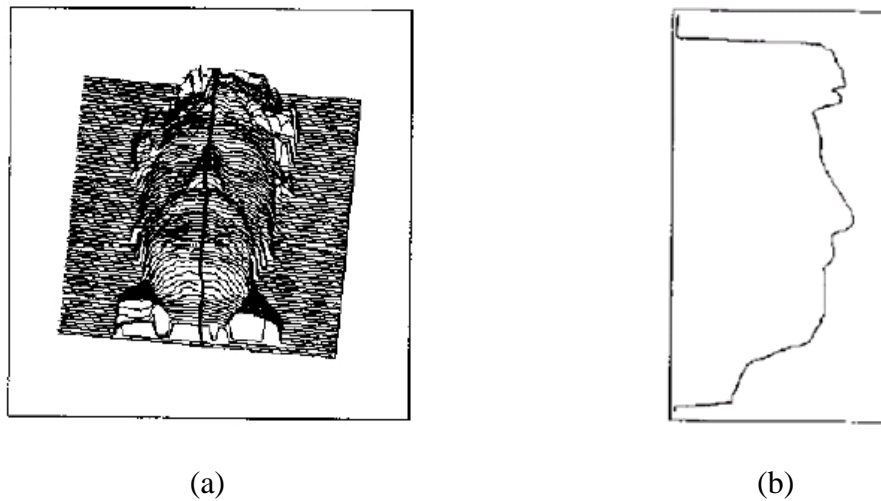
Fig.2-4. Quasi-symmetric plane (a) and profile curve (b) obtained from a given 3D facial image [8]

Tanaka et al. [53] presents an approach using curvature information from range images. They consider face recognition as a 3D shape recognition problem and improve previous approaches which only use the signs of curvatures in terms of principal curvature. In order to represent faces, by mapping maximum and minimum principal directions on two unit spheres they construct Extended Gaussian images (EGI) of

feature vector sets for face matching.
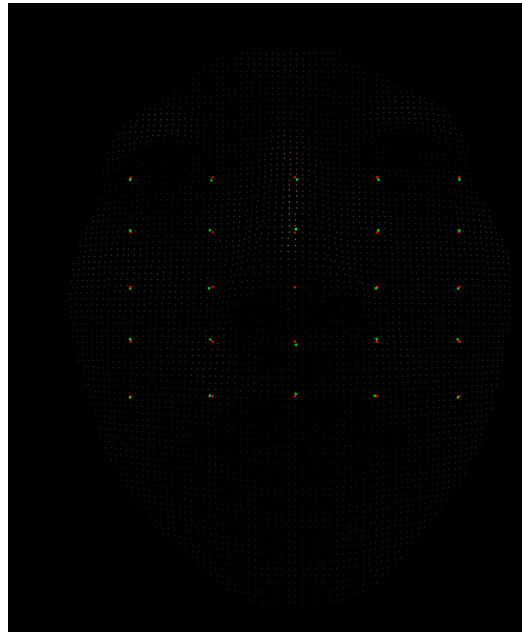
Fig. 2-5. Illustration of 25 points around the nose tip [9].

There is no doubt that many more studies of 3D face recognition employ other techniques. Li et al. [9] employ a feature set of 300 geodesic distances between all the pairs of the 25 feature points, as shown in Fig. 2-5, to represent the 3D face model for the purpose of face recognition. A recognition rate of 91.1% is achieved by Iterative Closest Point (ICP) method [54]. In order to use the minimum features to produce better recognition rates, Fatimah et al. [55] extract fifty three geometric features from twelve feature points and achieve a recognition rate of 86%. In other work of Fatimah et al., they prove that the eye separation provides the most powerful features for face recognition by evaluating a large number of features. Xu et al. [19] generate the combination of global geometric features and local shape variation information, such as the areas around the eyes, the mouth and the nose, to obtain the recognition rate of 96.1%. Xu et al. [56] analyse the geometric features of the registered faces in the lower

dimension space by PCA and achieve the recognition rate of 94%. Moreover, the low computational cost has been claimed due to its simplicity of matching in a lower dimensional space. It is worth pointing out that further studies [57-58] have suggested geodesic distance efficiently represents the 3D face model and is invariant of facial expressions because the skin has limited stretch ability.

In addition, other techniques like distance map, has been developed by Medioni et al. [59] between two face meshes to for the purpose of face recognition. They achieve the recognition rate of 97% and showed that 3D images provide better performance than 2D images. Wang et al. [60] map 3D images onto 2D domain using multiple conformal geometric map and achieve a recognition rate of 97.3% by using shape information only. Berretti et al. [61] develop a set of iso-geodesic stripes to represent the face model. They capture the characterising features of the face by measuring the spatial displacement between the stripes and achieve a recognition rate of 97.7%. In addition, the iso-geodesic stripes are considered in Feng et al. [62] and they claim that 20 striped used in their study are pose-invariant and expression-invariant. A recognition rate of 95% is achieved.

2.3 Review of Gender Classification Techniques

There is no doubt that human beings have amazing ability to recognise gender by simply observing a person's face. This is considered as an important aspect of human evolution and is involved in human face perception [63-69]. An important question remains on how gender is recognised by a human. Human beings can still conclude gender even with hair styles concealed, male's facial hair removed, and no cosmetic.

Bruce et al. [68] identify a set of potential cues for gender classification and explore the discriminative effects of removing or reducing different potential cues by measuring in several ways: (a) distances between key points on facial images (b) ratios and angles formed between key points on facial images (c) 3D distances derived by combination of full-face and profile photographs. They conclude that the gender of a face is presented in terms of several classes of information, local features (such as facial hair, eyebrows, and skin texture), relationships between features, and the 3D structure of the face. They focus on the shape differences between the two genders, and compare the average male and average female heads, as shown in Figure 2-6. They demonstrate that on average, the male face has a more prominent nose, brow, chin than the female face. The female face, however, has more profound cheeks than the male face. In addition, the nose region has the most discriminative features between male and female. Enlow [70] investigates the differences in facial shape between men and women in the nose area are due to their different oxygen requirements, as shown in Figure 2-6. They conclude that female faces have smaller nose.

(a)   (b)
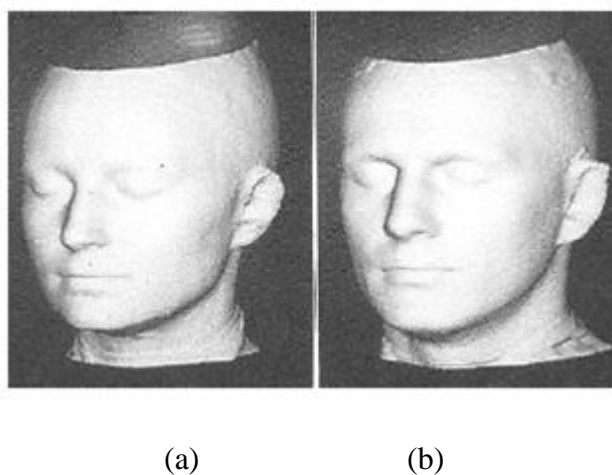
Fig. 2-6. Average laser scanned face surfaces of (a) female and (b) male [10]

As a basic task of face recognition technique, researchers have concentrated on developing techniques for gender classification since 1990s. This is mainly because it is an important aspect to face recognition applications.

Table 2-1. Other methods of classifying gender on 2D images

Researchers	Method	Database	Accuracy
Golomb et al. [71]	Two-layer neural network, SEXNET	90 face images	91.9%
Brunelli and Poggio [72]	HyperBF networks	168 images	79%
Tamura et al. [73]	Multi-layer neural network	30 subjects	93%
Wiskott et al. [74]	labeled graphs with topographical information and local templates	112 images	90.2%
Moghaddam et al. [75]	SVM with Gaussian RBF kernel	1800 subjects	96.62%
Lu [76]	SVM	800 subjects, 400 female and 400 male	92.55%
Scalzo [77]	Kernel spectral regression	200 female and 200 male	96.2%
Sun [78]	Genetic Algorithm,	200 female and	95.3%

	SVM	200 male	
Gutta et al. [79]	radial basis functions (RBFs), decisions trees (DTS) and SVMs	FERET	96%
Saatci et al. [80]	AAM and SVM	262 images	97.6%

This table shows 2D gender classification with multiple solutions. The highest accuracy rate is 97.6% from Saatci et al. [80] who develop a gender classifier using AAM to extract the features and SVM to classify. The best results are obtained using two expression classification cascades that are selectively trained on male and female images respectively as determined by an initial gender classifier. Thus, they conclude that the results can be improved by introducing an initial gender classification.

Tamura et al. [73] classify gender with multiple resolutions images using multi-layer neural networks. It shows the accuracy rate of 93%. Golomb et al. [71] train a fully connected two-layer neural network, SEXNET, to identify gender from 30-by-30 face images. Their experiments on a set of 90 images (45 males and 45 females) achieved an average error rate of 8.1%. Brunelli and Poggio [72] produce HyperBF networks for gender classification in which two RBF networks, one is for male and the other is for female. Trainin 16 geometry features on the face image (21 males and 21 females), it shows an average error rate of 21%. Wiskott et al. [74] use labelled graphs with topographical information and local templates. In the labelled graphs, the nodes are labelled with jets, a special class of local template built on the basis of wavelet transforms while the edges are labelled with distance vectors. They utilise a set of precomputed graphs, the "general face knowledge" to generate new graphs of faces by

elastic graph matching. They employ composite images of faces to determine certain features in order to classify gender. The experimental results show that on a set of 112 face images the average error rate is 9.8%. Moghaddam et al. [81] classify gender based on SVM with RBF kernel with respect to various traditional pattern classifiers, such as Linear, Quadratic, Fisher Linear Discriminant (FLD), Nearest-Neighbor. By exploring differences between these classifier methods, they find out that SVM classifier performs 96.62% identification rate and outperform all other classifiers. Lu et al. [76] evaluate the significance of different facial regions for the purpose of gender classification based on SVM classifier. By exploring the classification rate of seven regions respectively, such as whole face, internal face, upper face, lower face, eye, nose and mouth, they prove that the upper region yields the highest classification rate. Combination of upper face, left eye and nose, however, can improve the classification performance resulting in the rate of 92.55%. Based on these techniques, further studies have been developed. Scalzo et al. [77] construct a hierarchical feature fusion model by learning various features to produce optimal feature combination. They utilise three different classifiers, SVM, NN and kernel spectral regression (KSR) [82]. Sun et al. [78] utilise Genetic Algorithm (GA) to select a subset of features encoding important gender information by using PCA to reduce feature dimensions. Four classifiers are utilised to evaluate the genetic feature subset selection, including a Bayes classifier, a Neural Network (NN) classifier, a Support Vector Machine (SVM) classifier, and a classifier based on LDA. Their experimental results show that the SVM classifier outperforms the other three classifiers because it achieves the highest accuracy rate of 95.3%. Santana et al. [11] investigate the importance of contextual features, such as hair and neck tie, for gender classification, as shown in Fig. 2-7. They use 100 features extracted from PCA to represent the faces. Based on the SVM classifier they prove that the contextual features can be used to

classify gender due to the fact that uncropped C of the optimal areas (cropped A, cropped B, uncropped C), as shown in Fig. 2-7, achieved outstanding performance in terms of the accuracy rate. Wu et al. [83] utilise the 2.5D surface normals recovered from shape from shading to prove that the combination of shape information and texture information provides better results. Gutta et al. [79] use decision trees (DTs) and SVMs to implement the determinant components for deciding which of the techniques should be used to determine the classification output and determine the RBF kernel outperforms other non-linear kernels, such as polynomial and hyperbolic tangent. Nakano et al. [84] train the edge information by a neural network (NN) classifier for gender recognition. In particular, their input features are considered as the density histograms of the edge images. Nazir et al. [85] classify gender on the 2D images using Discrete Cosine Transform (DCT) to extract the optimal feature vectors and K-nearest neighbor classifier (KNN) for the purpose of classification. Matta et al. [86] show that not only the face appearance but also the features associated with the head and the mouth region provide support for gender classification.

It is worth pointing out that Ozbudak et al. [87] investigate the effects of masking on different parts of the face for the purpose of gender classification. Based on PCA, they conclude that the nose is the most distinctive feature, followed by the forehead, whereas the chin is the least distinctive feature to gender classification.

Fig. 2-7. Samples of different facial areas. From left to right: Cropped A (without hair line), Cropped B (including the hair line) and Eyes, Uncropped (including local context) [11]

With gender classification technology in two dimensional images having reached a mature stage, researchers have moved towards using three dimensional images.

Table 2-2. Other methods of classifying gender on 3D images

Researchers	Method	Database	Accuracy
O' Toole [88]	PCA	130 subjects, 65 female and 65 male	96.9%
Lu [89]	An integration scheme for gender and ethnicity classification using SVMs	1240 facial scans of 376 subjects	91%
Costen [90]	A sparse SVM classifier	300 images	94.42%
Shen et al. [91]	SVM training pixels of depth images	123 subjects (96 males and 27 females)	92.95%
Hu et al. [92]	PCA and SVM	590 male images and 355 female images	94.3%

In Table 2-2, O'Toole et al [88], apply PCA separately to the three dimensional structure and grey level image data. The features related to the gender are captured by individual components. In a series of simulations, the quality of information which is available in the 3D face data versus grey level data for predicting the gender is compared. They show that 3D structure data supports more accurate gender classification than grey level image data alone. Further studies of comparison of 3D and 2D images are from Shen et al. [91]. By contrast they conclude that the resolution of 3D facial images have little influence to the gender classification performance regarding to the comparison based on the accuracy rate of 92.95% and 99.73% testing on the depth image and the texture information respectively.

Across a range of gender classification on three dimensional imaging, Lu et al. [89] describe an integration scheme for ethnicity and gender identifications by combining the registered range and intensity modalities based on SVM classifier. They demonstrate that the 3D shape information provides effective capability for gender classification. The result based on 1240 facial scans of 376 subjects shows gender identification average error rate is 9.0%. Costen et al. [90] produce a sparse SVM classifier to select important features among a large number of candidate features generated from a relatively small training set of 3D appearance models and propose an algorithm for generating a complete set of sparse classifiers. Sparse classifiers are statistical algorithms for classification and relevant feature identification (specifying a smaller subset of discriminatory features). In theory, the sparse SVM uses 1-norm $\|w\|_1$ instead of 2-norm $\|w\|^2$, where w is the normal of the separating hyperplane. The squared 2-norm is not always the best choice for classification. Therefore, by exploring all the optimal, sparse classifiers, the sparse classifier assesses the feature selection and

parameter estimation processes. By a comparison table they clearly describe the SVM has 0.0% on training errors, 5.58% on testing errors, which has advantages over LDA. Hu et al. [92] propose a fusion-based gender classification by combining the internal face (region centred on the nose tip), upper region (region above the nose tip), lower region (region below the nose tip), nose and left eye and achieve the accuracy rate of 94.3%.

2.4 Review of Face Recognition under Expression Variations

Face recognition under expression variations is required in some applications and over last two decades many computer vision researchers have been attracted to focus on the problems of recognising faces under expression variations. Significant progress [93-96] has been made. The earliest study of Ekman [12], in the late 70s, has identified and classified the basic facial expressions, which are happiness, sadness, anger, fear, surprise, disgust and neutral. Some systems have been proposed to describe facial expressions. Ekman and Friesen (1978) have proposed the Facial Action Coding System (FACS), as shown in Fig. 2-8. They associate sets of muscles tenseness or relaxations, called Action Units (AU) to each basic expression. This has become the leading system to characterise facial expressions.

Fig. 2-8. Examples of Action Units (AU) [12]

Dynamic facial expression recognition is a well known topic in computer vision. Many researchers have contributed in the field. For example, Cohen et al. [97] have developed an expression classifier based on a Bayesian network. In general, a Bayesian network is a graphical model that encodes probabilistic relationships among variables of interest. In the particular graphical area, each node in the graph represents a random variable, while the edges between the nodes represent probabilistic dependencies among the corresponding random variables. They also propose a new architecture of Hidden Markov Model (HMM) [98] for automatically segmenting and recognising human facial expression from video sequences. A Hidden Markov Model is a statistical Markov model, in which each (internal) state is not directly observable (the term hidden) but produces an observable random output (external) state. Pantic and Patras [99] present a dynamic system able to recognise facial AUs and so expressions, based on a particle filtering method. In this context Bartlett et al. [100] use SVM classifier. Finally Fasel and Luettin [101] study and compare methods and systems presented in the literature to

deal with dynamic facial expression recognition. They focus particularly on the robustness comparison in case of environmental changes.

Lu et al. [102] match 2.5D facial images in the presence of expression variations and pose variations to a stored 3D face model with neutral expression by fitting the two types of deformable models, expression-specific and expression generic, generated from a small number of subjects to a given test image which is formulated as a minimisation of a cost function. Basically, mapping a deformable model to a given test image involves two transformations, rigid and non-rigid transformation. Therefore, the cost function is formed by translation vector and rotation matrix for rigid transformation, and a set of weights α. Kakadiaris et al. [103] address main challenges concerning the 3D face expressions recognition as follows.

- *Accuracy gain*: For using 3D facial expression recognition independently or combined with other modalities, a significant accuracy gain of the 3D system with respect to 2D face recognition system must be produced in order to justify the introduction of a 3D system.

- *Efficiency*: 3D acquisition captures and creates larger data files per subject which causes significant storage requirements and slow processing. The data preprocessing for efficient data must be addressed.

- *Automation*: A system designed for the applications must be able to function fully automatically.

- *Testing database*: Larger and widely accepted databases for testing the performance of 3D facial expression recognition system should be produced.

Kakadiaris have addressed the majority of the challenges by utilising a deformable

model and mapping the 3D geometry information onto a 2D regular grid. The advantage of this is combining the 3D data with the computational efficiency of 2D data. They achieve the recognition rate of 97%.

Lee et al. [104] propose an expression-invariant face recognition method. They extract the facial feature vector and obtain the facial expression state by the facial expression recogniser from the input image. The two main strategies for expression transformations are direct and indirect transformations. Direct transformation transforms a facial image with an arbitrary expression into its corresponding neutral face, whereas indirect transformation obtain relative expression parameters, shape difference and appearance ratio by model translation. By transforming them into its corresponding neutral facial expression vector using direct or indirect facial expressions transformation, they compare the recognition rate of each proposed method based on three different distance-based matching methods, nearest neighbor classifier (NN), LDA and generalised discriminant analysis (GDA).They achieve the highest recognition rate 96.67% based on NN, LDA using indirect expression transformation.

Al-Osaimi et al. [105] introduce a new definition called the shape residue between the non-neutral and the estimated neutral 3D face models and present a method for decomposing an unseen 3D facial image under facial expressions to neutral face estimates and expression residues based on PCA. The residues are used for expression classification while the neutral face estimates are used for expression robust face recognition. In a result, 6% increase in the recognition performance is achieved when the decomposition method is employed.

Li et al. [106] use low-level geometric features to create sparse representation models collected and ranked by the feature pooling and ranking scheme in order to achieve satisfactory recognition rate. They intentionally discard the expression-sensitive features, which are considered as higher-ranked. The recognition rate 94.68% is achieved.

2.5 Review of Face Recognition Systems

Face recognition systems detect faces in moving or still images and recognise them. The flow chart of a particular automatic face recognition system is as shown in Fig. 2-9.
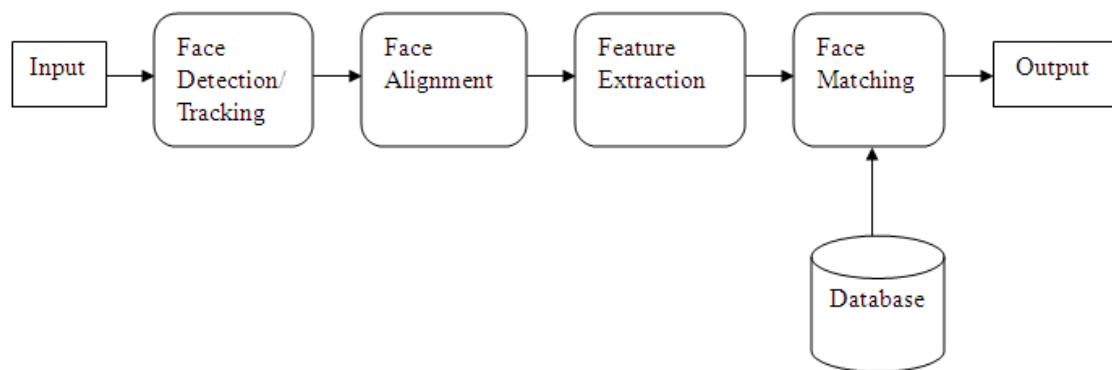
Fig. 2-9. Flow chart of a face recognition system

In general, automatic face recognition system can be formulated as follows: given still or video images of a scene, identify one or more persons in the scene using a stored database of faces. The solutions involve segmentation of faces (face detection) from cluttered scenes; face alignment (localisation), more accurate localisation of the face and scale of each detected face. The input face image is normalised concerning geometrical properties, such as size and pose, (geometrical transforms or morphing) and

concerning photometrical properties such illumination and grey scale; face representation (feature extraction) based on segmentation of faces; and recognition (face matching).

In an automatic human face recognition system applied in the field-deployable environments, key subtasks can be divided and grouped into three relevant components in order to improve the efficiency, computing speed and performance.

i. Registration and modeling of facial surfaces in an efficient way aims to reduce the computational complexity of the registration algorithm and help to improve the performance in the recognition part [107].

ii. Extraction of 3D facial features component, which in most cases distinguish various faces in terms of eyes, nose and mouth. At present most popular methods for facial feature extraction are based on point clouds, facial profiles, surface curvature-based features, 2D depth image-based approaches and surface normals [108].

iii. Algorithm and methodology using 2D/3D facial data in an efficient way.

Lu et al. [109] have developed a face recognition system that utilises 3D shape information to make the system more robust to address the problem of large head pose changes. Two different modalities provided by a facial scan, which are shape in 3D models and intensity in 2D images, are utilised and integrated for face matching. They have designed a hierarchical geodesic-based resample scheme to derive facial surface models for establishing correspondence across expressions and subjects. Based on the developed representation, they extract and model 3D non-rigid facial deformations such

as expression changes for expression transfer and synthesis. For 3D face matching purposes, a user-specific 3D deformable model is built driven by facial expressions. An alternating optimization framework is applied to fit the deformable model to a test facial scan, resulting in a matching distance. To make the matching system fully automatic, an automatic facial feature point extractor is developed. This 3D face recognition system is able to handle large head pose changes and expressions simultaneously, including automatic feature extraction, integration of two modalities, and deformation analysis to handle non-rigid facial movement , such as expressions.

(a)   (b)

Fig. 2-10. 3D face acquisition system (a) stuctured light projected onto a face subject (b) 3D reconstruction from (a) [13]

Beumier et al. [13] propose a structured light system to capture 3D facial images, as shown in Fig. 2-10. The 3D facial image matching is carried out at both central and lateral profiles, as shown in Fig. 2-11. They investigate the nose as a significant geometric feature. Combining 2D images and 3D images they extract the profile curves from them. However, the sensor noise is reported as a major issue affecting the matching accuracy.
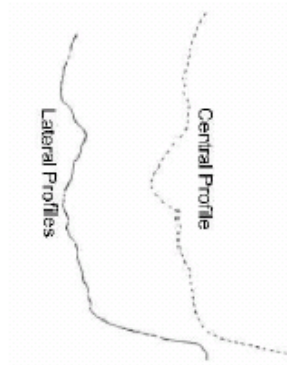
Fig. 2-11. Central and lateral profiles after normalisation [13]

Chang et al. [18] have developed a face recognition system based on comparison and combination of 2D texture information and 2.5D depth information. A 2.5D image is a simplified 3D (x, y, z) surface representation that contains at most one depth value for every point in the (x, y) plane. They demonstrate that independently using 2D or 3D information has similar performance characteristics. Combination for a face recognition system, however, shows that significant improvements can be made. It is worth pointing out that employing 2D texture information, to a certain degree, costs more computational time.
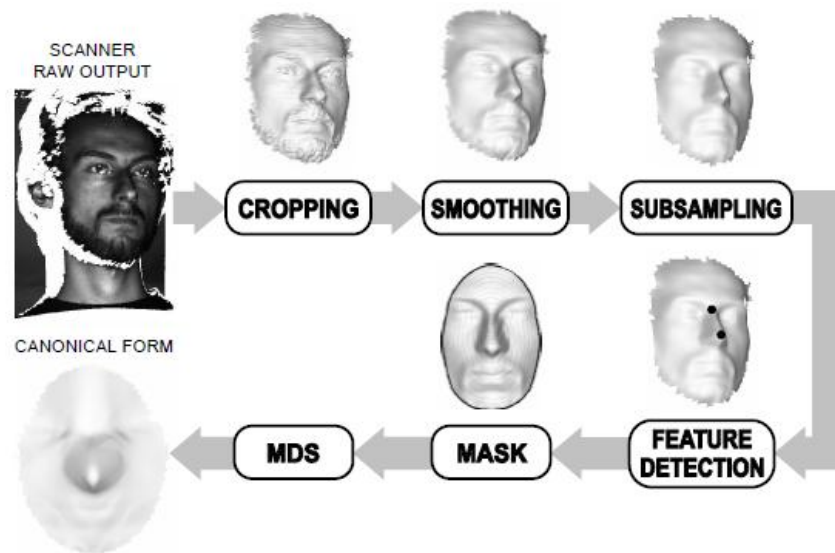
Fig. 2-12. Scheme of the 3DFACE system pipeline [14]

Bronstein et al. [14] present a geometric framework, called 3DFACE system, as shown in Fig. 2-12, for 3D face recognition under expression variations. It is worth pointing out that in this proposed system, data preprocessing involves face cropping followed by smoothing and subsampling. By modeling facial expressions as isometrics, they use canonical form to preserve the intrinsic geometric properties of facial surfaces for face recognition, which are expression-invariant. They represent facial surfaces with the characteristic of an expression-invariant by using the isometric embedding as a method to construct expression-invariant. Their results show high recognition rate in the presence of facial expressions.

Li et al. [110] develop a set of multiple geometric descriptors to represent the face model, which is remeshed in a feature-sensitive manner. They consider the expression-insensitive regions (the upper face), excluding the mouth region. The intrinsic descriptors are used to describe the face model, such as geodesic distance, angles, areas and curvatures. Combining the descriptors by applying a weight to each

element of descriptors is the key to achieve the optimized performance. The descriptors combinations of angles and geodesic distance perform best with the recognition rate of 95.56%.

2.6 3D Face Recognition Challenges

Compared to 2D face recognition techniques, 3D face recognition methods are relatively new, although it has been studied and developed over a few decades. Indeed, a 3D model provides more information on the shape of the face, which is less affected by illumination and pose variations. Another factor has driven rapid development of 3D face recognition methods. The development of 3D acquisition systems and the 3D capturing process are becoming cheaper and faster. This definitely makes the 3D face recognition method more applicable to real situations. There are still a few problems and challenges in 3D face recognition:

- *Noisy facial images*: Although the quality of 3D acquisition systems has improved over the last few years, there still remains the problem of making an impact on the performance of several existing method.

- *Feature points localisation*: Indeed, some researchers have localised significant feature points over 3D geometry meshes with the help of employing 2D texture information. It seems to be a challenge when dealing with 3D images without 2D texture information as it is difficult to locate sufficient feature points (MPEG-4 standard) solely relying on 3D geometry meshes.

- *Expression variations*: This seems to occur in a real word scenarios as even subtle expression variations can be captured into the 3D acquisition system and affect the recognition performance.

- *Computational cost*: Achieving less computational cost for real world applications has become a big challenge, since large computational cost are already produced by using 3D face images compared to 2D texture information.

Chapter 3 Face Characterisation towards Recognition Using Curvature Methods

3.1 Introduction

For many applications, like face recognition, recognition of psychological characteristics from face [111], facial surgery [112-113], basically it is an important technique to measure and evaluate 3D face models by characterising faces. The face characteristics mainly concentrate on the facial features on the eyes, nose and mouth. Therefore characterising the optimal features and evaluating the geometric characteristics of the face models based on the significant geometric descriptors, like distances, curvatures, area, angels and normals, strengthen the face recognition performance.

In this chapter, we present a novel and computationally fast method for characterising face models towards 3D face recognition. The face model can be either a point cloud or a 3D polygonal mesh. Our face characterisation method aims to construct a framework with evaluating limited profile-based features in order to characterise face models semi-automatically. This is achieved by finding two intersections, one between the symmetry plane and the face model, the other one between the horizontal plane and the face model. The intersections will be determined by a set of feature points along the profiles and measured and evaluated by the curvature method. These profile-based face characteristics are essential to characterise the face model with limited features and can be used for 3D face recognition.

3.2 Problem Domain and Objectives

3.2.1 Problem Domain

In general, face recognition presents some issues which are related to the data retrieval process, the effective characterisation of face models, and efficient face matching with fast computation. The first issue is particularly relevant to the problem we want to address in this chapter.

It has been noted that like facial geometry, including open eyes, nose, mouth, as well ethnic, age and gender factors, characterises faces. In particular, for the 3D face recognition purpose, characterising the face geometrics has been developed by using various measurements and descriptors, such as various curvature estimations, angles, distances and normals.

It is clear that more information on 3D face models creat higher computational cost. Although a large number of methods for 3D face recognition have been proposed that employ whole regions or some certain sub-regions of the facial surface, methods that employ limited features from facial sub-regions remain largely unexplored. Furthermore, the few algorithms of this flavour that have been developed, have met with limited success. Another concern is that characterising face models using sub-regions can be unstable due to noise. The last but not least open problem that remains unsolved with regards to 3D face recognition is to develop algorithms that work consistently in different facial expressions. We address these issues in this chapter and present a novel method that employs Gaussian curvature to the profiles.

3.2.2 Objectives

Utilising efficient profiles or subspaces containing pivotal features which could characterise face models are the issues needed to be addressed. For 3D face recognition systems, in this chapter, we specifically aim at the algorithm and method of characterising face models in an efficient way. The objective is to establish a framework for characterising facial models utilising features comparatively invariant to expressions, focusing on a certain region which includes significantly distinguishing features. Curvature-based features in this framework are extracted based on facial symmetry characteristics in the upper region, shown in Fig. 3-1 (a), since this region is expression insensitive and includes discriminative features. Thus, in our proposed method, we intend to discard the lower region, as shown in Fig. 3-1 (b), which is comparatively sensitive to expressions. Our method focuses on how to extract expression-insensitive features which are unique to each individual facial surface. Therefore our algorithm can reduce the computational time where computational cost matters.

| (a) | (b) |
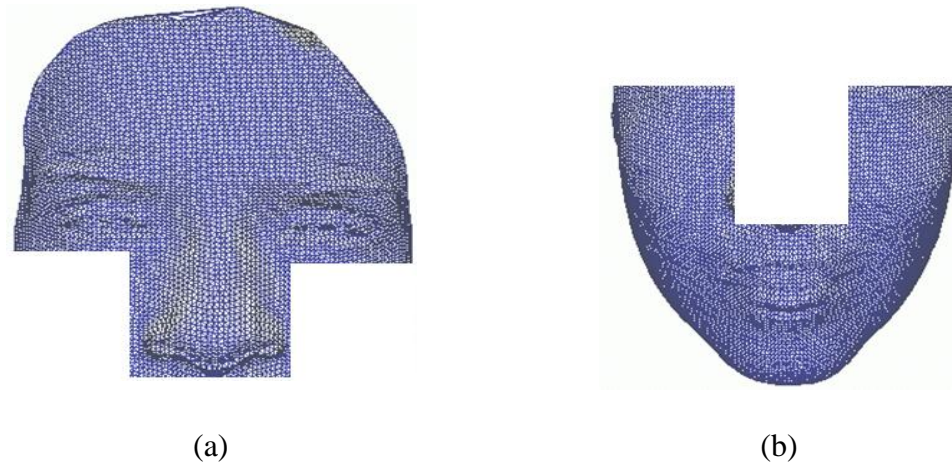
Fig. 3-1. Illustration of expression-invariant and expression-variant regions (a) The expression-invariant region including eyes, and nose (b) The expression-variant region including mouth chin and cheeks.

3.3 Data Format for Face Models

The correctness of the profiles extracting task usually depends on how well the face data is captured and preserved. 3D cameras and 3D scanners are widely used for face model acquisition.

The 3D face models are captured and generated from a single shot with a 3D camera, which commonly operates on the basis of stereo disparity of a high-density projected light pattern. The 3D camera is used to produce a 3D point cloud of the facial surface, which is then registered into a polygonal mesh. In this chapter, the particular experimental face data used are triangular meshes from in-house data. Another camera can be used to capture texture information, which is subsequently mapped onto the 3D model, as shown in Fig. 1-7.

In this chapter, we intentionally discard the texture of the face model due to the purpose of reducing computational cost under the condition of illumination-insensitivity. Thus geometric information of face models is acquired precisely as triangular meshes composing of a set of points in spatial space to represent face models.

Finally a 3D facial surface is generated using standard 3D reconstruction techniques and output in prevalent Wavefront's OBJ file format or VRML file format as are our facial data for this proposed method saved. The OBJ file format is a common data format that represents 3D geometry itself, i.e. the position of each vertex, the UV position of each texture coordinate vertex, normals, and the faces. The faces are triangles which are defined by three neighbouring points in our method, as shown in Fig. 1-7 (a). The 3D face model is a set of points in three-dimensional space, with each point lying on some object surface. This means that the point cloud actually describes the nearest visible surface to the 3D camera or scanner.

Unlike 2D facial images, the 3D face model has a distributed number of points across a spatial space. To achieve expected experimental results, 8 randomly selected in-house facial models are utilised for feasibility analysis first, whose vertices number is in the range of 10000 to 50000 from the face models capture process.

3.4 Discrete Curvature Method

3.4.1 Introduction

In computer graphics and geometric design applications, the surfaces of discrete form

such as meshes, subdivision surfaces and point surfaces become more and more important. Meanwhile various curvature estimation techniques have been developed and applied. According to the fact that face models are based on triangular meshes, the curvature estimation techniques on mesh surfaces can be broadly divided into two categories; discrete [114] and continuous [115].

The first refers to approximating curvatures by formulating a closed form for differential geometry operators that work directly on the discrete representation of the underlying surface that generated the triangle mesh. The latter involves fitting a surface locally, then computing the curvatures by interrogating the fitted surface. Due to face models being composed of triangle meshes, the discrete methods for triangle meshes will be described in this section.

The widely used discrete methods are listed as follows:

- Discrete Gaussian and mean curvature estimation
- Taubin's method [116] with suggested improvements by Surazhsky et al [117]

The discrete Gaussian and mean curvature estimation techniques are constructed respectively by Moreton and Sequin [118], Taubin [116], Meyer and Desbrun [119]. By exploring the experimental results for comparing various curvature estimation methods, Fang [120] finds out that Meyer's method based on Voronoi produces the outcome with low error rates for the triangle meshes. In our proposed method, we rely on the Voronoi method of Meyer and Desbrun to produce appropriate curvature on face models.

Prior to Meyer method, the notion of discrete Gaussian curvature on a triangular mesh is related to the notion of angles [121-122] . Let P be a polyhedral surface. The total angle $\theta(x)$ around the vertex $x \in P$ is the sum of angles of all the plane polygons incident to x. For any point $x \in P$ the curvature ω is defined as

$$\omega(x) = 2\pi - \theta \tag{3.1}$$

Let x be surrounded by triangular faces U with areas S1, S2, S3, . . ., and unit normals n1, n2, n3, . . . , as shown in Fig. 3-2 (a). The spherical image of the polygonal surface is a set of points on the unit sphere (the heads of unit vectors parallel to n1, n2, n3 . . .), as shown in Fig. 3-2 (b). Let us connect these points by arcs of great circles to form a spherical polygon on the unit sphere, as shown in Fig. 3-2 (c). The area A of the spherical polygon is equal to the angle deficit of p. The area of each triangular face adjacent to x can be portioned into three equal parts corresponding to the vertices of the face. So the total area related to x is $\sum S_k/3$. Thus the Gaussian curvature at x can be approximated by formula (3.2).

(a)   (b)   (c)
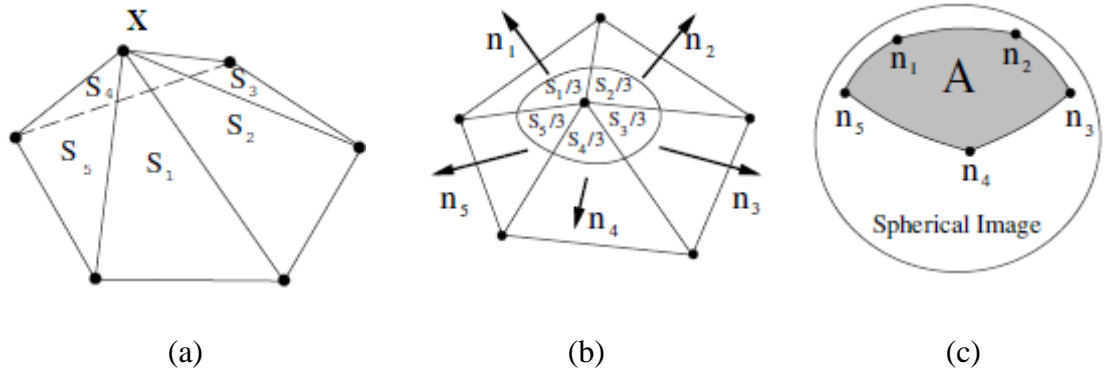
Fig. 3-2. Illustration of mapping a surface to Gauss map based on Gauss Theorem (a) a surface with a vertex x surrounded by neibouring faces (b) illustration of normals of each face (c) Gauss map

3.4.2 Meyer Voronoi Method

A key point of using the 1-ring neighbourhood around the vertex (point) is sufficient for approximating curvature at the vertex. Therefore, the Gaussian curvature of a vertex is related to angles and faces that are connected to that vertex.

The Gaussian curvature K of an inner vertex V_i (Fig. 3-3) is as formula (3.2).
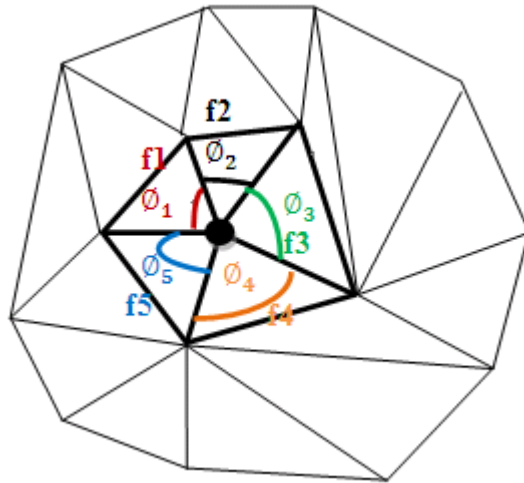
Fig. 3-3. The Gaussian curvature of an inner vertex

In Fig. 3-3, there are five sets of angles and faces which are distinguishable by colours, i.e. $\emptyset_1$ and f_1 in red denote the angle labeled in a red curve and the triangle *face1* with this corresponding inner angle. $\emptyset_2$ and f_2 in black denote the angle labelled in a black curve and the triangle *face2* with this corresponding inner angle. $\emptyset_3$ and f_3 in green denote the angle labeled in a green curve and the triangle *face3* with this corresponding inner angle. $\emptyset_4$ and f_4 in orange denote the angle labelled in a orange

curve and the triangle *face4* with this corresponding inner angle. $\emptyset_5$ and f_5 in blue denote the angle labeled in a blue curve and the triangle *face5* with this corresponding inner angle.

$$K = \frac{2\pi - \sum_{i=1}^{k} \emptyset_i}{\frac{1}{3}A} \tag{3.2}$$

where $A = \sum_{i=1}^{k} f_i$ is a sum of each triangle's area in the 1-ring neighbourhood, and $\emptyset_i$ denotes the angle at a vertex.

The Gaussian curvature K of a boundary vertex is that of a boundary line from boundary vertex, as shown in Fig. 3-4.
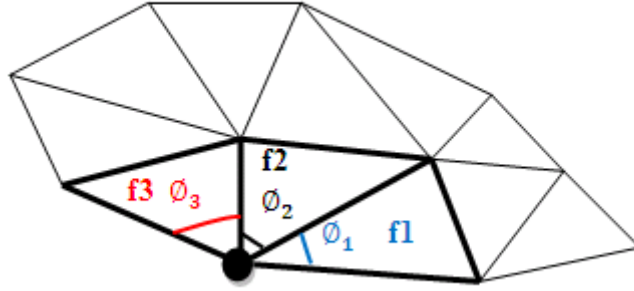
Fig. 3-4. The Gaussian curvature on a boundary vertex

In Fig. 3-4, there are three sets of angles and faces which are distinguishable by colours, i.e. $\emptyset_1$ and f_1 in blue denote the angle labeled in a blue curve and the triangle *face1* with this corresponding inner angle. $\emptyset_2$ and f_2 in black denote the angle labeled in a black curve and the triangle *face2* with this corresponding inner angle. $\emptyset_3$ and f_3 in red denote the angle labelled in a red curve and the triangle *face3* with this corresponding inner angle.

$$K \ = \ \frac{\pi - \sum_{i=1}^{k} \emptyset i}{\frac{1}{3} A} \tag{3.3}$$

where $A = \sum_{i=1}^{k} f_i$ is also a sum of each triangle's area in the 1-ring neighbourhood, and $\emptyset_i$ denotes the angle at a vertex.

Considering that facial surfaces we use are triangular meshes, we apply Gaussian curvature method of Meyer in our proposed method for curvature analysis.

3.5 Analysis of V Shape Profiles

In this section, feasibility of our method is discussed by describing the earlier experiments based on the fact of the symmetry characteristic of face models.

3.5.1 Feature Extraction

Human faces are not perfectly symmetric and the degree of symmetry differs individually. However, on average the deviation from perfect symmetry is not very strong. This is the result of a study by Ferrario [123] about the morphometry of the orbital region.

Here we create two planes respectively with two groups of three points exactly on the face surface, which are named P_0, P_1, P_2 and P_0, P_3, P_4, as seen in Fig. 3-5. The six landmark points are localised manually. P_0 is origin of the coordinate system, P_1 is the corner of one eye, P_3 is the corner of the other eye. P_2 and P_4 are mouth corners which combine with other two corresponding points to build up planes.
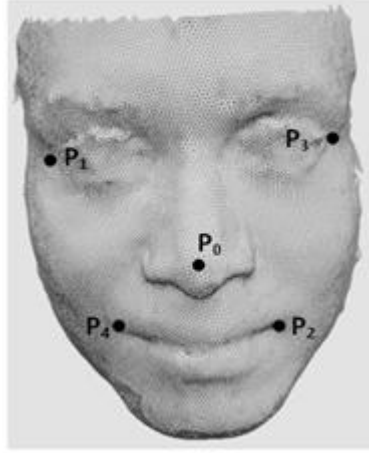
Fig. 3-5. Five landmark points localisation   Fig. 3-6. Profiles segmentation
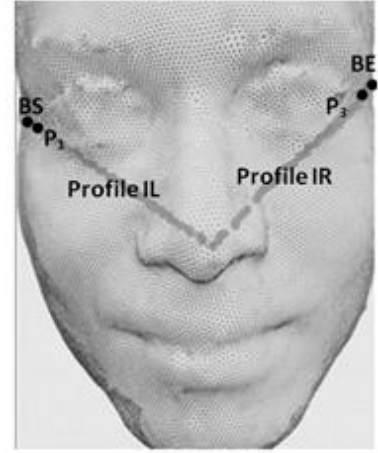
The plane built up through P_0, P_1 and P_2 has intersects with the face surface. We only extract the segmentation of the x values on the left side of faces, named profile *IL*. The plane determined by P_0, P_3 and P_4 intersects the face surface. We only extract the segmentation of all the x values that are positive including nose tip named profile *IR*, as seen in Fig. 3-6. On the other hand, *IL* is the intersection from nose tip point (P_0) through left eye corner (P_1) up to the boundary point (*BS*) of the face model. *IR* is the intersection from nose tip point (P_0) through right eye corner (P_3) up to the boundary point (*BE*) of the face model. The measurements we used for the profiles will be discussed in detail in the following section.
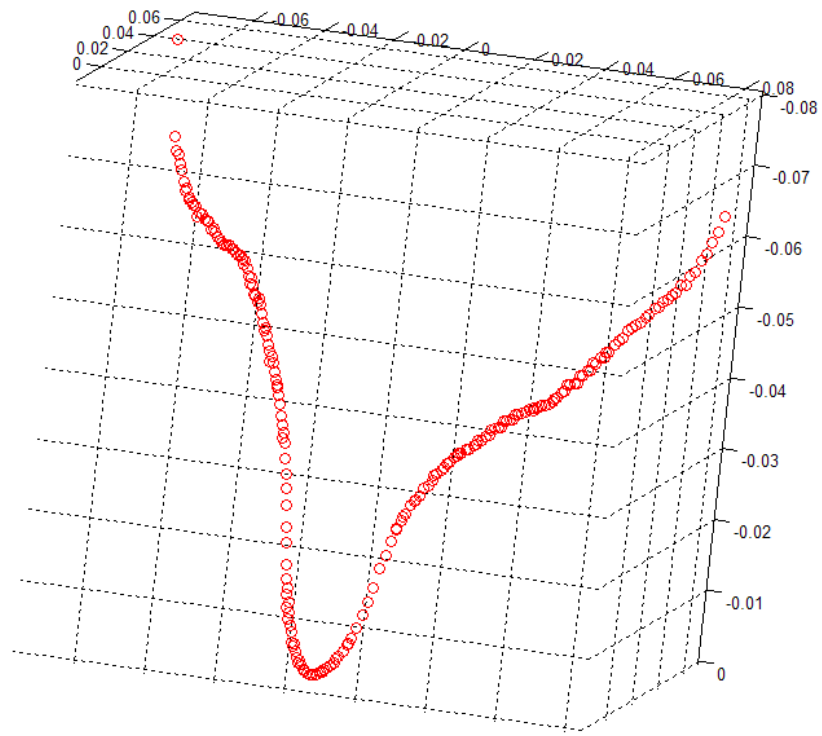
(a)
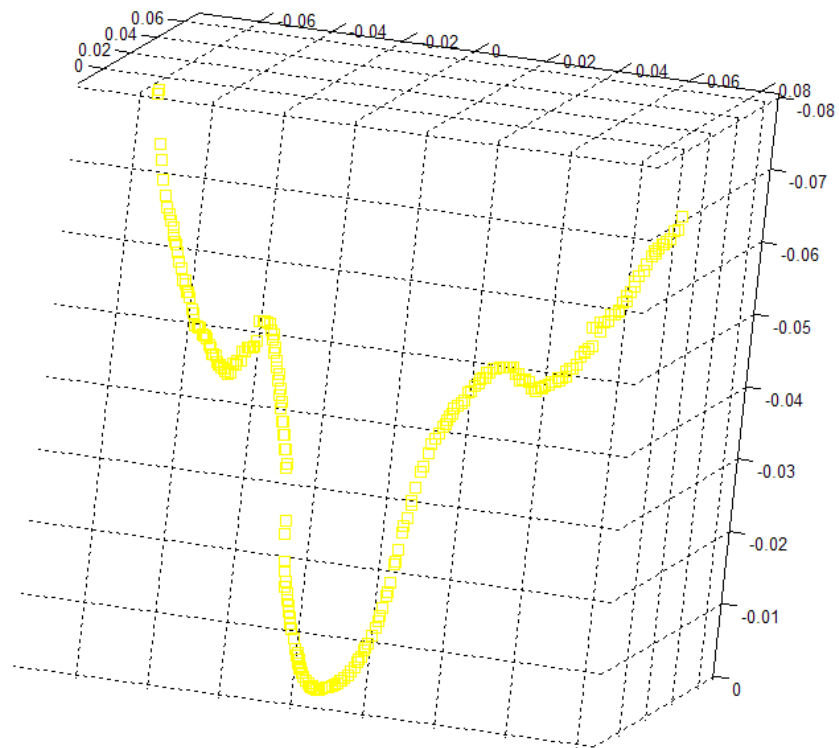
(b)

Fig. 3-7. V shape profiles curve of (a) face model 1 (b) face model 2
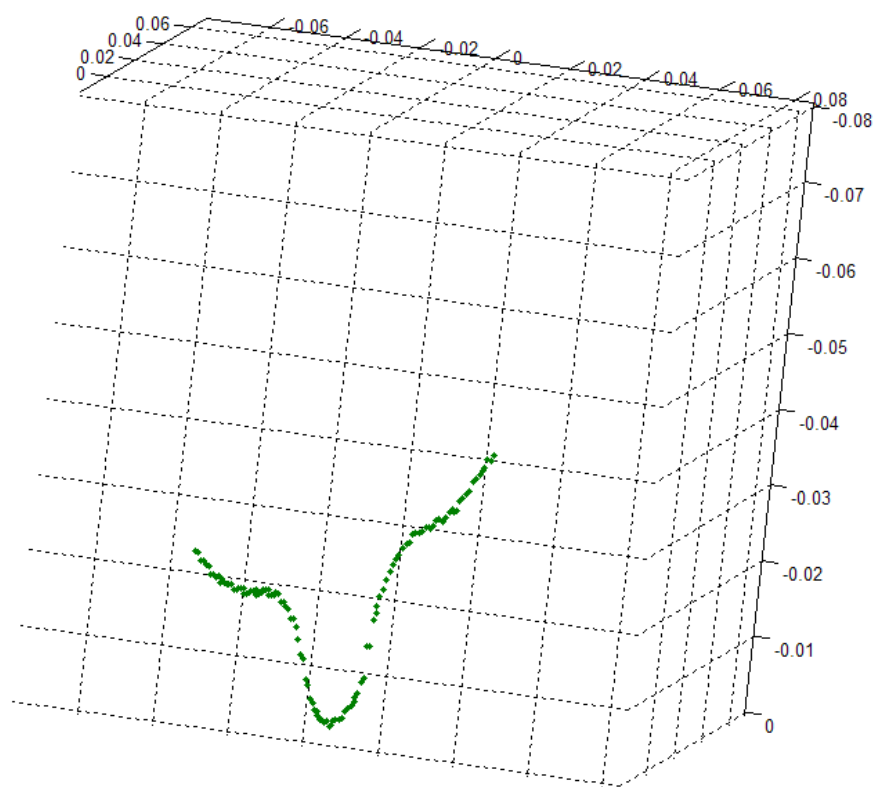
(c)

Fig. 3-7. V shape profiles curve of (c) face model 5
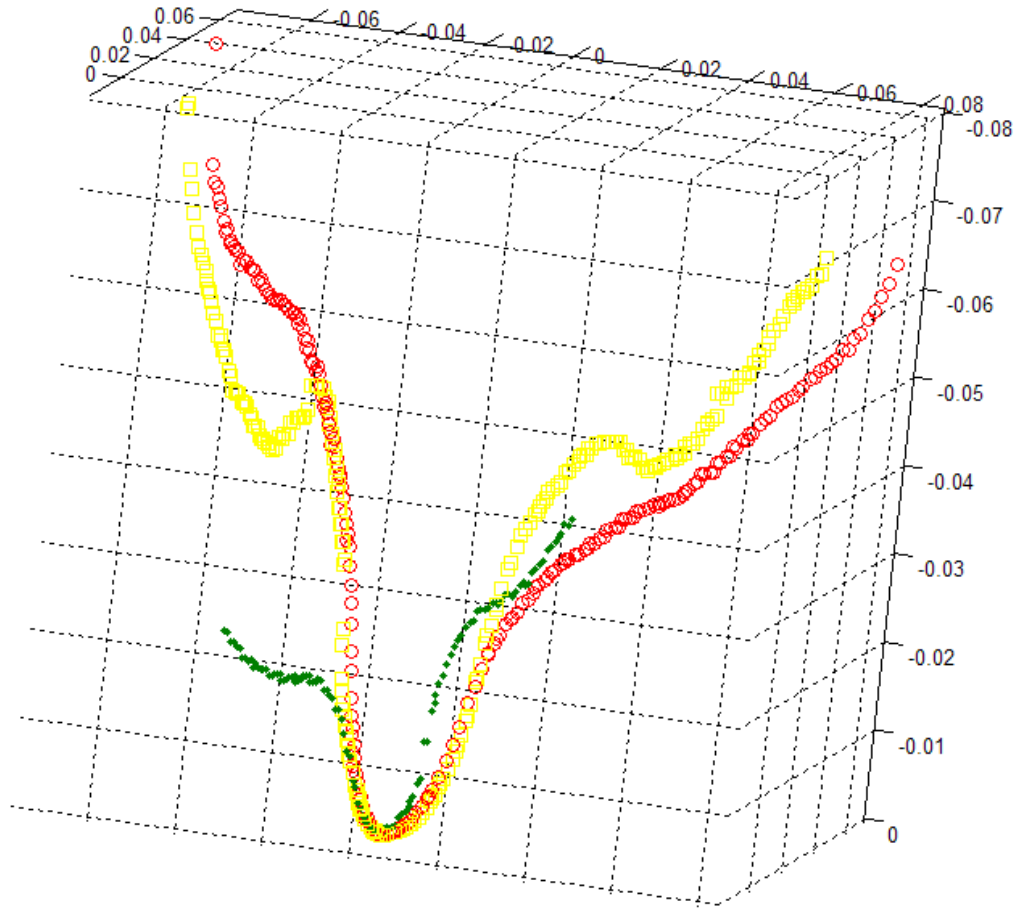
(d)

Fig. 3-7. V shape profiles curve of (d) 3 Random face models

In Fig. 3-7, by randomly selecting three face model V shape profile curves, obviously we can see curve variations. In Fig. 3-7 (d), it is clearly demonstrated that V shape profile curves from normalised face models vary in the spatial space. The nose tip is labelled with a hollow black circle, from which it stretches in two directions with ending points, BS and BE.

The next step is to apply the Gaussian curvature method to the profiles on face models to analyse the characteristics of faces. A dataset for this method comprises eight normalised in-house face models, which will be described in the next section.

3.5.2 Results and Analysis

IL profile curvature plot and *IR* profile curvature plot in Matlab are shown in Fig. 3-8.
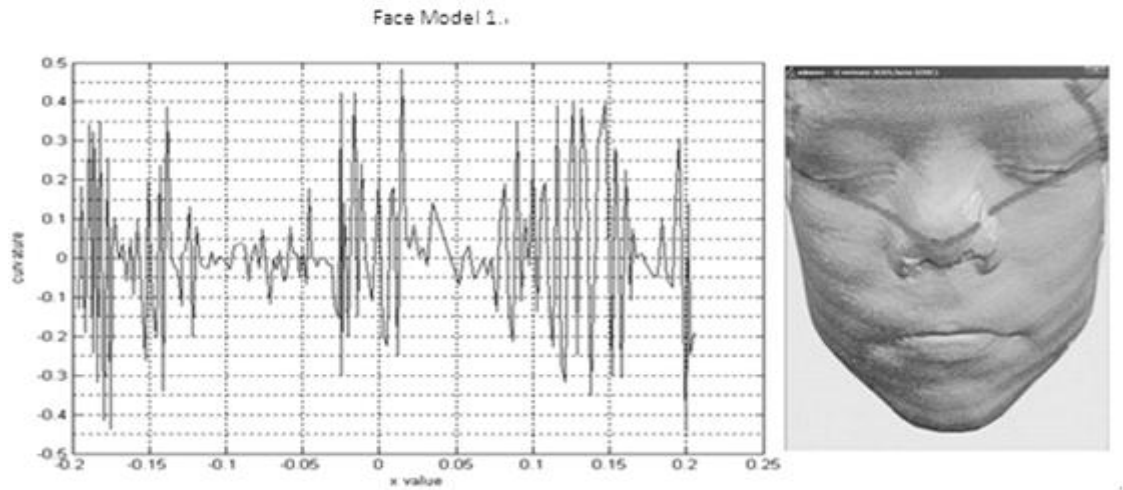
(a)
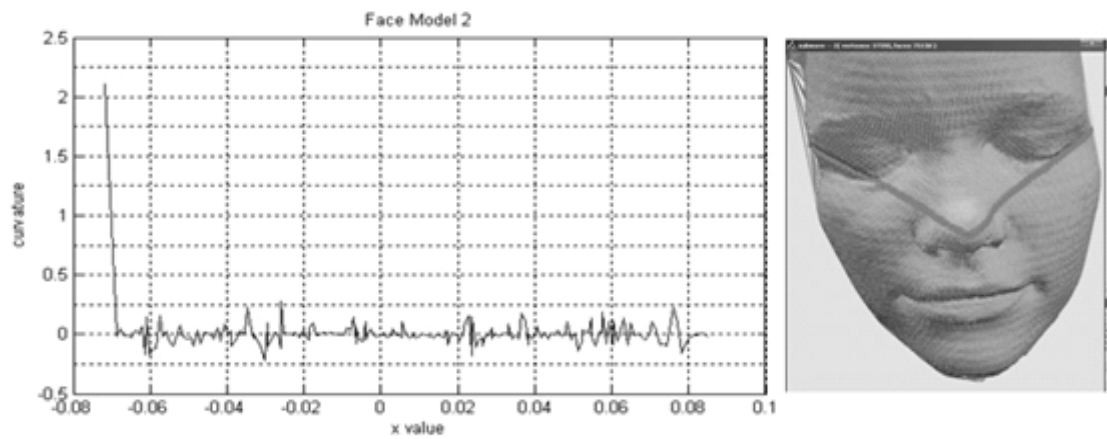
(b)

Fig. 3-8. *IL* and *IR* profiles curvature plot of (a) face model 1 (b) face model 2
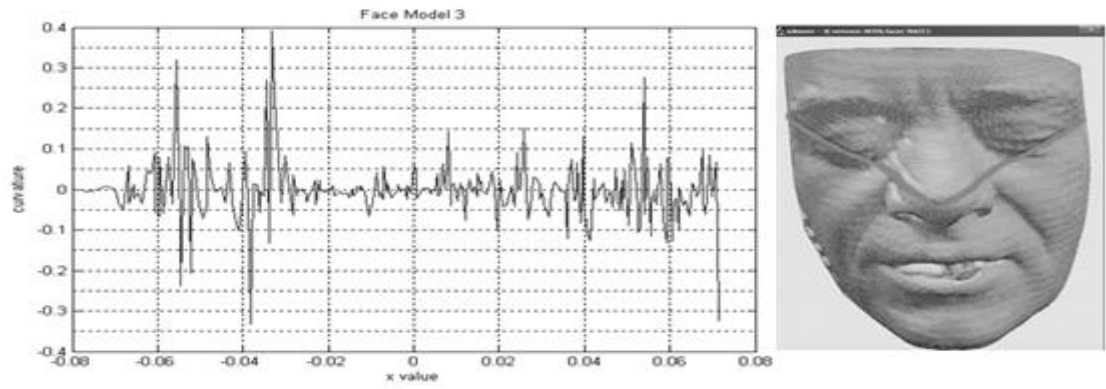
(c)
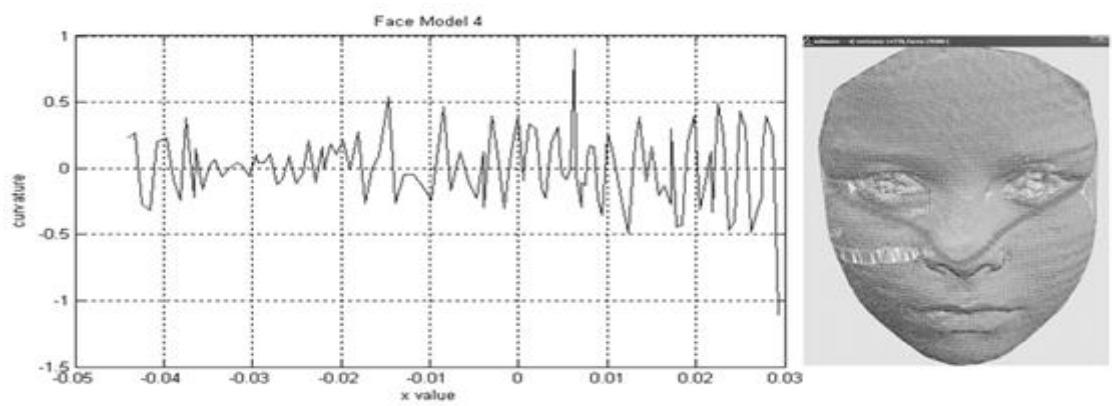
(d)
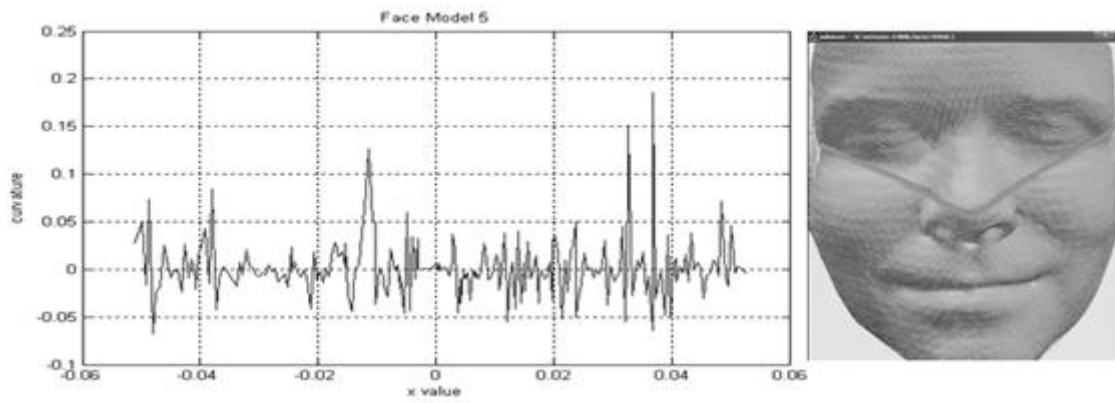
(e)

Fig. 3-8. *IL* and *IR* profiles curvature plot of (c) face model 3 (d) face model 4 (e) face model 5
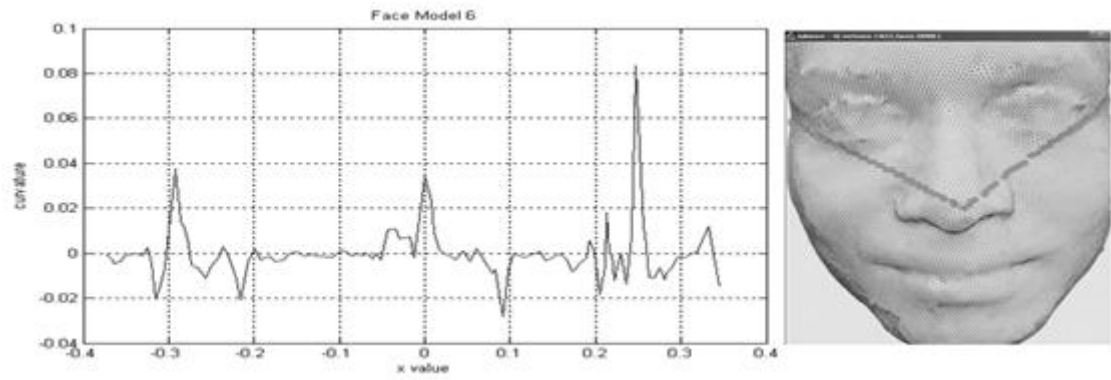
(f)
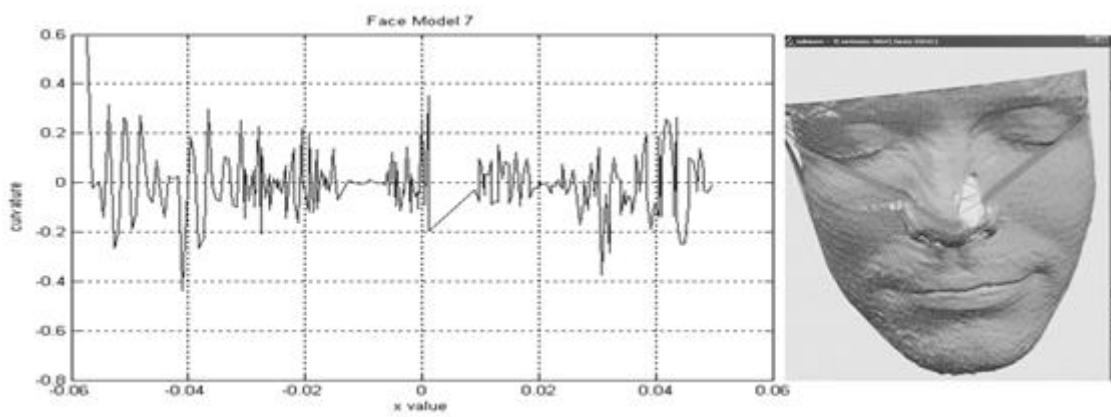
(g)
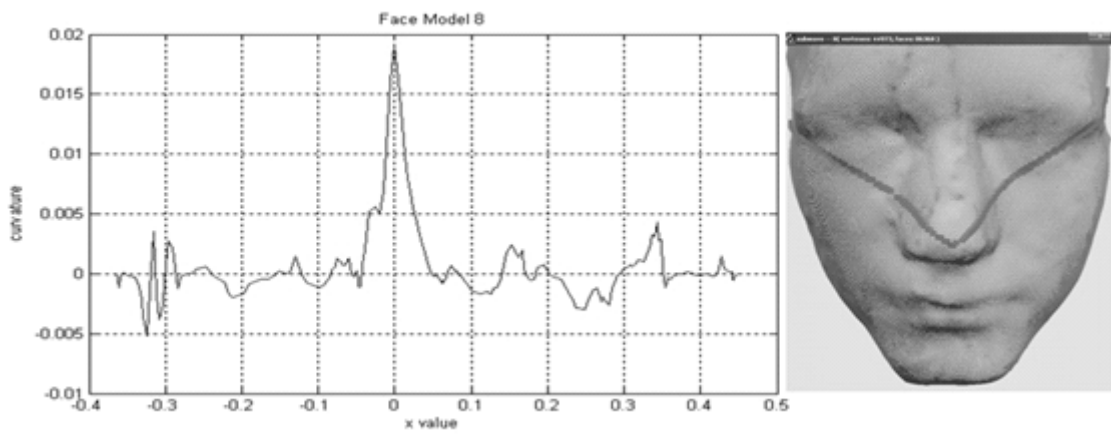
(h)

Fig. 3-8. *IL* and *IR* profiles curvature plot of (f) face model 6 (g) face model 7 (h) face model 8

Each curvature plot of the profiles *IL* and *IR* is from the boundary point *BS*, as shown in Fig. 3-6, down to the origin and again up to the boundary point *BE*, as shown in Fig. 3-6. In the curvature plot, the x-axis displays the x value of each point on profile *IL* and *IR* from left beginning towards the right end, while y-axis means the curvature value of the points along with increasing x value. Obviously it indicates the origin when x equals to 0. Ideally, as we expect, the curvature value of the origin, the nose tip, should be the peak value, the highest of all. Each curvature plot should look roughly symmetric, moreover the sub-peak values should be in the eye corners area and the curvature shape of the remaining region, which is part of the cheek, should be smooth. Face models 2, 4, 6 and 8 have smaller numbers of vertices than face models 1, 3, 5 and 7, which are considered as dense images. Dense images generate high frequency in curvature plots, whereas sparse images generate low frequency in curvature plots. However, high frequency might be caused by noises, for example face model 7 has noise on the left nose wing and a gap on the right nose wing. Moreover, due to the fact that Gaussian curvatures are not considered to be absolute values, curvature plots are distributed above zero and below zero.

After examining these eight curvature plots, only the face model 8, however, has a result close to the ideal expected. Secondly, the curvature plots of face models 1, 2, 3, 5, and 6 are roughly symmetric, whereas the peak values of them are not at the nose tip. The curvatures computed for models 4 and 7 do not provide the expected results. The reason for that is the horizontally extracted profiles do not go through the middle of the eyes. The point that face model 7 has a small gradient, to most extent, directly makes some influence on the result. Another reason impacting non-ideal results is noise on the face models. For example, face model 4 has the most noise, like holes which are results

of the 3D face acquisition facilities. Furthermore, the landmark localisation is another cause. By unique test, pre-experimental results prove that the V shape profiles are unique to each individual. On the other hand, they can provide sufficient information to characterise faces in certain circumstances.

3.6 Analysis of T Shape Profiles

Our basic idea is to utilise the symmetry of faces to establish unique profiles for each face based on curvature. The baseline of our method is that the face models are normalised. It generally means the local coordinate system takes nose tip point as the origin and all the values of points P(x, y, z) are in the range of [-1,1]. The dataset of eight face models will be utilised for experiments.

3.6.1 Segmentation of Face Region

Knowing the symmetry characteristic of faces through earlier work [124], enables the computational time to be reduced. The region which preserves numerous discriminative features of the whole face and symmetry characteristic is determined as in Fig. 3-9 (a). This sub-surface essentially contains eyes and nose. Furthermore, the region is comparatively insensitive to expressions. We intentionally discard the mouth region since it varies greatly under expression variations.

(a)   (b)

Fig. 3-9. Central region contains (a) eyes and nose (b) five landmarks localisation

3.6.2 Extraction of Baseline Profiles

T shape profiles are comprised of two profiles, one of which is the symmetry profile. It is comprised of those points which are the intersection between the symmetry plane of P_0, P_3, P_4 and the facial model. The profile starts from point P_0, through P_3 and ends at point P_4, as shown in Fig. 3-9 (b). The other one is the horizontal profile across the eyes. It is comprised of those points which are the intersection between the horizontal plane of P_1, P_0 and P_2 and the face model.

It is worth pointing out that the landmarks for building up planes are located manually by using MAYA toolbox, as shown in Fig. 3-9 (b). The point P_0 refers to the middle of the two eyes. P_4 refers to the nose tip which is the origin and P_3 refers to the middle of the nose bridge. P_1 and P_2 are outer eye corners respectively. The plane through P_0, P_3 and P_4 is represented by the formula (3.4).

$$\overrightarrow{P_0P_1} \times \overrightarrow{P_0P_2} = \begin{vmatrix} \vec{\imath} & \vec{\jmath} & \vec{k} \\ x_2 - x_1 & y_2 - y_1 & z_2 - z_1 \\ x_3 - x_1 & y_3 - y_1 & z_3 - z_1 \end{vmatrix} \qquad (3.4)$$

To obtain the intersection points between the two surfaces, a formula (3.5) computes the

closest points to form the profiles since the facial surface is a triangle mesh with discrete points and

$$T = \frac{\sum_1^{F_N} d|f_i V_0, f_i V_1| + d|f_i V_0, f_i V_2| + d|f_i V_1, f_i V_2|}{18 * P_N} \qquad (3.5)$$

where T denotes tolerance and F_N means the number of the faces (triangles) the face mesh has. V_0, V_1 and V_2 denote the three respective vectors (points) which build up a triangle, f denotes each individual triangle, and d means the distance between every two points of three in each triangle.

How to define a profile is the key problem in this method. We select points to extract a profile obeying a rule that the distance between the individual point on the face surface and the plane is less than T, which means the closest points to the symmetry plane whose distances are less than tolerance T. In this way, the profiles are established by all those selected points, named I_h and I_v respectively. I_h, as shown in Fig. 3-10, stands for the extracted profile, from the start point P_1 to the end point P_2, presented in a horizontal way through the three points, P_0, P_1, P_2. I_v, as shown in Fig. 3-9 (b), stands for the extracted profile, starting from point P_0 to point P_4, presented in a vertical way through the three points P_0, P_3, P_4.
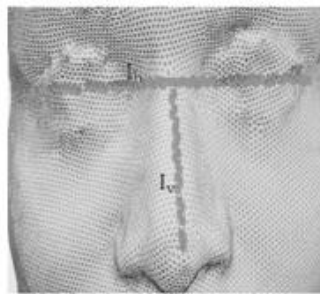
Fig. 3-10. Illustration of the extracted T profile
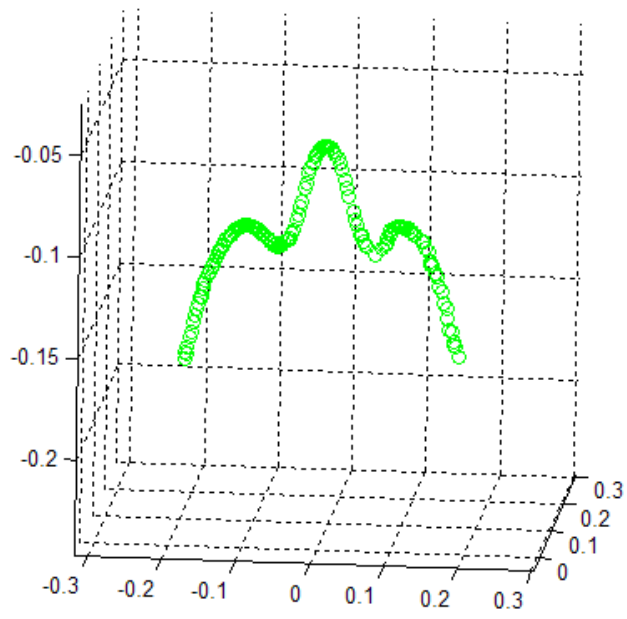
(a)
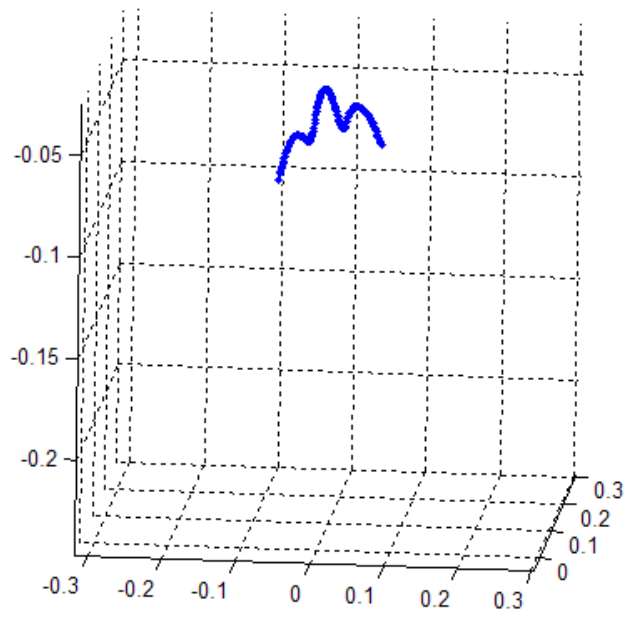
(b)

Fig. 3-11. Horizontal profile curve of (a) face model 1 (b) face model 2
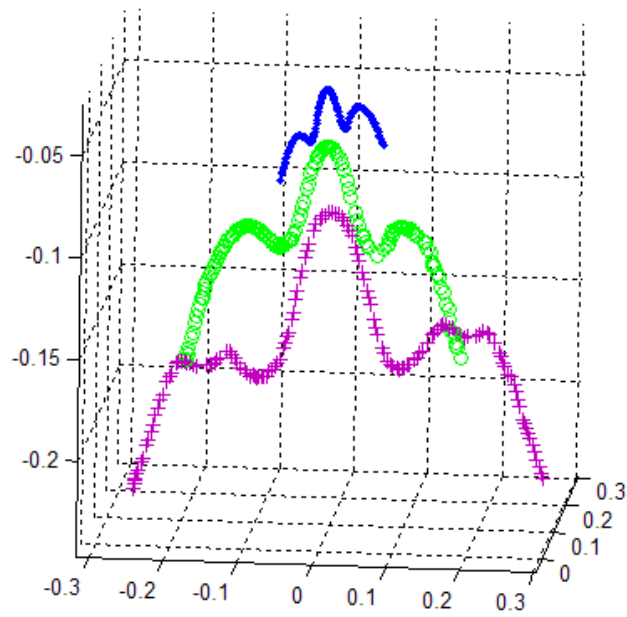
(c)

Fig. 3-11. Horizontal profile curve of (c) random three face models

In Fig. 3-11, are presented horizontal profile curves from three random faces by labelling mid-eye point with circle and outer eye corners with squares. To investigate the variations, we intentionally rearrange curves in different ratios which are illustrated in (d).
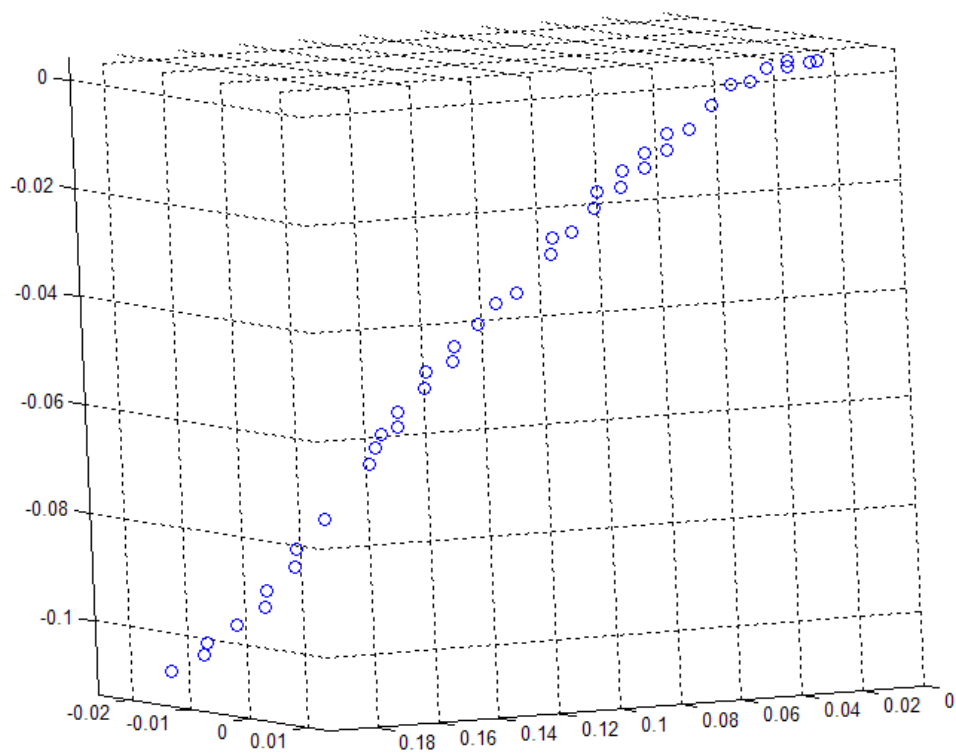
(a)
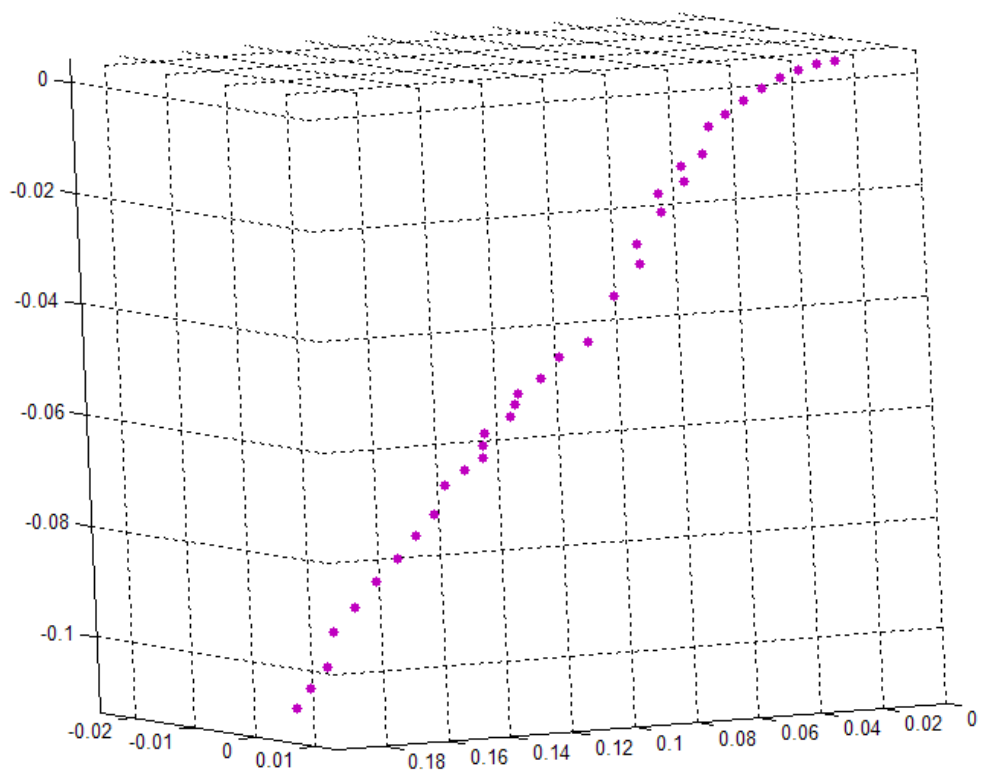
(b)

Fig. 3-12. Vertical profile curve of (a) face model 1 (b) face model 2
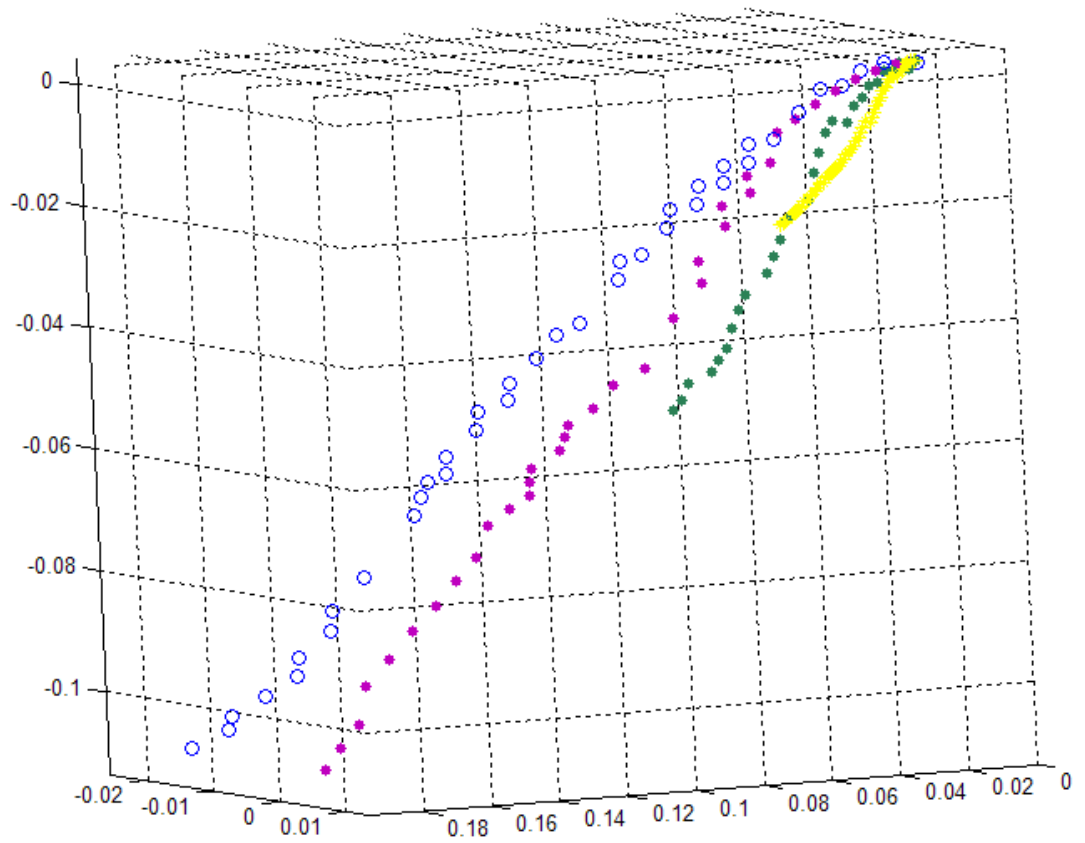
(c)

Fig. 3-12. Vertical profile curve of (c) random four face models

In Fig. 3-12, are displayed vertical profile curves which are part of T shape profiles. It shows two randomly selected curves and a combination of three curves in different ratios. The nose tip is labelled by a black circle. In (c), curve shape variations support our expected experimental results in advance. Each individual curve is presented by different labels. In addition, vertical profile curves present symmetry of faces which is one key facial characteristic.

3.6.3 Results and Analysis

In this part, the curvature plots of the profiles will be illustrated. Similarly to the previous work, the curvature is plotted in Matlab. For I_h profile, the curvature plot is in the direction going from point P_1 to P_2. For I_v profile, the curvature plot is in the direction going from nose tip P_4 up to the mid-eyes point P_0.

The curvature plots will be divided into two groups for illustration, which are a group of horizontal profiles curvature plots and another group of vertical profile curvature plots.

3.6.3.1 Curvature plots for horizontal profiles
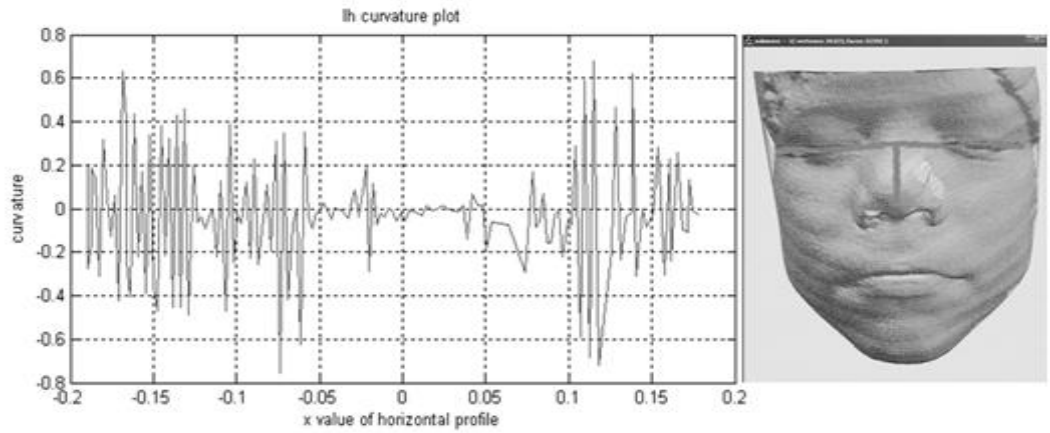
(a)

Fig. 3-13. Curvature plots of horizontal profiles cross eyes from (a) face model 1
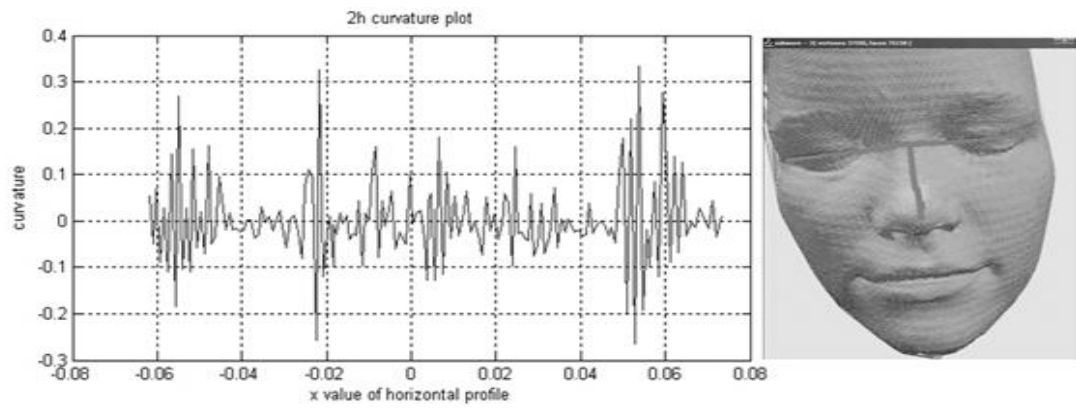
(b)
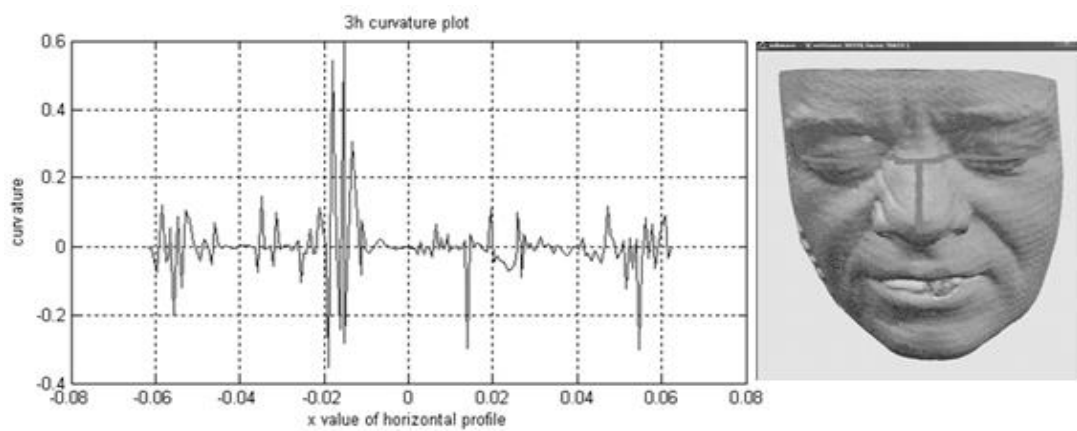
(c)
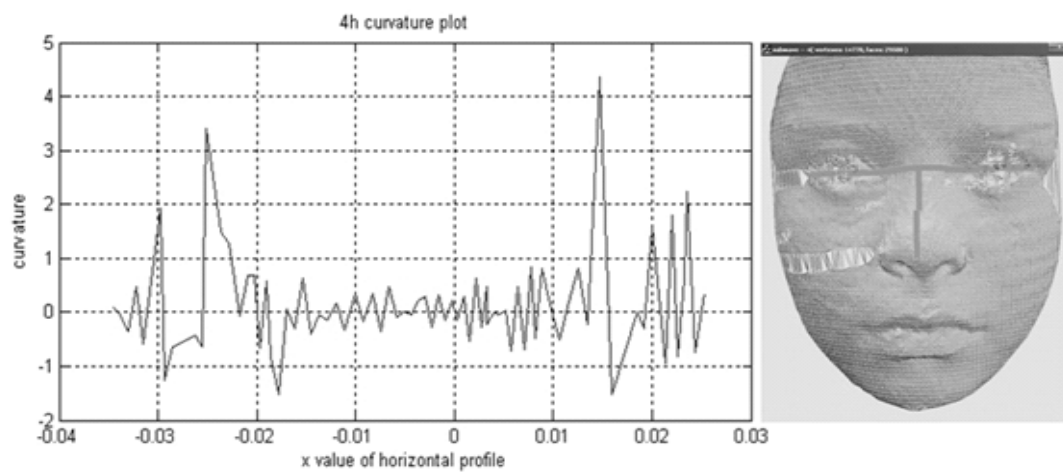
(d)

Fig. 3-13. Curvature plots of horizontal profiles cross eyes from (b) face model 2

(c) face model 3 (d) face model 4
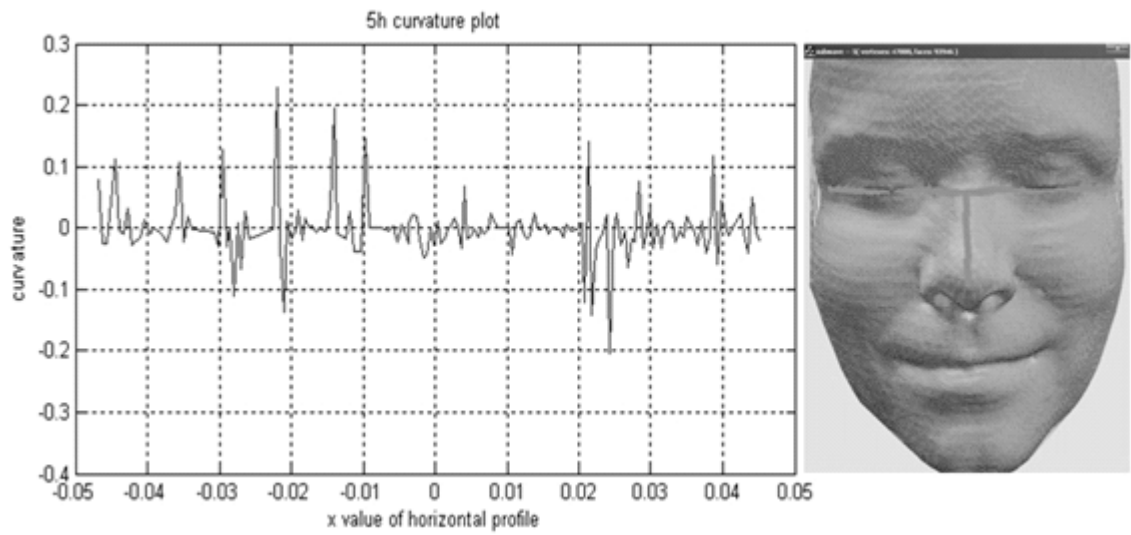
(e)
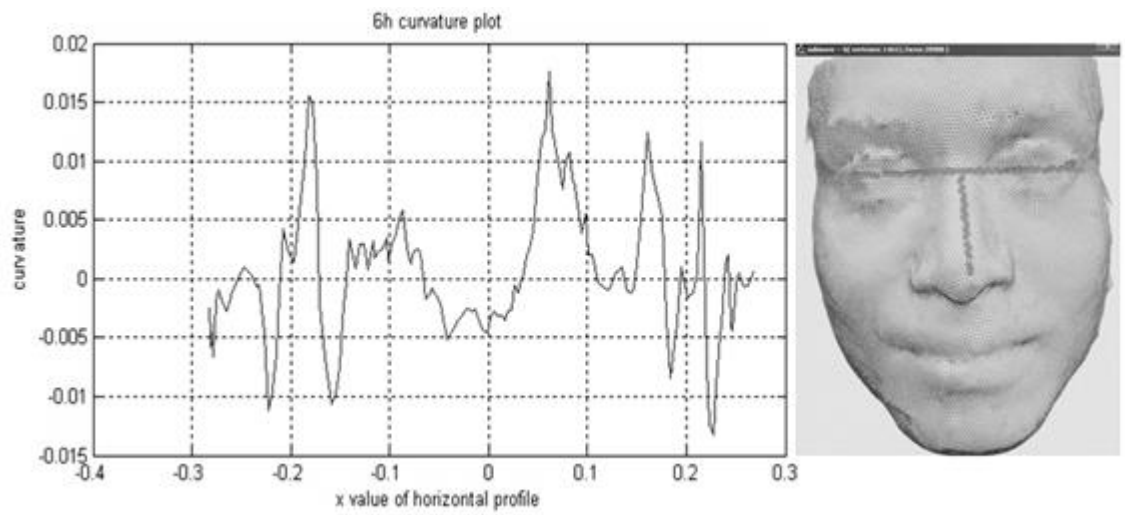
(f)

Fig. 3-13. Curvature plots of horizontal profiles cross eyes from (e) face model 5 (f) face model 6
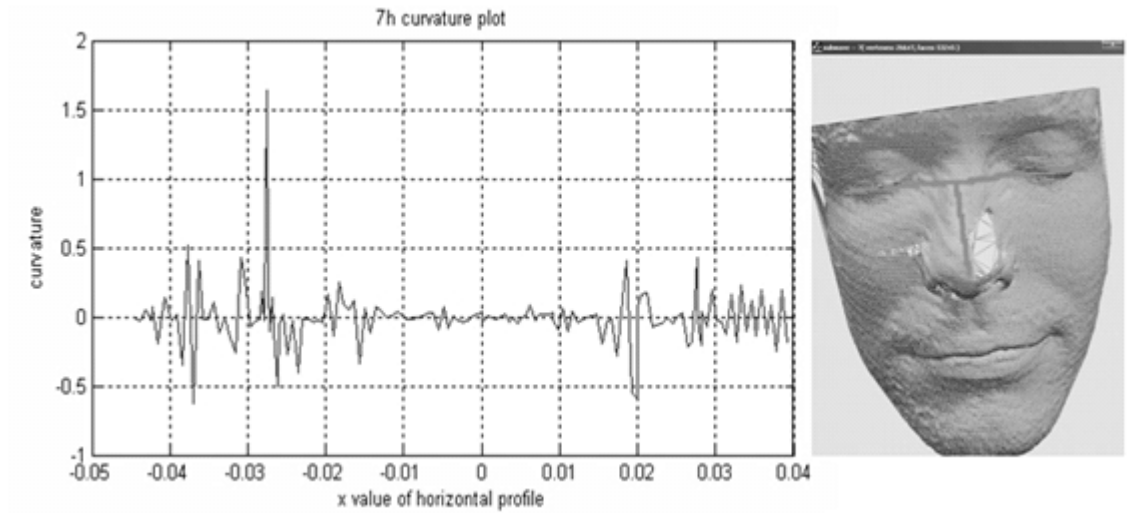
(g)
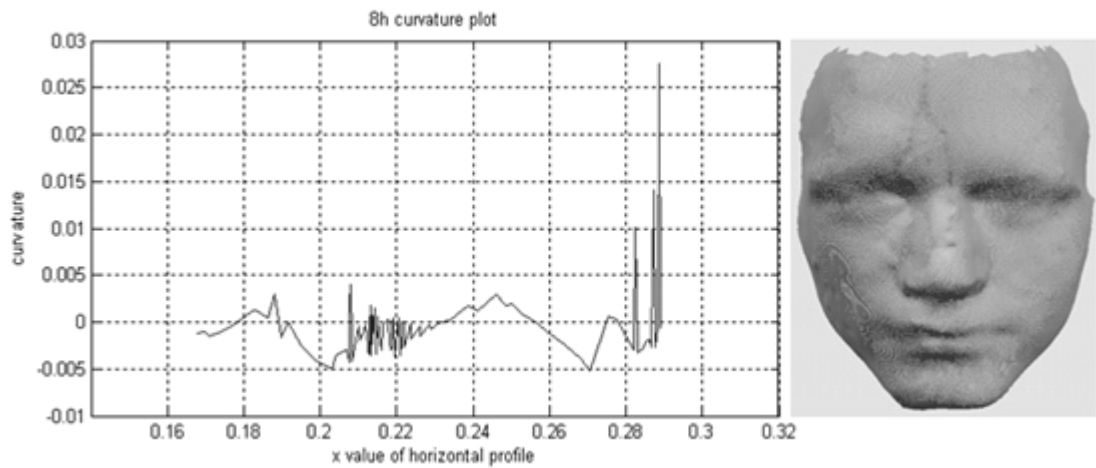
(h)

Fig. 3-13. Curvature plots of horizontal profiles cross eyes from (g) face model 7 (h) face model 8

In Fig.3-13, are included the horizontal profiles curvature plot on the left and the corresponding face model on the right. It gives the curvature shape of horizontal profile in the direction from P_1 to P_2. Obviously in the presence of shapes, we can tell they are from different face models. However, practically it is believed that two slightly different face models from one particular face can be derived at different times. Moreover, due to

smaller numbers of vertices in face models 4, 6 and 8, their curvature plots generate low frequency compared to others'. High frequency in curvature plots is possibly due to either noise or large number of vertices. Regarding to peak and valley values, peak numbers are far bigger than absolute values of valley numbers because peak numbers sit on convex surface.

In contrast to face models' intrinsic characteristics, the peak values of curvature plots corresponding to eyes region points and the shape of curvature plots are roughly symmetrical. Peak values reflect the actual shape through central profiles of eyes. It accounts for the fact that the eyes region is comparatively more curved. It is worth pointing out that for each plot, the shape around the point that x equals to zero slightly varies. It illustrates that curvature of the mid-eyes region is low. Moreover, the range of the curvature plot is also a key factor for face recognition.

Table 3-1. Curvature range comparison

Face model Index	Curvature valley value	Curvature peak value
Face model 1	-0.8	0.8
Face model 2	-0.3	0.4
Face model 3	0.4	0.6
Face model 4	-2	5
Face model 5	-0.4	0.3
Face model 6	-0.015	0.02
Face model 7	-1	2
Face model 8	-0.01	0.03

As shown in these plots, the curvature for face model 1 is in the range of [-0.8, 0.8], for face model 2 is in the range of [-0.3, 0.4], for face model 3 is in the range of [0.4, 0.6], for face model 4 is in the range of [-2, 5], for face model 5 is in the range of [-0.4, 0.3], for face model 6 is in the range of [-0.015, 0.02], for face model 7 is in the range of [-1, 2], and for face model 8 is in the range of [-0.01, 0.03]. These ranges reflect the shape of the central profile through eyes in terms of Gaussian curvature. It is believed that the T shape profiles are comparatively insensitive to facial expression variations. For each individual, technically the shape of horizontal eye profile and its curvature are unique. Therefore, this range of curvature can be also regarded as a candidate for matching.

A particular example of a curvature plot is for face model 3, in Fig. 3-13 (c). The horizontal profile, however, deviates from the left central eye point. Consequently extracted profile accuracy can impact on curvature plots shape.

The affected factors for results are not only the profile deviation, but also the noises on the face models when scanning. Furthermore, face alignment and pose, as well as landmarks localisation for the purpose of the extracted profiles also influence it. In summary, these curvature plots corresponding to their horizontal profiles show the results as we expect. Once we have analysed the curvature plots of the horizontal profiles, we investigate the curvature of the vertical profiles starting from the nose bridge to the nose tip in the next sub-section.

3.6.3.2 Curvature plots for vertical profiles

1v curvature plot

Vertical profile from the nose bridge to the nose tip

(a)

2v curvature plot

Vertical profile from the nose bridge to the nose tip
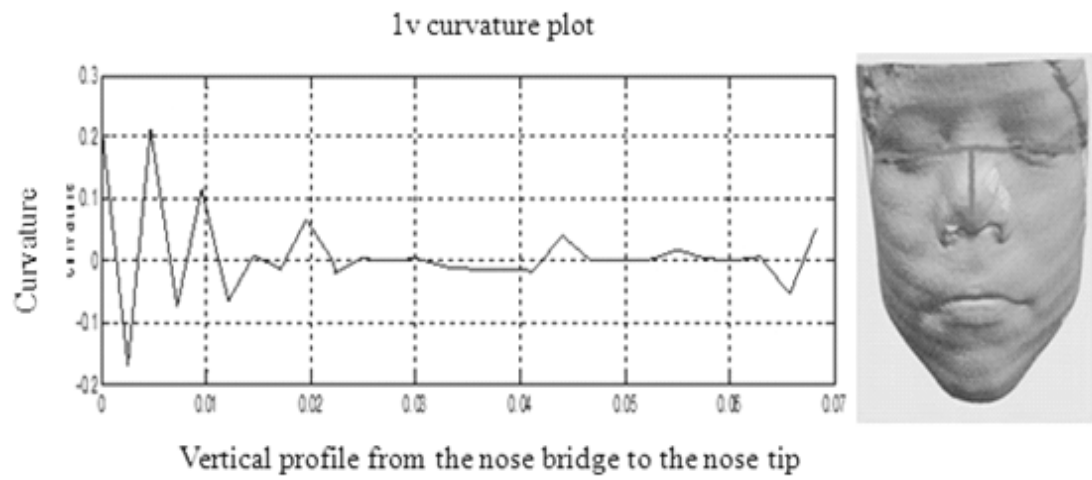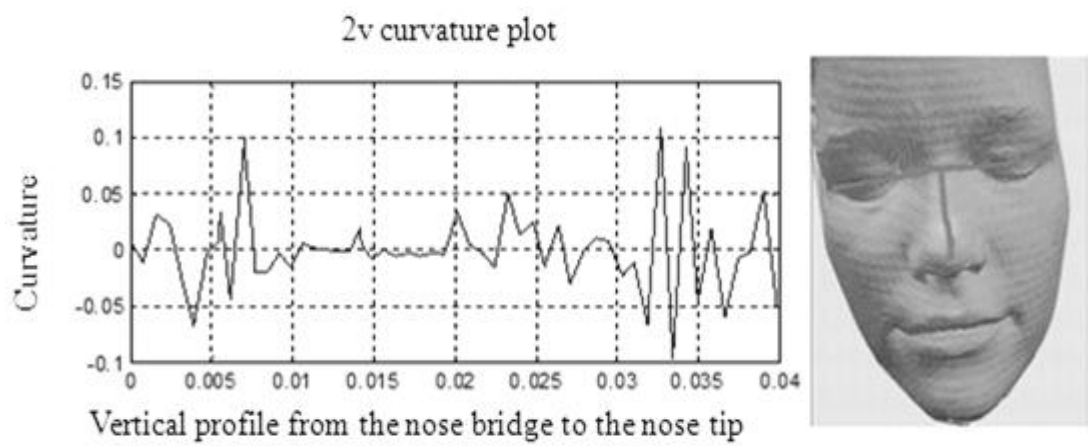
(b)

Fig. 3-14. Curvature plots of vertical profiles along from nose bridge to nose tip from (a) face model 1 (b) face model 2
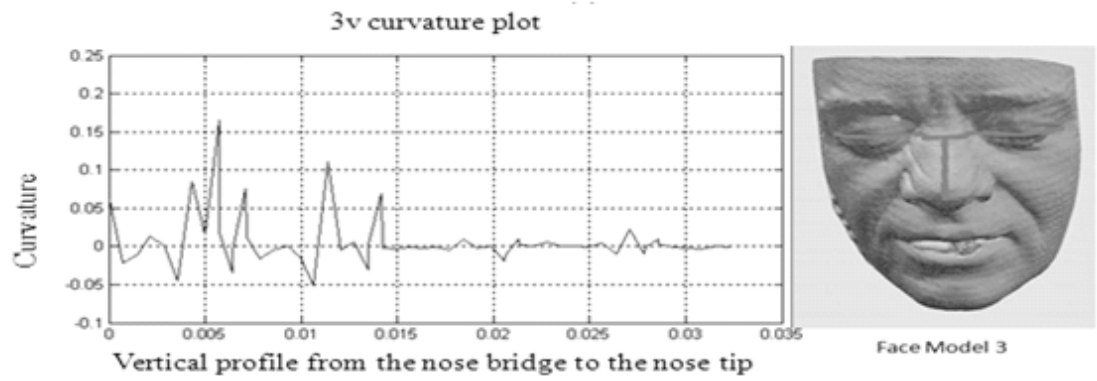
(c)
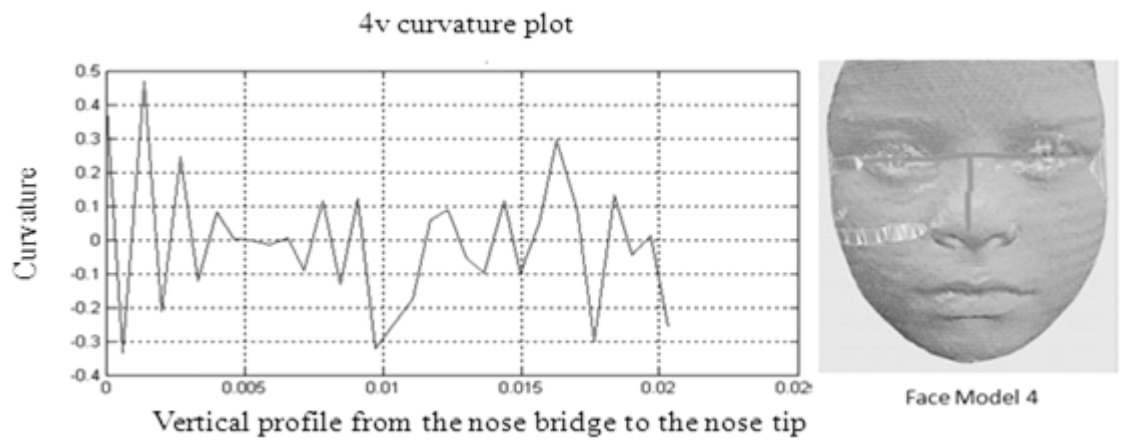
(d)
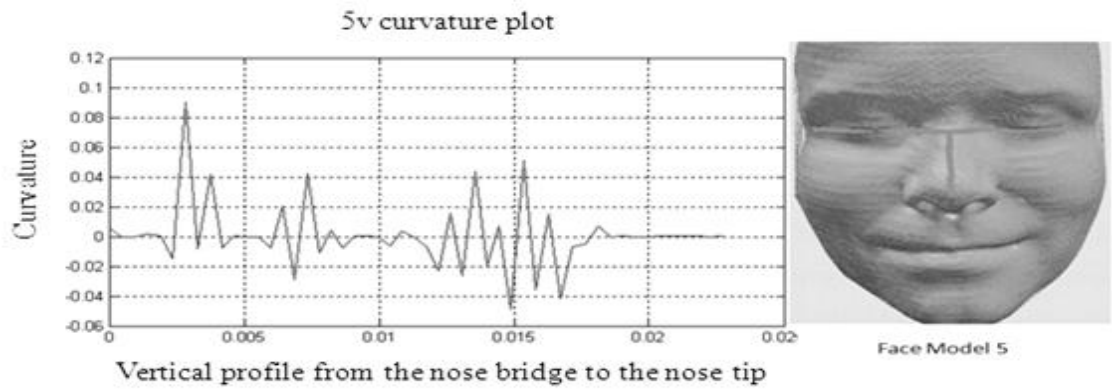
(e)

Fig. 3-14. Curvature plots of vertical profiles along from nose bridge to nose tip from

(c) face model 3 (d) face model 4 (e) face model 5
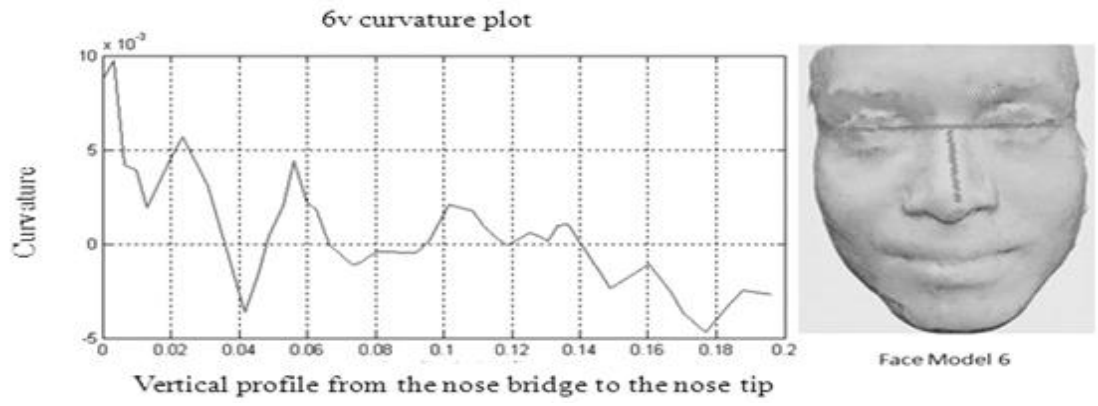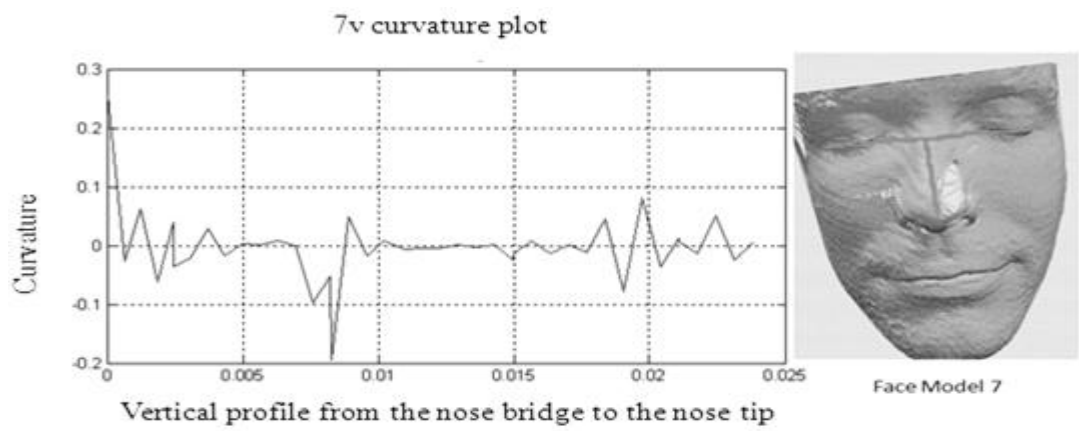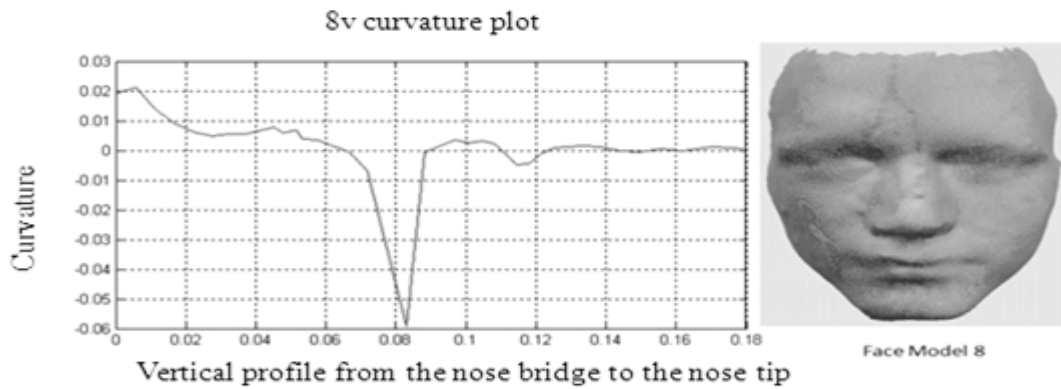
Fig. 3-14. Curvature plots of vertical profiles along from nose bridge to nose tip from (f) face model 6 (g) face model 7 (h) face model 8

In Fig. 3-14, are included the vertical profile curvature plot on the left and the

corresponding face model with vertical profile from the nose bridge to nose tip on the right.

These curves in the diagrams show the changing shape and range of curvature from nose tip P4 up to the mid-eyes point P0. Given that the curves start with the peak value, apart from face models 2, 3 and 5, in general, it obeys the condition that nose tip has the highest curvature along the vertical profile. In addition, from our observation, the curvature decreases from the nose tip to the mid-eyes point.

However, some unexpected cases occur, for example a big fall in the middle of the curvature plot for face model 8; curvatures for the nose tip of face models 1, 2, 3 and 5 are approaching zero. By analysing the number of vertices each face has, face models 1, 2, 3 and 5 have far denser images than others. This yields a displacement of the nose tip. Small changes of the nose tip can cause a large decrease in performance. Finally it disrupts extraction of the features and causes an unexpected result that the highest curvature of the vertical profile is not obtained on the nose tip. Thus, in those cases possessing various conditions are common in practice, such as small errors in localisation, and different levels of the noises, a recognition error is almost certain to result.

To summarise, the curvature-based method using the T shape profiles is promising for recognising faces although the database of eight face models is limited. In fact, the computational cost is comparatively low since our curvature-based method reduces face information to the T shape profiles for efficient face recognition. It has been showed that the curvatures of the T shape profiles are unique to each individual and it

can characterise the face models. In fact, it is necessary to evaluate our proposed method on a large database.

3.6.4 Experimental Results

Our curvature-based face recognition method using the T shape profiles is evaluated on GavabDB and BU-3DFE databases. We standardise the T shape profiles by selecting thirty points to compose the horizontal profile, and fifteen points to compose the vertical profile. The accuracy of the matching method is measured based on the Euclidean distances in order to find the nearest matching between the probe image and the gallery. The recognition rates of GavabDB and BU-3DFE are 90.3% and 91%, respectively.

Some researchers have developed face recognition methods on neutral faces. Table 3-2 summarises recognition rates of our curvature-based method in comparison with other existing methods. Chang et al. [57] achieve their highest recognition rate of 96.6% using multiple overlapping regions around the nose. However, complex computation accompanies the high recognition rate. In fact they compute curvature at every single point of the faces in order to detect landmarks on faces. Additionally, larger database leads to the higher recognition rate. In their experiment, a collective database of 546 subjects is involved and a total of 4,485 face images are implemented. Thus, more computation and a large database lead to the highest recognition rate. In terms of the database we used, we compare our method to the method of Mahoor et al [6] because we implement our methods on the same database. They achieve comparatively a higher recognition rate than ours. However, our method does not require some processes in

such a way that we reduce the computational time. In their method, a preprocessing of the database is involved, i.e. using filters to remove spikes, smoothing the face models, filling the gaps. Spikes and noises occur in the dark area, like inside mouths and nostrils. Taking this into consideration, there is no need for our curvature-based method to employ these processes. In addition, it is worth noting that their ridge image with contour lines is built by finding the points which have maximum principal curvature. They create a ridge image for each involved image, both a given image and an image in the gallery. There is no doubt that this process increases computational time. Among these methods of face recognition on neutral faces, there is another study based on the same database. Moreno et al. [17] achieve the lowest rate of 78% using thirty-five feature sets. In summary, our system achieves an acceptable recognition rate of 91% which employing a smaller feature set.

Table 3-2. Our curvature-based face recognition method in comparison with other existing methods

Authors	Database	Feature sets	Number of Vertices on a whole face	Recognition rate	speed
Chang [57]	Collective database of 546 subjects	Overlapping regions around the nose	Varies due to its big collection	96.6%	N/A
Tang [125]	BJUT-3D	Whole face based on normal and depth info.	200,000	95.6%	N/A
Li [126]	FRGC v2.0	Whole face deformation model	4500 after resampling	93.3%	N/A
Li [9]	CASIA	300 geodesic distances between all pairs of the 25 points around nose region PLUS upper face		91.1%	N/A
Mahoor [6]	GavabDB	Contour lines	13,000	93.5%	1.275 seconds on a PC Intel Core Duo 1.86 Ghz processor
Heseltine [127]	York Uni.	Combine various measurements on whole face	5000-6000	91.8%	Face alignment
Our curvature-based method	BU3D-FE	45 dimension	8000	91.0%	N/A
Our curvature-based method	GavabDB	45 dimension	6000 after cropping face	90.3%	N/A
Gupta [128]	105 subjects	300 dimension of features		89.9%	N/A
Moreno [5]	GavabDB	35 feature sets	2186 vertices	78%	N/A

3.7 Conclusions

In this chapter we have shown the curvature-based method of face recognition. First of all, our proposed method was evaluated on the V shape profiles. Once the feasibility of our proposed method has been proved, our feature sets, the T shape profiles were extracted from the region of the nose and the region of the eyes, respectively. We analysed the curvature plots of the profiles of the face models based on their shape and range variation, and the symmetry characteristic. The proposed method based on the T shape profiles proved curvature could characterise the distinct features on faces. Our propose method has been evaluated on two databases and achieved the reasonable and acceptable recognition rates. Thus, our curvature-based method reduced the face information to the two distinct profiles as our feature sets, which could characterise the face models. By using these minimum feature sets, our proposed method reduced the computational time and achieved a recognition rate of 91%.

Chapter 4 Gender Classification for Face Recognition

4.1 Introduction

There is no doubt that human beings have an amazing ability to recognise gender by simply observing a person's face. This is considered as an important aspect of human evolution and is involved in human face perception [63-64, 66-69, 129]. An important question remains is how gender is recognised by a human. As a basic task of face recognition technique, researchers have concentrated on developing techniques for gender classification since the 1990s. This is mainly because it is an important aspect of face recognition applications. In computer vision, pattern classification widely covers many research areas and gender classification is a typical pattern classification problem. To classify the gender, exposed face models are commonly used.

In this chapter, we present a novel method of classifying gender based on feature landmarks in the absence of the face alignment and normalisation in order to efficiently use the limited feature set to achieve a good classification rate. The employed multiple regions on 3D face models are determined from work on discriminative features between genders in the face surgery area. Combined with the adopted method, the proposed gender classification utilises the new geometric descriptors of area and volume to describe the multiple regions because the area and volume are the optimal descriptors based on the demonstration in the method. Our aim of fast computation is not only resulting from the limited feature set we used, but also from the term 'ratio of denominator' we introduced. More specifically, the ratio of denominator applied to the descriptors of area and volume is to eliminate the preliminary processes of face

alignment and normalisation in order to improve the computational time. The classification rate is achieved by SVM classifier with RBF kernel.

4.2 Problem Domain and Objectives

Some progress has been made on the gender classification area over the last two decades based on 2D face intensity images [81, 130]. They prove that SVM classifier produces significantly better results than other classifier techniques. However, most of the works are based on 2D intensity work and gender classification on 3D geometric models remains unexplored. Therefore, 3D facial models become the main experimental subjects in order to achieve this task of gender classification with a more advanced technique at lower computational cost. However, how to extract intrinsic and discriminative features of facial surfaces to classify gender becomes the primary objective because the feature set used for classification is the foundation of the classification and can affect the classification accuracy. The 3D geometric features represent the facial surface structure associated with the specific facial gender. Traditionally, people utilise the global face model (the whole face image) to achieve this task. In our proposed method, the significances of multiple sub-regions are considered with respect to the internal features. In addition, most gender classifications involving the face alignment and normalisation make the computation complex. This is considered as another issue to be solved in our method.

Motivated by these issues, in this chapter, we generate a 3D gender classification by proposing a novel method based on multiple sub-regions extracted from 3D face models. This chapter essentially has three key contributions. Firstly, rather than extracting key

points that other systems employ, we achieve gender classification by analysing limited shape features describing five regions. The second contribution is that wisely, considering a 3D face recognition system as a 3D face recognition engine, by plugging in this gender classification method, the engine directly reduces the searching range. Thus the identification task is achieved by saving half the computational cost of what other systems use. Additionally, we do not rely on expensive preprocessing techniques such as face alignment and normalisation that other methods employ since our proposed method employs a ratio scheme.

4.3 Method of Discriminative Features

In [131], the basic differences between male and female faces are listed. By exploring them all, we understand the optimal features to be used in our study are necessarily very important gender markers. Among them, forehead is one of the most important gender markers. The ridge of bone that runs right across the forehead just above the eyes is usually far more pronounced in males, whereas females appear to be gently rounded overall with a fairly flat front. Male eyebrows tend to be fairly straight and thick, while females usually have a thinner shape. The female nose appears to be smaller, shorter and have a narrower bridge than that of the male. In addition, female cheeks tend to be fuller and more rounded. Last but not least, female lips are often fuller than those of the male, and in terms of the mouth's vertical distance, the female's is narrower than the male's.

4.3.1 Scale Invariant Measurements

In our proposed method for gender classification, we focus on 3D face data constructed

with the triangular mesh, as seen in Fig.4-1 (a). Methods of extracting prominent facial features which discriminate between the genders in humans are utilised. We extract these facial features by locating landmarks on selected multiple sub-regions of faces. The features broadly define the shape of forehead, eyebrows, nose, mouth and cheeks, as shown in Fig 4-1 (b).

(a)   (b)

Fig. 4-1. Illustration of sub-regions (a) a sample face model (b) discriminative multiple sub-regions on this face model

The invariant measurements of facial surfaces are an important goal in computer vision since facial surfaces are insensitive to orientation, is an important goal in computer vision. Some relevant work has been developed on this topic, describing various measures or ratios of distances, which are invariant with respect to projective and perspective transformations [132-133]. In our proposed method, by taking geometric invariants into consideration, the employed features are measured in terms of the ratio of the multiple sub-regions area and volume to those of the corresponding central face region, as shown in Fig. 4-2 (b). This central face region is determined by five landmarks, as shown in Fig. 4-2 (a). All the area and volume parameters will be represented as the ratios of the area and volume of the corresponding central face region. Our proposed method does not require the facial surface to be either aligned or

normalised because the 3D facial surface is insensitive to pose and free to transformations. By employing the ratio, their features are invariant without alignment in advance. SVM classifier with (RBF) kernel is applied to the ratio of the selected features to generate the gender classification results. A series of simulation results will be discussed later and an average error rate will be pointed out.

(a)   (b)

Fig. 4-2. Illustration of the central face region segmentation (a) five landmarks localisation before the central face region segmentation, outer eye corners, mid-eye points, nose bridge and outer mid-lower lip (b) face central region after segmentation

4.3.2 Localisation of Landmarks and Extraction of Features

To compare our method on localisation of landmarks and extraction of features to previous studies, the existing methods are discussed. Gender classification entails three stages: feature extraction, feature measurement and classification. Brunelli and Poggio [134] select 16 geometry features for their classification system, such as distance of eyebrow, eyebrows thickness and nose width. Samal et al [135] experiment much more about 406 geometric features.

Xu et al [136] demonstrate that with more and more geometric features taken into consideration, the classification performance rises steadily and significantly. The highest recognition rate is achieved when all eight geometric features are employed. Referring to a set of measurements defined by Farkas [137], and the MPEG-4 facial feature points definition [138], as shown in Fig.4-3, we define sets of landmarks for extracting multiple sub-regions. This process is achieved using MAYA tools.
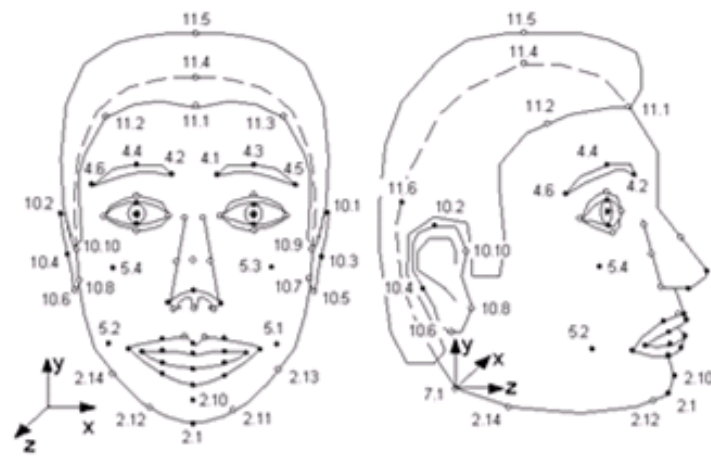
Fig.4-3. Facial feature points [15]

The landmarks for each region to be extracted are located manually. In Fig. 4-4, is shown the landmarks for each feature region. Each feature is extracted as a rectangular shape across the corresponding landmarks. The forehead landmarks and the hairline define the forehead region. The cheek region is determined by the vertical and horizontal profiles through the eye-corner point and nose wing end point separately. We only concentrate on one side of the cheek. The eyebrow region is extracted through the top and corner of eyebrow points and the eyes centroids. The nose region is defined by the bridge of nose (lowest point along nose), the end points of nose wings and the base point. The lip region is the rectangle through the top,

bottom and corner points of the lip. Each extracted feature is shown in Fig. 4-5.

(a)

(b)

(c)

(d)

(e)
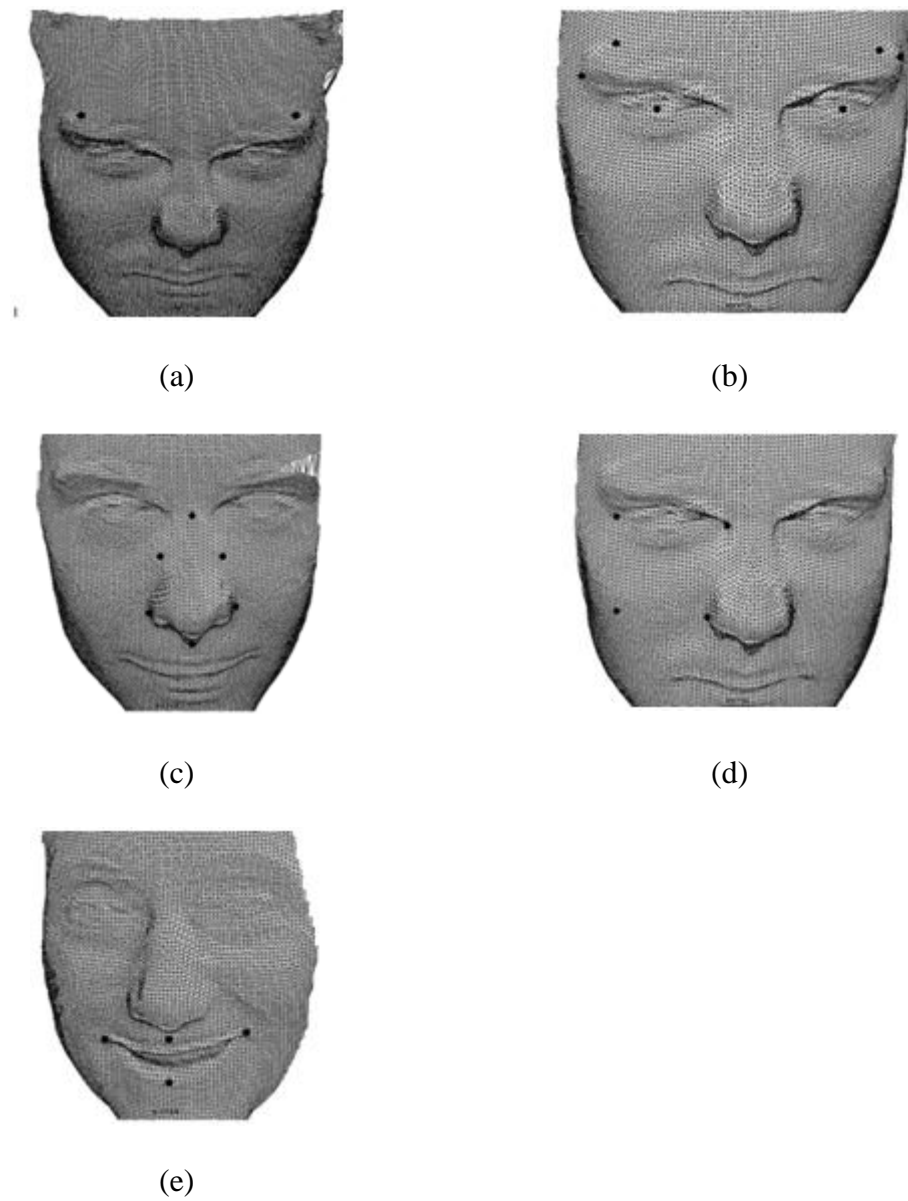
Fig. 4-4. Illustration of landmarks for individual sub-regions (a) forehead (b) eyebrow (c) nose (d) cheek (e) mouth

(a)

(b)

(c)

(d)

(e)
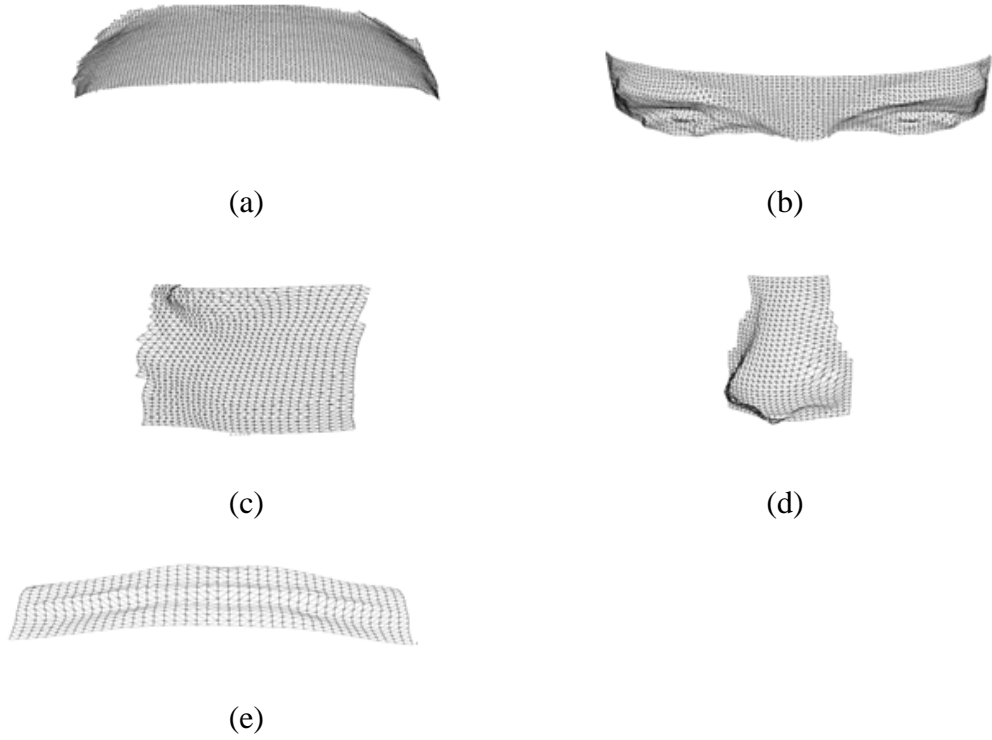
Fig. 4-5. Five extracted sub-regions from a face model (a) forehead region (b) eyebrows region (c) cheek region (d) nose region (e) mouth region

4.4 Measurements of Area and Volume

Face models with triangular meshes we use in our proposed method for gender classification can be considered as a particular non-closed polyhedral object of which each face is a triangle. In terms of area and volume, we access triangular meshes of which face models are composed.

In our study, we take volume and area of surfaces into consideration to measure face models' features. This is in contrast to other curvature, length and width measurements applied in some studies [68, 72, 92]. Our face models have been set up to have no self-intersection. The algorithm to calculate the volume and area of a closed,

non-self-intersecting polygon mesh is based on the Divergence Theorem from calculus [139]. The divergence theorem is commonly known as Gauss's theorem [139]. Given a differentiable vector field F defined in a compact region R which is simply connected, the volume integral of the divergence of F over R is,

$$V_R = \int S_R F \cdot N ds \tag{4.1}$$

where N is the outer unit normal to the boundary of R, S_R is the surface area of R. $F * N$ is the dot product of F with N, ds is the infinite element of surface area. The particular triangular meshes require $F = \frac{(x,y,z)}{3}$ and $div(F) = 1$ to be applied in formula (4.1). Thus the V_R becomes the volume of the region, so

$$V_R = \int \frac{S_R N ds}{3} \tag{4.2}$$

Given that the boundary of R is a list of polygon, we can approximate the surface integral with a Riemann sum. Let there be m polygons, the $i\text{-}th$ polygon having area A_i, normal $N_i = (U_i, V_i, W_i)$ and containing a point(X_i, Y_i, Z_i). For example, the point could be chosen as a vertex or centroid. Make certain normals all point outward. The volume is approximately

$$Volume(R) = \sum_{i=1}^{m} \frac{(x_i u_i + y_i v_i + z_i w_i) A_i}{3} \tag{4.3}$$

$$Area(R) = \sum_{i=1}^{n} area(P) \tag{4.4}$$

where n is the number of polygons, p defines an individual polygon. The approximate area is calculated by using each polygon area together.

Given six sub-regions and one central region, their measurements are computed based on formulas (4.3) and (4.4). These central region measurements are considered to use for normalisation in order to generate the ratios of area and volume of each sub-region to those of the central region. In such way, normalising are only applied to the utilised

area and volume rather than aligning raw face models at the preprocessing stage.

4.5 Comparison Results on Multiple Databases

We compared the classification rate of the proposed method on GavabDB with the BU-3DFE database. To investigate this, the experiments are done   iteratively five times for each database, where for every simulation, the training and testing data are set as follows: we take advantage of the fact that the male and female images in the GavabDB dataset are arranged in a random order. The experimental results are estimated with five-fold cross validation, i.e. a five-way dataset split, with four-fifth of the database used for training and one-fifth of the database used for testing, with four subsequent rotations as the other four simulations. The average size of the training set is 48 (38 males and 10 females) and the average size of the test set is 13 (7 males and 6 females). The first 13 images are selected as a training set, leaving the rest of 48 images as a testing set for one simulation. The second simulation uses the last 13 as a training set. The other three simulations randomly select 13 images three times as training sets from the middle of 35 images, therefore allowing all the images to be tested at least once. Evaluating our proposed gender classification method with this five-way cross validation is due to the realistic training proportion of 11% to 22%. We set female 0 and male 1 for SVM classifier with the RBF kernel. The SVM parameters are heuristically set prior to actual training and testing.

We also conduct the experiment on BU-3DFE database which contains 56 female and 44 males. It is necessary to randomly select 80 individuals in which the same amount of females and males are assured for each simulation. Similarly in GavabDB, this database

is split into the training set of 80 individuals and the test set of 20. We assure that for each simulation each individual that appears in the training set is excluded from the corresponding testing set in order to meet the realistic scenario in practice.

The classification is performed by SVMs, which is known as a superior method when compared to traditional pattern classifiers in solving the problems of gender classification [81]. In the context of pattern classification, the training principle is to find the optimal hyperplane that separates the positive and negative samples with maximal margin. In [81, 130], they claim that SVM outperforms the rest when dealing with gender classification. In particular, Moghaddam et al [81] investigate SVM classifier performance with various kernels and find out that Gaussian RBF kernel performs the best in terms of error rate. Thus, SVM with RBF kernel is determined to classify gender.

In SVM classifier, a 61*10 matrix for GavabDB contains, in particular, the area and volume ratios corresponding to the forehead, nose, eyebrows, cheek and lips features. Another 100*10 matrix built for BU-3DFE contains, in particular, the area and volume ratios corresponding to the forehead, nose, eyebrows, cheek and lips features. The error rates of all the simulations tested with 61 facial geometry meshes are reported in Table 4-1. Comparatively, the error rates of all the simulations tested with 100 individuals are reported in Table 4-2.

Table 4-1. Classification rates on GavabDB

Experiment	Error rate		
	Male	Female	Overall
E1	17.05%	19.88%	18.23%
E2	15.95%	18.73%	17.39%
E3	17.84%	14.56%	15.89%
E4	18.43%	17.45%	17.91%
E5	15.24%	19.63%	17.80%

Table 4-2. Classification rates on BU-3DFE

Experiment	Error rate		
	Male	Female	Overall
E1	12.50%	8.33%	10.42%
E2	11.11%	9.09%	10.00%
E3	10.00%	10.00%	10.00%
E4	18.18%	11.11%	14.65%
E5	11.11%	9.09%	10.00%

From Table 4-1, it is clearly seen that E1 has the highest error rate whereas E3 has the lowest. Regarding to the error rate of 17.44% using five-fold cross validation, it is a comparatively acceptable error rate when compared to other existing gender classification results. The main reasons for these errors are possible due to face geometry noises, beards, fuzzy boundary and uncertain landmarks location.

In Table 4-2, the average error rate of 11.01%. There is no doubt that the error rate of

BU-3DFE database is lower than that of GavabDB. This is probably due to two reasons, which are, firstly that BU-3DFE is composed of almost twice the number of individuals as that of GavabDB; secondly, 83 feature points defined on the face models in BU-3DFE enhance sub-regions extraction without losing useful information as the fact of locating features points on geometry models is more complicated than that on textured models.

Table 4-3. The classification rates of our proposed method

Database	Classification Rate
GavabDB	82.56%
BU-3DFE	88.99%

Table 4-3 summarises the classification rates of 82% and 88% on the two databases. However, the classification rates are higher than 90% in other studies, which are described in the literature review. One possible means to improve the classification rate is to use addition feature sets. For example, distance-based features on face models may carry useful information about the face size and shape. Thus, an adjustment is introduced to modify the gender classification. Taking advantage of 83 landmarks in BU3D-FE database, as shown in Fig. 1-8, we evaluate the distance-based features between these 83 landmarks. We use this set of 83 landmarks because they have the discriminating power. Based on the fact that two distinct points induce one distance, these landmarks are used to construct around 3000 distances. Regarding to the male and female categories, two mean distances are computed for the male and female sets, respectively. They are employed in the gender classification along with the other five features in order to improve the classification rate. For example, when a given image

has been classified into the male set, this adjustment will be used to reassess the result of the given image. By comparing it to the female and male mean distance-based features, the given image may be either corrected to the right set or proved to be already successfully classified. By introducing this adjustment in the gender classification, it results in the correction of 5% to 10%, as shown in Table 4-4.

Table 4-4. Comparison of classification rates of our proposed method before adjustment and after adjustment

	GavabDB	BU-3DFE
Before adjustment	82.56%	88.99%
After adjustment	93.5%	95.1%

Table 4-5. Comparison of our method and other methods

Researchers	Method	Database	Accuracy
O' Toole [88]	Head structure, PCA	130 subjects, 65 female and 65 male	96.9%
Hu et al. [92]	Multiple regions as feature sets, PCA and SVM	590 male images and 355 female images	94.3%
Our proposed method	Measurements of multiple regions and an adjustment as feature sets trained by SVM	BU-3DFE 56 female and 44 male.	94.1%

Shen et al. [91]	SVM training pixels of depth images	123 subjects (96 males and 27 females)	92.95%
Our proposed method	Measurements of multiple regions and an adjustment as feature sets trained by SVM	GavabDB 45 male and 16 female	92.5%
Lu [89]	Multimodal gender classification using range images and intensity images, SVM	1240 facial scans of 376 subjects, 139 female and 237 male	91%

A list of methods of gender classification using 3D shape is given in Table 4-5. Based on this table, a set of strategies dealing with gender classification are observed. In terms of feature sets, the first strategy uses multiple regions. The second strategy uses all the points on the head structure and finds the projection coefficients by PCA. The third strategy employs 3D shape information and 2D intensity information of the whole face region. Interestingly, in terms of classifiers, it is observed that SVM is currently the best classifier.

4.6 Combination of Gender Classification and Curvature-based Method

We have evaluated our curvature-based method in previous chapter and our gender classification in this chapter. The performance of the combination of gender classification and curvature-based face recognition is investigated in this section. The

sequences of the combination are begun with the gender classification. The given image is first classified into male or female category. Then, the curvature-based method is used to match the find the match from the correspondent database (known as male or female database). Finally the decision is made and the recognition rate is compared.

Table 4-6. The recognition rates of our combination methods in comparison with other studies

Authors	Database	Feature sets	Number of Vertices	Recognition rate	Speed
Chang [57]	Collective database of 546 subjects	Overlapping regions around the nose	Varies due to it's a big collection of databases	96.6%	N/A
Tang [125]	BJUT-3D	Whole face based on normal and depth info.	200,000	95.6%	N/A
Li [126]	FRGC v2.0	Whole face deformation model	4500 after resampling	93.3%	N/A
Li [9]	CASIA	300 geodesic distances between all pairs of the 25 points around nose region PLUS upper face		91.1%	N/A
Mahoor [6]	GavabDB	Contour lines	13,000	93.5%	1.275 seconds on a PC Intel Core Due 1.86 Ghz processor
Our proposed method(gender+curvature)	BU3D-FE	51 dimension	8000	92.4%	N/A
Heseltine [127]	York Uni.	Combine various measurements on whole face	5000-6000	91.8%	Face alignment
Our proposed method(gender+curvature)	GavabDB	51 dimension	6000 after cropping face	91.67%	N/A
Our proposed method(curvature only)	BU-3DFE	45 dimension	8000	91.0%	N/A
Our proposed method(curvature only)	GavabDB	45 dimension	6000 after cropping face	90.3%	N/A
Gupta [128]	105 subjects	300 dimension of features		89.9%	N/A

Authors	Database	Feature sets	Number of Vertices	Recognition rate	Speed
Moreno [5]	GavabDB	35 feature sets	2186 vertices	78%	N/A

The results in Table 4-6 show the effect on the recognition rates of employing the gender classification. Firstly, employing the gender classification improves the final recognition rate. We begin with the database of GavabDB, the gender classification improves the recognition rate by 1.37%. The other database of BU-3DFE is observed to improve the recognition rate by 1.4% by using the gender classification. By the comparison of the results of GavabDB and BU-3DFE, there is a trend toward higher recognition rate with larger database size. Secondly, gender classification can reduce a substantial amount of search range in the database for the curvature-base method. If a given image is input, the given image is classified into the male or female category by the gender classification. For instance, with a database with N subjects, N_m male and N_f female, the saving in computational effort could be as much as $\frac{N_m}{N_m + N_f}$ or $\frac{N_f}{N_m + N_f}$, whichever is the larger. Once the corresponding category is determined, the recognition process can be achieved by matching the given image to the corresponding category for searching. If without the gender classification, the given image would be matched against all the images across the whole database.

4.7 Conclusions

We have presented a method based on geometric feature measurement for gender classification on 3D face models. The differences between males and females on facial surfaces are accounted for by area and volume geometry measurements instead of width, length and length geometry feature measurements. We introduced and evaluated ratios of multi-regions based on anthropometric and facial surgery research work using SVM with radial basis function (RBF) kernel The experiments have finally been made for

comparison between two databases in order to assess the method with respect to non-aligned facial surfaces in the database. Further studies were carried out in order to improve classification rates.

To improve the classification rate, we employed a distance-based adjustment and proved the robustness of this adjustment. Further work on evaluating the combination of the proposed gender classification and curvature-based face recognition has been extended, so that it demonstrated that the proposed gender classification can boost the proposed curvature-based method for neutral face recognition.

Chapter 5 Face Recognition under Expressions Using Curvature Methods and Neutralisation of Facial Expressions

5.1 Introduction

It has been noticed that face expressions can affect the accuracy and the performance of face recognition systems since the geometry of the face significantly changes as a result of facial expression. To deal with this challenging problem, some researchers have addressed the expression issue [16, 57, 102]. In particular, some existing methods rely on extracting stable face features, such as profile curves [140] and geometric invariants [141]. Even though 3D face recognition has achieved excellent results, it still encounters difficulty in handling facial expression variations.

The first aim of this chapter is to investigate the effects of the curvature-based method (Chapter 3) in face recognition under expression variations. The T shape profiles are considered as expression-invariants. Gaussian curvatures are employed as the descriptors of the 3D feature sets as these do not change when the surface translates or rotates. Thus, we employ the method for face recognition under expressions and find out its potential in dealing with expressions.

Another aim of this chapter is to investigate the neutralization of facial expressions of happiness in order to find out the distinct features for face recognition under expression variations. More specifically, the goal of this study is to determine the features that are distinctive and can be effectively used for 3D face recognition under expressions. This

study addresses this problem by investigating the expression-sensitive region due to a large amount of significant progress regarding the expression-insensitive region. It concludes that the feature points, for example mouth corners remain comparatively more stable after the neutralisation process. The proposed face recognition method in the presence of facial expressions relating to the neutralised feature sets will be showed and discussed in the next chapter.

5.2 Problem Domain and Objectives

It is claimed that the upper face is the expression-invariant region. Initially, our thought was that working on the expression-invariant regions and avoiding the expression-variant regions may be a solution to the problem of expressions. In fact, our curvature-based method (Chapter 3) is working on the expression-invariant region. Our concern was how well the curvature-based method using T shape profiles, considered as expression-invariants, helps face recognition under expression variations. Another concern was how to collect the relevant features from the facial images for face recognition under expression variations and determine a set of fast computation geometric descriptors. Furthermore, evaluating the significance of the features, which are sensitive to expression variations, is the other concern. Once the feature sets are determined, another objective is to find out the optimal model to learn the relationship of the feature sets between expressions and neutral. Finally, in an attempt to avoid face models preprocessing to reduce the computational time, we use additional distance-based descriptors for the purpose of normalisation.

With the outcomes above, our aims in this chapter are to, firstly investigate the act of

curvature-based method in dealing with expressions, secondly neutralise the feature sets by modeling the relationship between faces with and out expressions. We are motivated by two factors to achieve the first aim. Firstly, although facial expressions are complicated, human faces have limited deformation. In fact, while an expression occurs on 3D face models, the nose and eyes region are invariant to expressions; their lower faces (the mouth) vary to expressions. In our case, the T shape profiles employed in our proposed curvature-based method lie in the upper region, which is considered as the expression-invariant. Secondly, a valuable observation is that there exist some geometric features that are relatively invariant to expressions. It is observed that the curvatures at the T shape profiles do not change much while a face model yields expressions due to the limited stretch of the nose and the eyes. Thus, our proposed curvature-based method will be evaluated to deal with face recognition under expression variations. In order to achieve the second goal, we carry out an initial study of features determination in the specific expression-sensitive region, i.e. the mouth region. To achieve this, it is considered to find the variations between expressions and neutral cases. The initial study is described in the section of neutralisation.

5.3 Curvature-based Method for Face Recognition with Expressions

In this section, our proposed curvature-based method using T shape profiles is employed in order to investigate its face recognition performance under expression variations.

5.3.1 Experiments and Results

In the following, we present the results obtained with the proposed method. In the experiments, with 5- fold cross-validation, our proposed method is evaluated on the two databases, GavabDB and BU-3DFE, respectively. The face images with neutral expressions are in the gallery set and the face images with various expressions are in the probe set. Prior to the final results, we extract the T shape profiles on the face models with expressions, as shown in Fig. 5-1 and Fig. 5-2.

(a)

(b)

(c)

(d)
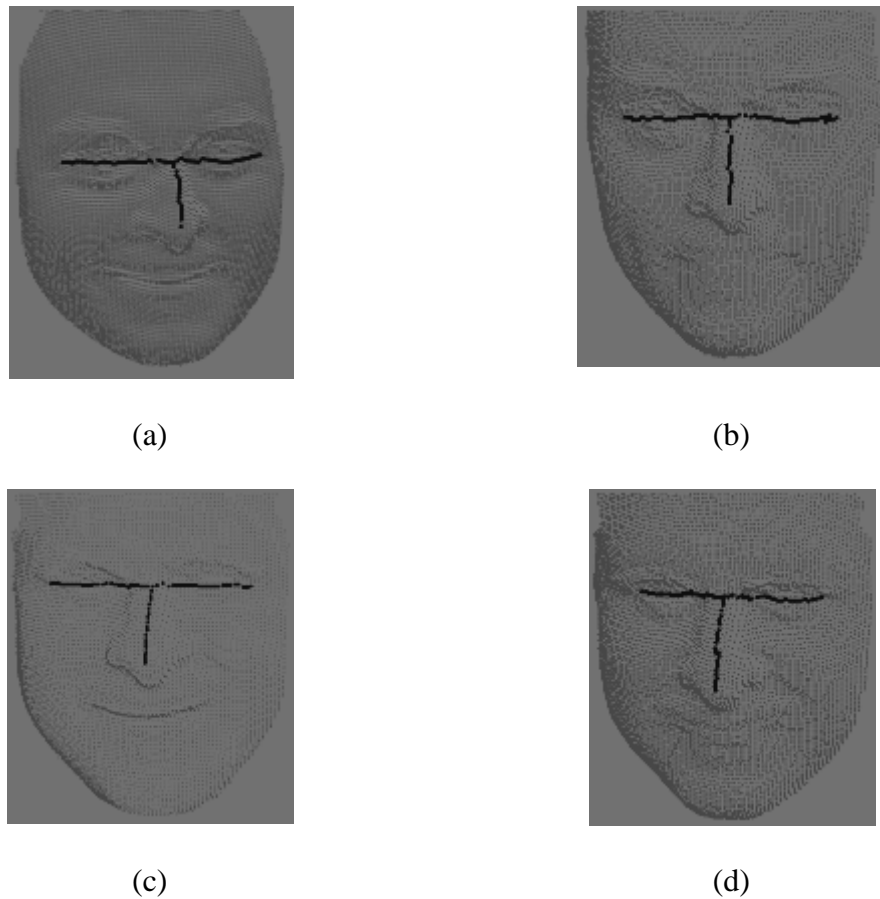
Fig. 5-1. The T shape profiles of two random subjects in GavabDB. One random subject (a) of laugh (b) of neutral. The other random subject (c) of laugh (d) of neutral

(a)   (b)   (c)

(d)   (e)   (f)
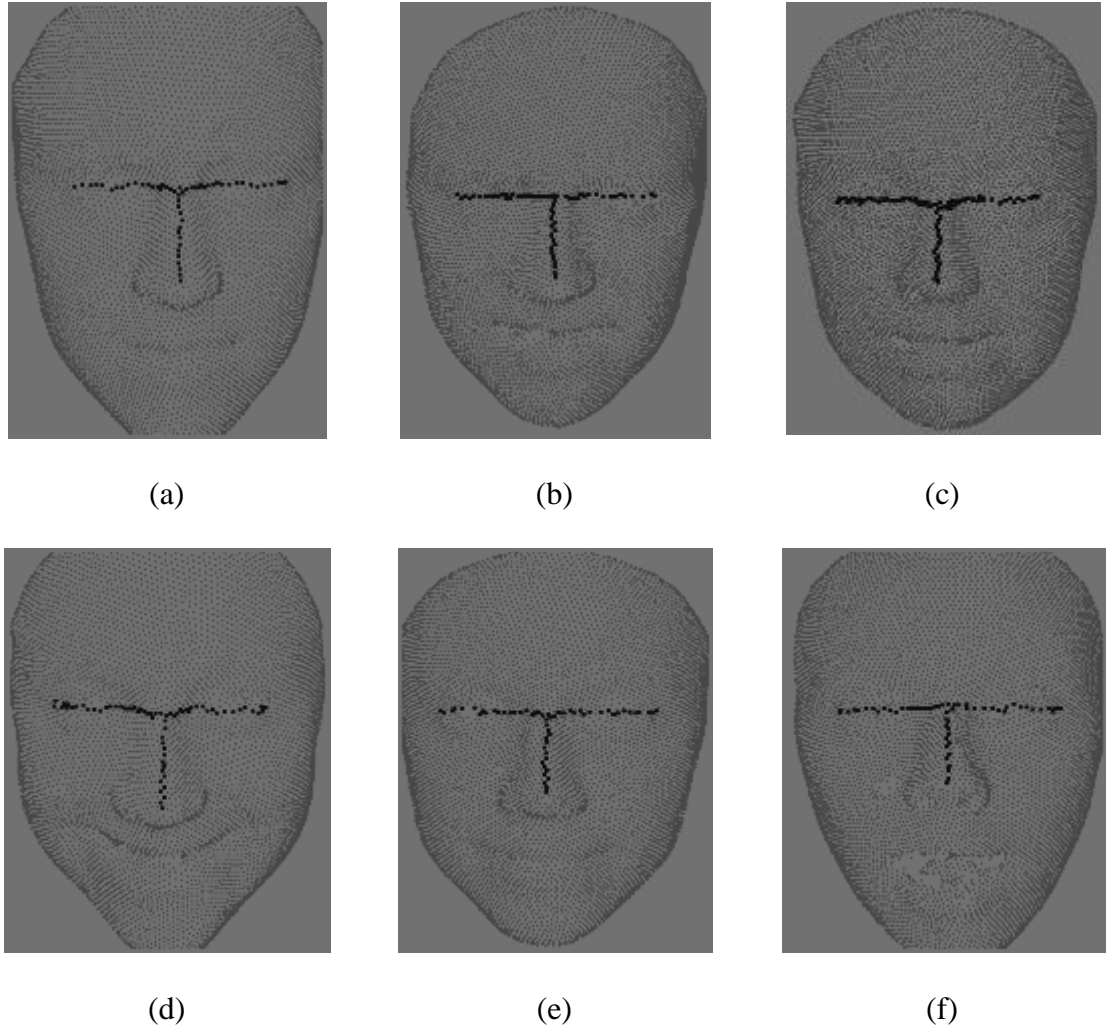
Fig. 5-2. The T shape profiles extracted on the face models of the six significant expressions (a) angry (b) disgust (c) fear (d) happy (e) sad (f) surprise

Fig. 5-1 illustrates the T shape profiles on the neutral face models and the expression face models of two random subjects. While Fig. 5-2 illustrated the T shape profiles on the six significant expressions face models of one particular subject. It is observed that the T shape profiles lying in the expression-invariant regions (the eyes and nose) do not change much under expression variations. In contrast, the cheek and mouth regions vary comparatively much under expression variations. Once we have visualised the T shape profiles, next, we will visualise the curvature plots of the T shape profiles under

108

expression variations, as shown in Fig. 5-3.
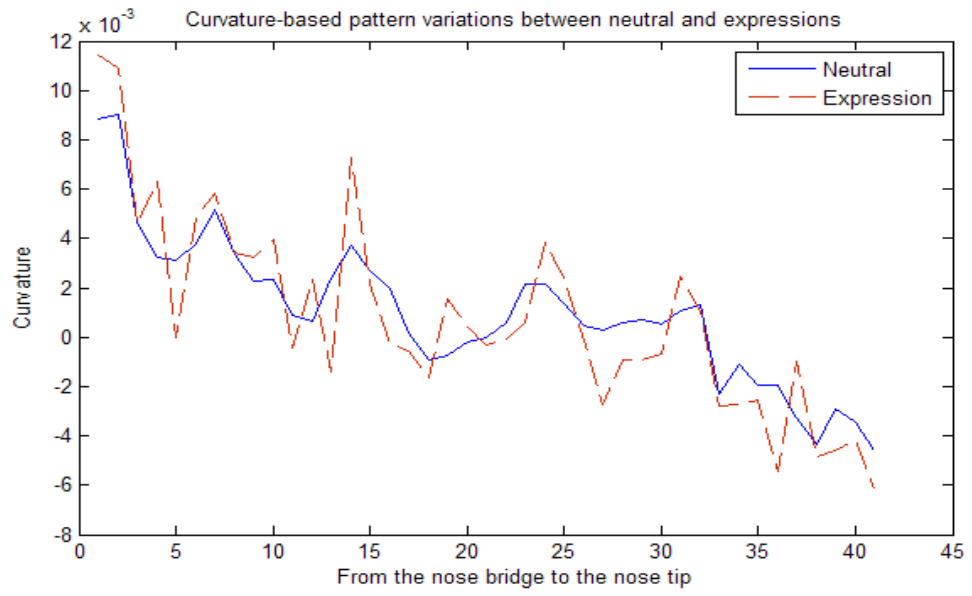
(a)
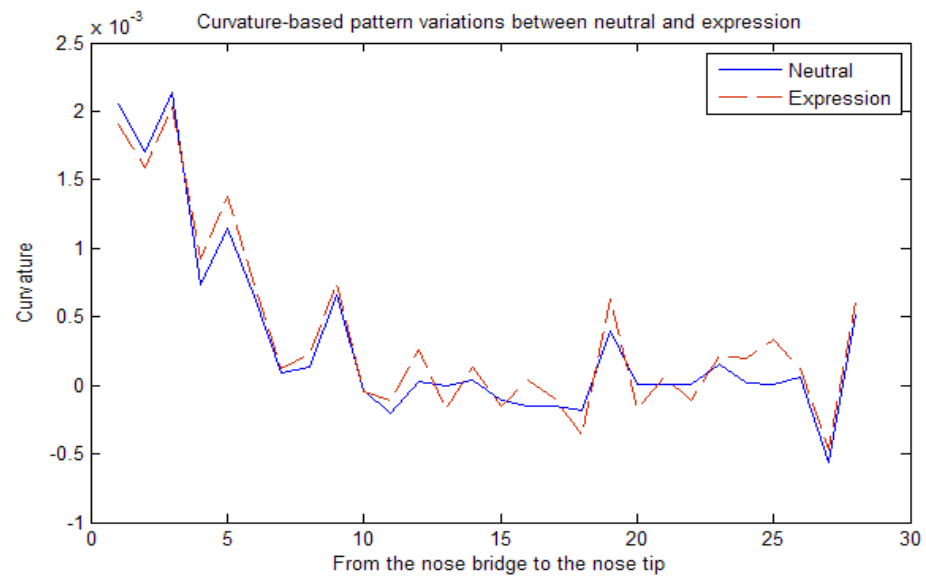
(b)

Fig. 5-3. Samples of curvature plots variations between neutral face and expression

(a) vertical profile (b) vertical profile
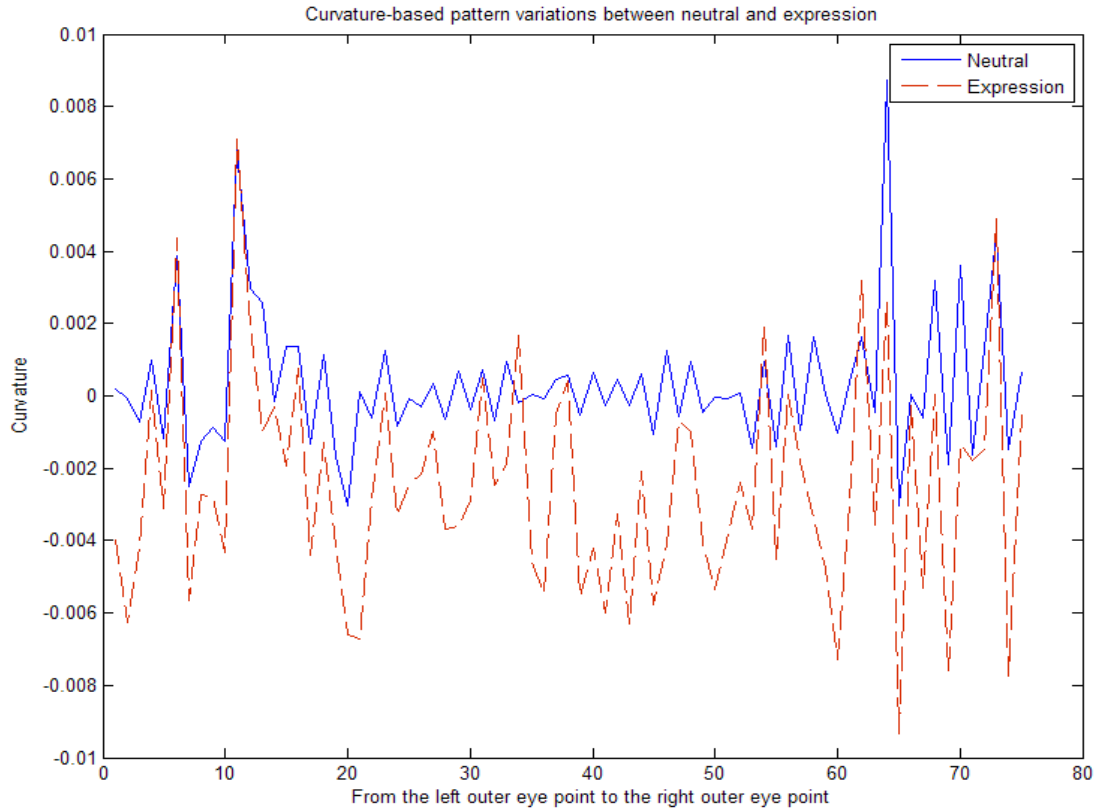
(c)

Fig. 5-3. Samples of curvature plots variations between neutral face and expression

(c) horizontal profile

In order to further investigate the variations of the profiles between neutral and expressions, we select a few curvature plots of random sample subjects. More specifically, the pattern variations of the curvature-based plots between neutral (blue) and expression (red) are shown in the Fig. 5-3. The pattern variations are analysed into two categories, the vertical profile and the horizontal profile. Fig. 5-3 (a) and (b) illustrate the vertical profiles starting from the nose bridge to the nose tip, while Fig. 5-3. (c) illustrates the horizontal profile starting from the left outer eye to the right outer eye. It can be observed that the vertical profiles vary less under expression variations than the horizontal profiles. In particular, we analyse the pattern variations in Fig. 5-3 (b). As

expected, the pattern variations show the reasonable variations between neutral and expressions. The curvature plot on expressions presents the approximate patterns of the curvature plot on neutral. Also these two curvature plots are in the same range. Although the curvature values on each individual vertex are changed when expression are produced, these subtle variations do not affect the results of matching for a couple of reasons. One is the patterns are roughly the same when neutral and expressions, the other reason is the curvature values, known as the patterns, are unique even when non-neutral expressions.

Table 5-1. Recognition rates of our proposed method in comparison with other methods

	Our proposed method		Alyuz [94]	
Database/Region	GavabDB	BU-3DFE	Eye	Nose
Recognition rates	85.78%	86.50%	88.25%	85.93%

The recognition rates achieved by our proposed curvature-based method in comparison with other methods are listed in Table 5-1. By observing the experimental results, the proposed method achieves the recognition rate of 85.78% on GavabDB, 86.50% on BU-3DFE. Using the point sets, Alyuz achieve the recognition rate of 88.25% on the local region of the eyes, 85.29% on the local region of the nose. In fact, Alyuz has investigated other regions and the fusion of the regions, i.e. the cheek, the chin. He claims that, as the individual regions, the eyes and the nose produces higher recognition rates than the cheek and chin regions; and the combination of these regions outperforms others in terms of the recognition rates. In order to compare to our proposed method, we only focus on his results on the eye and nose region.

Based on the comparison between databases, the proposed method achieves a higher recognition rate on BU-3DFE than GavabDB because one subject has more than one image stored into the gallery data set. It was found out by Faltemier et al. [142] that by using a gallery composed of multiple images of each individual subject it is possible to achieve higher performance. Besides, BU-3DFE has a larger number of subjects than GavabDB. Based on the comparison between our proposed method and the method generated by Alyuz, he achieves a better recognition rate with the eyes region. An investigation of this case in which our recognition rates are lower, shows that it is mainly due to the displacement of the landmarks determining the T shape profiles. Although our recognition rates are comparatively lower, we use much smaller feature sets and reduce the computational time. Besides, we have investigated the application of the curvature-based method using the T shape profiles in handling the problem of expressions and pointed out its potential to handle expressions.

Although its promising start to deal with expressions has been proved, the recognition rates still need improvement. Face recognition under expression variations become challenging due to the deformation of the face geometry by expressions. To solve the deformation, neutralisation is a possible solution. We will find out how the neutralisation will support face recognition under expressions next.

5.4 Processing Faces with Expressions

Most of the research work has been focused on the expression-invariant regions, i.e. the upper face, in order to solve the problem of expressions. In particular, Bronstein et al.

[14, 141] make an assumption that the mouth is closed in all expressions. However, this constraint is not practical or realistic. Chang et al. [57] match individually multiple regions around the nose and integrate individual matching to build a final matching. They claim that the nose is the most stable and reliable region on face models during expression changes. The recognition rate, however, is around 80%, which needs improvement. A gap has been observed that there has been no investigation of the expression-variant region, i.e. the lower face. This will be the target of the initial study of face expressions neutralisation. In order to learn the variations of the mouth region according to changes in expression, we neutralise the mouth region by partitioning it into multiple sub-regions so that the upper and lower lips can be learned individually.

5.4.1 Partition of Mouth Region

To neutralise the mouth region, we consider partitioning it into multiple sub-regions by hierarchical sampling. Human faces can be represented by a fiducial set of landmarks defined in Farkas [137]. To achieve our task, a fiducial set of landmarks (thirteen landmarks including two mouth corners) along the middle line of the mouth region, as shown in Fig. 5-4, are located to form the first layer of the hierarchical sampling, as shown in Fig. 5-5. From our observation, the movement of the different parts of the mouth region varies during changes in expression, i.e. the upper lip and the lower lip, the different parts of the upper lip, and the different parts of the lower lip. This is why we make the decision to locate the landmarks in the middle of the mouth region to neutralise the upper and lower lip separately. Furthermore we locate the landmarks along the upper lip and lower lip to neutralise the sub-regions individually.

(a)   (b)
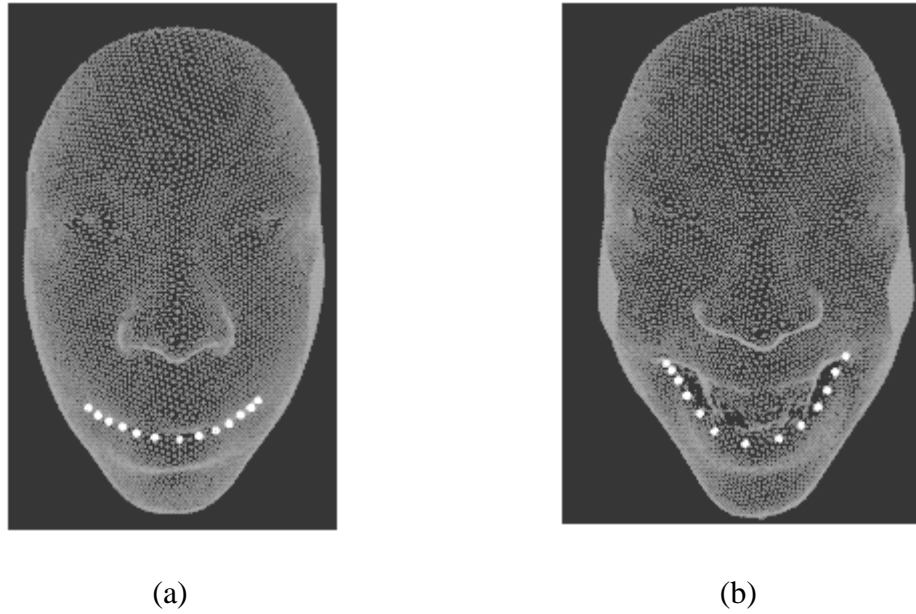
Fig. 5-4. Landmarks in the middle of (a) neutral face of a sample subject (b) laugh face of the same sample subject

In Fig. 5-5, the hierarchical sampling from the fiducial landmark set (first layer) to the final sampling of the sub-regions (final layer) is shown. In order to partition the mouth region into twelve sub-regions, the fiducial set of landmarks comprising the nose tip, two mouth corners and three sets of eleven landmarks along the top, middle and low mouth respectively, are considered as constraints and the first layer in the hierarchical partition, as shown in Fig. 5-5 (a). The second layer is determined by the first layer. The geodesic path through the nose tip, the landmark of the top mouth and the corresponding landmark of the low mouth, is derived by finding the intersection between the plane of these three points and the facial surface. By reconstructing the intersections, the thirteen geodesic paths comprise the points on the mouth. The points on eleven geodesic paths are indicated by vertical lines and marked in red, as shown in Fig. 5-5 (b). The points on the paths are used as newly extracted points for the next layer. The third layer of landmarks is constructed based on the newly extracted points

from the second layer. In particular, the two sub-regions adjacent to mouth corners are constructed by computing a mouth corner to its corresponding geodesic path. By computing the facial points between two adjacently vertical paths, the final layer of the hierarchical scheme is further constructed. The facial points are marked in green in Fig. 5-5 (c) and comprise twelve sub-regions of the top and low mouth, as shown in Fig. 5-5 (d). The derived sub-regions encode the mouth movement of different expressions.

(a)

(b)

(c)

(d)
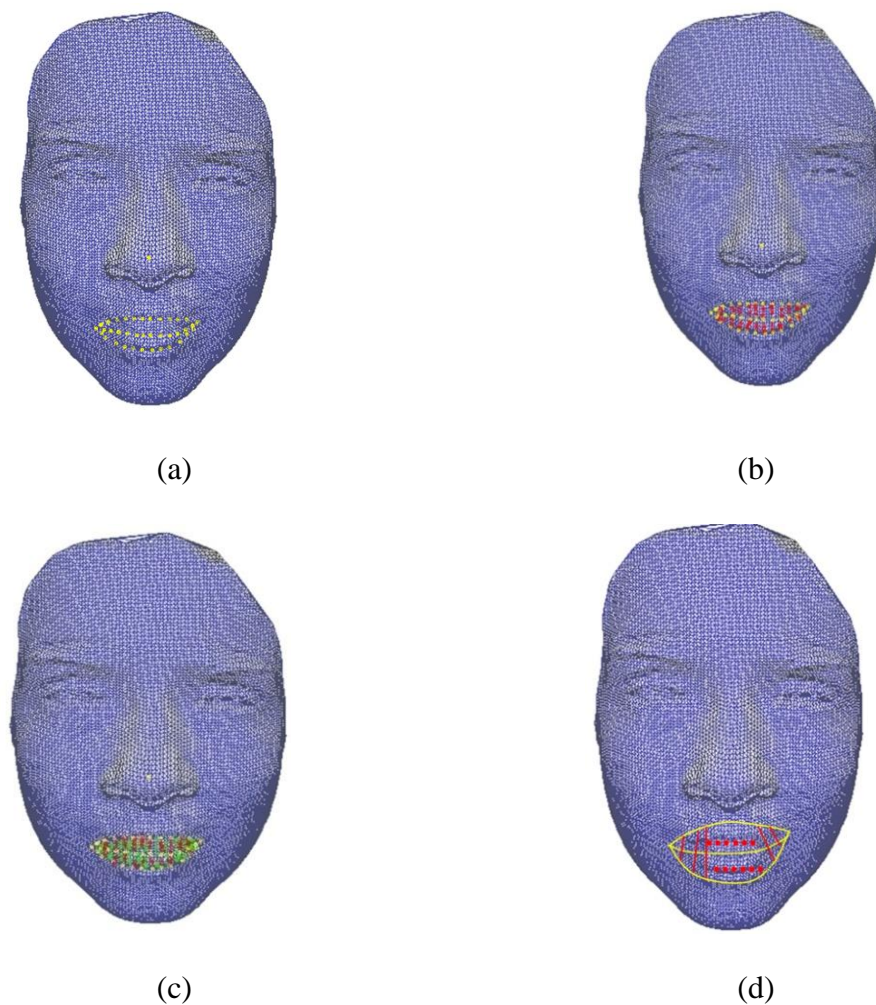
Fig. 5-5. Neutral face partition by hierarchical sampling (a) first layer (a fiducial set of landmarks) (b) second layer (c) third layer (d) final sub-regions illustration (middle sub-regions represented by omission)

5.4.2 Measurements of Ratio and Vector

To neutralise the mouth region, we evaluate two measurements of ratio and vector on each individual sub-region. Depending on the movement of each sub-region, we derive a number of measurements for each particular sub-region.

(a)

(b)
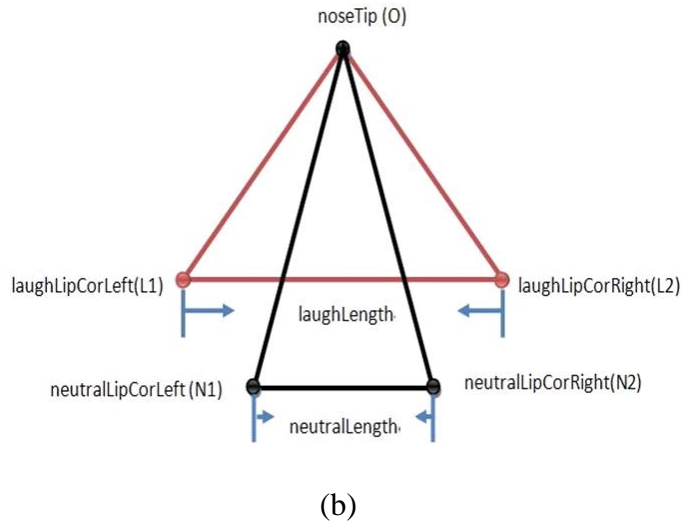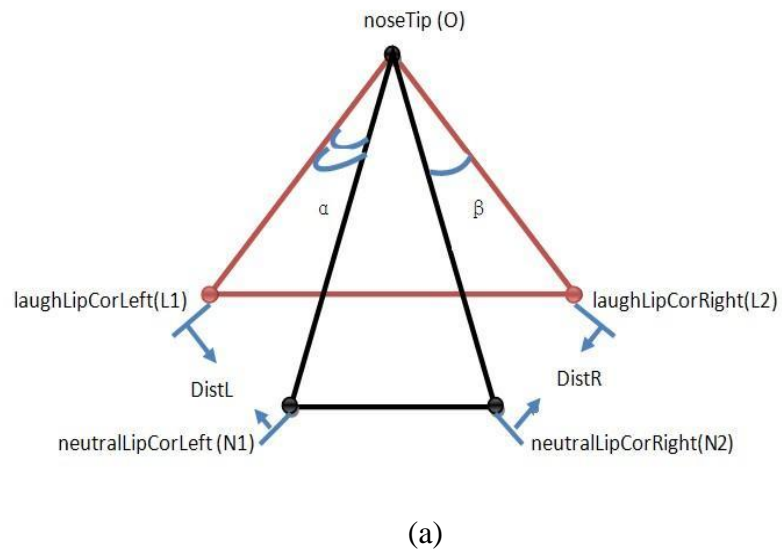
Fig. 5-6. A sample illustration of the points, *DistL* and *DistR* in (a) and *neutralLength* in (b) used for constructing the measurement of the sub-region including the mouth corners.

Ratio measurement

The ratio is derived from the distance of the point in the first layer on neutral face and the corresponding point in the first layer on expression face, divided by the length of the middle line on neutral face, named *neutralLength* in Fig. 5-6 (b). For example, in the case of conducting the ratio measurement of the outer left sub-region including left mouth corner, we derive the ratio by *DistL*, as shown in Fig. 5-6 (a), divided by *neutralLength*; in the case of conducting the ratio measurement of the outer right sub-region including right mouth corner, we derive the ratio by *DistR* divided by *neutralLength*. Finally, a number of ratio measurements for each sub-region are derived. These ratios are applied in the corresponding sub-regions individually and then assembling these sub-regions to achieve the task of neutralisation of the mouth region with expressions.

Vector measurement
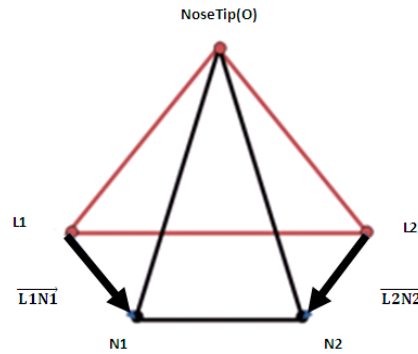
Fig. 5-7. Vectors and points illustration of the particular sub-regions including two mouth corners (*L1* and *L2* are the laugh mouth corners; *N1* and *N2* are the neutral mouth corners). The vectors are named $\overrightarrow{L1N1}$ and $\overrightarrow{L2N2}$.

The vector is considered as the distance of the point in the first layer on neutral face and the corresponding point in the first layer on expression face and the direction of the movement of the point in the first layer during changes in expression. For example, in the case of conducting the vector measurement of the outer left sub-region including left mouth corner, we compute the distance between points *L1* and *N1*, and the direction of *L1* movement towards *N1* to obtain the vector, named $\overrightarrow{L1N1}$, as shown in Fig. 5-7; in the case of conducting the vector measurement of the outer right sub-region including right mouth corner, we compute the distance between *L2* and *N2*, and the direction of *L2* movement towards *N2* to derive the vector, named $\overrightarrow{L2N2}$, as shown in Fig. 5-7. Finally, a number of vector measurements for each sub-region are derived. These vectors are applied in the corresponding sub-regions individually and then assembling these sub-regions to achieve the task of neutralisation of the mouth region with expressions.

5.4.3 Grouping of Smile Levels

In the GavabDB database, each individual has two images of smile associated with two intensities of smile, named smile and pronounced smile, as shown in Fig. 5-8. Thus, in order to evaluate the performance of neutralisation, we study on expression of the smile.

Fig. 5-8. Comparison of smile intensities (a) smile (b) pronounced smile [3]

Prior to the neutralisation, several steps need to be carried out. In order to explore the relationship between the mouth open and the mouth size, we first set up an experiment to study the movements of the mouth corners over the mouth width (known as *neutralLength* in Fig. 5-6 (b)) in terms of ratio and geodesic distance. The results associated with geodesic distances are summarised in Fig. 5-9 and the results associated with ratios are summarised in Fig. 5-10.
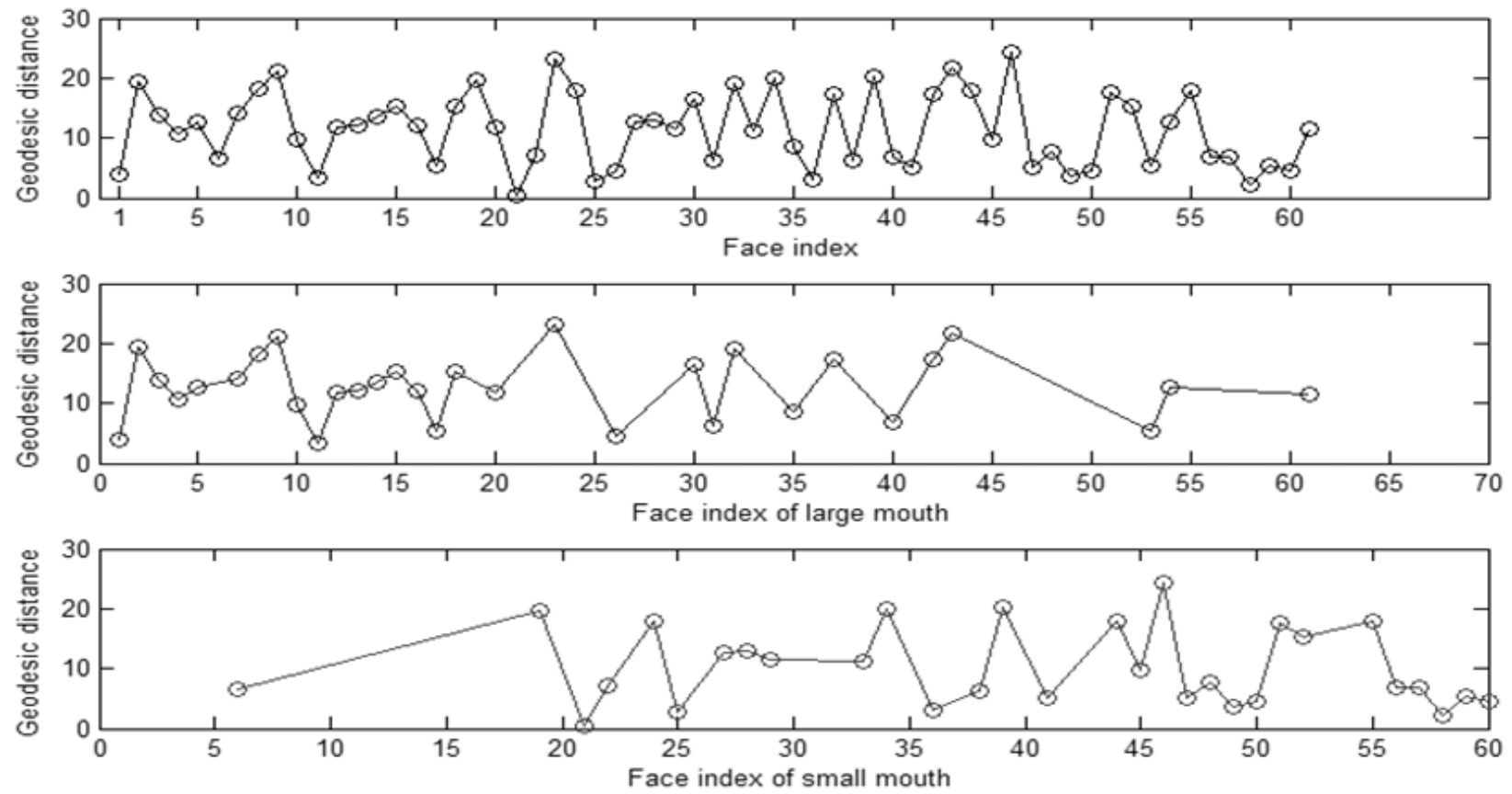
Fig. 5-9. Mouth corners movement from neutral to laugh over the neutral mouth width based on the measurement of distance.

Top: in an overview. Middle: over the large mouth width. Bottom: over the small mouth width.
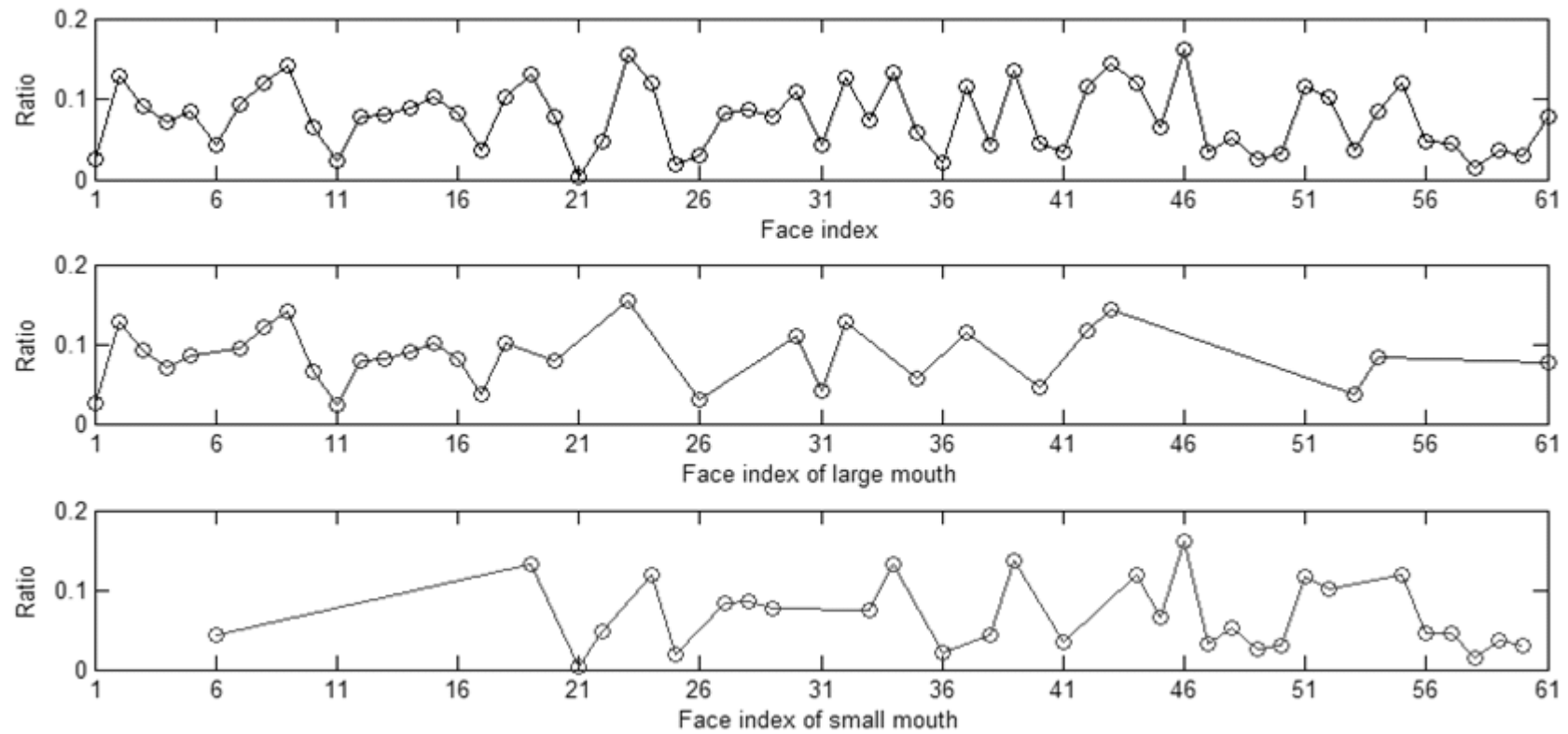
Fig. 5-10. Mouth corners movement from neutral to laugh over the neutral mouth width based on the measurement of ratios.

Top: in an overview. Middle: over the large mouth width. Bottom: over the small mouth width.

In Fig. 5-9, the geodesic distances of the movement of mouth corners from neutral to smile in the range of [0, 0.2] are shown. The middle figure demonstrates that faces 1, 11, 26 and 53 produce small movements, although they have large mouths. Furthermore, the bottom figure demonstrates that faces 19, 34, 39 and 46 produce big movements, although they have small mouths. To further verify the relation, the study in terms of the ratio is carried out. In Fig. 5-10, the top figure shows the ratio is in the range of [0, 4]. Due to the existing noises on the mouth data, faces 39 and 51 are generated with unacceptably high ratios, which mean these two faces produce far larger movements of the mouths than width of neutral mouths when smiling. The middle figure demonstrates that faces 1, 2, 4, 8, 10, 13, 14, 18, 20, 32 and 35 produce small movements, although their mouth sizes are considered to be large. The bottom figure demonstrates that faces 6, 19, 25, 29, 33, 46 and 49 produce big movements, although their mouth sizes are considered to be small. Thus, the results imply that the mouth size and the mouth movement are not highly correlated in principle or in practice.

In the GavabDB [3] database, each subject has only one expression of smile with two intensities, smile and pronounced smile, as shown in Fig. 5-8. There are two requirements driving us to utilise the set of pronounced smiles: our goal of the initial study is to investigate the variations during expression changes. The profounder movement of the mouth region, the significant variation induced; our visual observation shows that some individuals barely produce movement when they make the expression of smile.

Once we decide to use the pronounced smile as our experimental dataset, after our observation of the pronounced smile of each individual, they are found to be not at the

same level, as shown in Fig. 5-11. According to the mouth open, evidently these two individuals produce different levels of the pronounced smile with respect to their emotions and personal characteristics. Due to its influence, we decide to divide the pronounced smile set into two groups regarding to the mouth open: the simple smile (29 individuals) and the accentuated smile (32 individuals). These two groups will be considered and experimented separately for the purpose of neutralisation. In order to determine an optimal measurement, we evaluate the ratios and vectors by applying them on the mouth regions to neutralise the mouth regions in the next section.
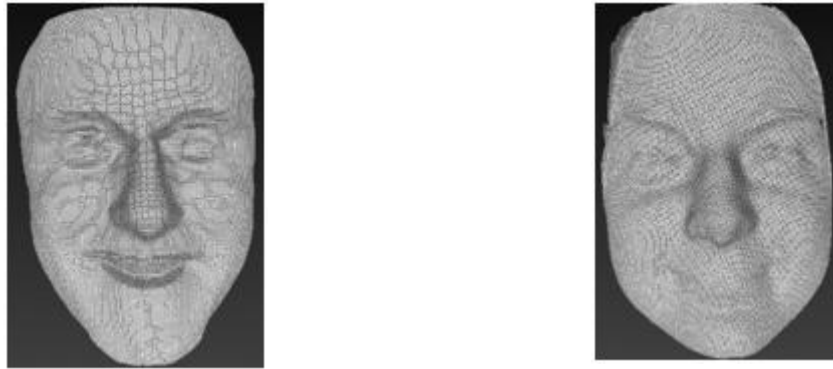
Fig. 5-11. Different smile levels of two individuals in the pronounced smile set on aspects of mouth open vertically and horizontally. Left: accentuated smile. Right: simple smile

5.4.3.1 Neutralisation of simple smiles

Since the mouth regions of each individual at neutral and smile are partitioned into twelve sub-regions respectively based on same method in section 5.4.1, we apply the set of ratios and vectors into the individual sub-region respectively in the simple smile set (29 individuals) for the purpose of neutralisation. We divide the simple smile group into

the training set of 24 individuals and the testing set of 5 individuals. The measurements of ratios and vectors are generated from the training set. The results are shown in Fig. 5-12.

Results and Analysis of Ratio vs. Vector

(a)   (b)
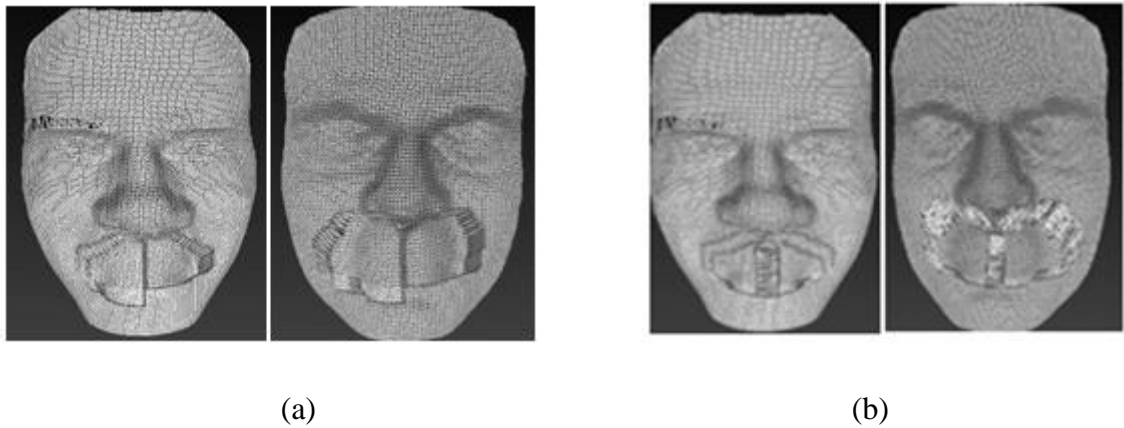
Fig. 5-12. Neutralisation of face model examples with simple smiles based on ratios in comparison with the models based on vectors. (a) ratio-based neutralisation of two subject examples (b) vector-based neutralisation of two subject examples.

Fig. 5-12 shows the facial models of ratio-based and vector-based neutralisation in comparison in the simple smile group. The face models of ratio-based neutralisation, as shown in Fig. 5-12 (a), demonstrate the vertically discontinuity between left half and right half mouth regions. The bottom border of the mouth region is not smoothly connected to the face model. However, in Fig. 5-12 (b), the facial models of vector-based neutralisation are shown. Although different patterns of triangular meshes between the mouth region and the face model are present, the connection between them is generated smoothly. Therefore, we conclude that the neutralised mouth regions based

on vectors present in a reasonable way and approach towards reality.

5.4.3.2 Neutralisation of accentuated smiles

In this section, we experiment on the set of accentuated smiles (32 individuals) based on ratio and vector respectively, in order to evaluate the optimal measurement. The mouth region has been partitioned into twelve sub-regions as we mentioned earlier on. The set of ratios and vectors are applied into corresponding sub-regions for the purpose of neutralisation. The accentuated smile group has been divided into the training set of 26 individuals and the testing set of 6 individuals. The measurements of ratios and vectors are generated from the training set. The results are shown in Fig. 5-13.

Results and Analysis of Ratio vs. Vector

(a)   (b)
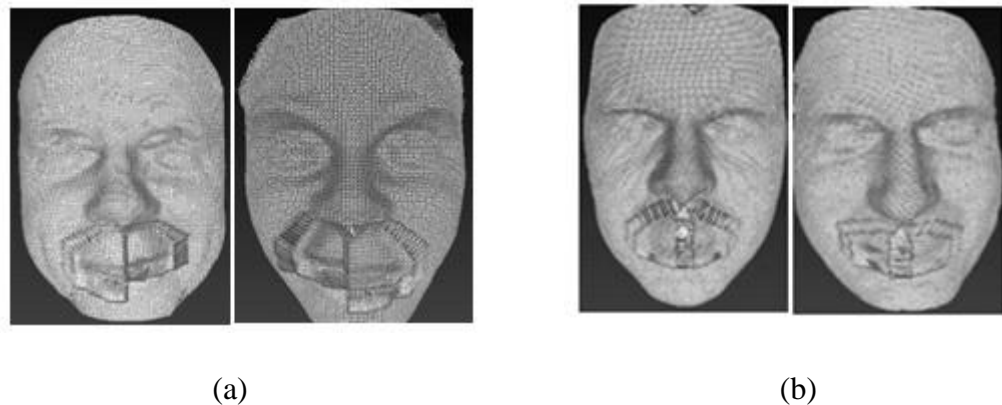
Fig. 5-13. Neutralisation of face model examples with accentuated smiles based on ratios in comparison with the models based on vectors. (a) ratio-based neutralisation of two subject examples (b) vector-based neutralisation of two subject examples.

Fig. 5-13 presents the facial models of ratio-based and vector-based neutralisation in

comparison in the accentuated smile group. The face models of ratio-based neutralisation, as shown in Fig. 5-13 (a) demonstrate the vertically discontinuity between left half and right half mouth regions. The bottom border of the mouth region is not smoothly connected to the face model. However, Fig. 5-13 (b) shows the facial models of vector-based neutralisation. The connection of them is generated smoothly, although there are different patterns of triangular meshes between the mouth region and the face model. A visible gap between the upper lip and the lower lip exists in both ratio-based and vector-based neutralisation, which might be due to the training and testing settings. We conclude that the neutralised mouth regions based on vectors present in a reasonable way approach towards reality.
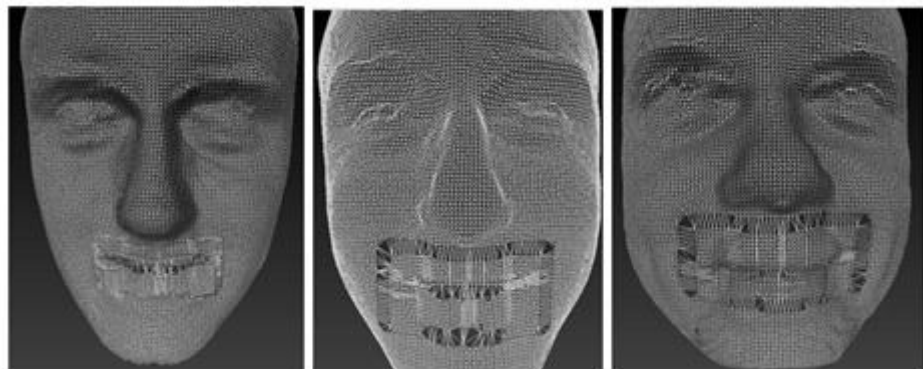
Fig. 5-14. Illustration of neutralisation of vector-based face model samples with satisfactory presents

We have explored the results of ratio-based and vector-based neutralised face models. It is believed that the measurement of vectors outperforms that of ratio with regard to the purpose of neutralisation. The randomly selected face models after neutralisation based on vectors are shown in Fig. 5-14. Smooth meshes over the mouth region and connections to the face mesh are two advantages over ratio-based techniques. However,

there are two barriers to implement matching methods on the neutralised face models, which are noise and computational complexity. Noise manipulates the final presentation and influences the neutralised face models by inducing the spikes and vertical discontinuity. All the points in the mouth region are involved in the neutralisation process that induces massive computational time.
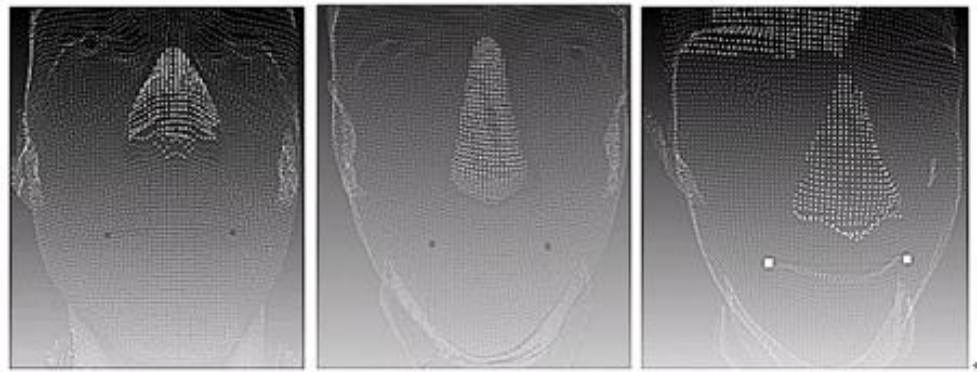
Fig. 5-15. Illustrations of neutralised mouth corners (square points) in comparison with those in the corresponding neutral face of three random subjects.

Fig. 5-15 demonstrates the locations of the neutralised mouth corners in comparison with the corresponding face model. It is evident that the neutralised mouth corners contact the actual mouth corners when neutral. Therefore, the mouth corners are reliable for recognition and stable in the neutralisation process. A valuable outcome of this initial study is that of all the points in the mouth regions, the mouth corners posses the significant meanings and powers under expression variations. Based on Farkas' study [137], the mouth corners are considered as feature points in a fiducial set of landmarks on face models. Thus, we will use a set of feature points on face models to construct a framework of features for the purpose of recognising faces under expression variations in the next chapter.

5.5 Conclusions

In this chapter, we have investigated our proposed curvature-based method in dealing with face recognition under expressions. The investigation concluded that it generated reasonable recognition rates and was a promising start to solve the problem of expressions. To achieve a better result, another solution to the problem of expressions was neutralisation. We set up an initial study of neutralising faces with expressions in order to investigate the variations of expression-variant region (the lower face region). The neutralisation process was carried out on the partition of the mouth region into twelve sub-regions. The ratio-based and vector-based measurements were employed for neutralisation. It has been demonstrated that vector-based measurement outperformed ratio-based measurement. Furthermore, we have concluded that the neutralised face models would have an influence on the results of recognition due to noises existing in the mouth region; the neutralisation process would induce computation complexity for a face recognition system since the process involves each point comprising the mouth region. The conclusion of the initial study showed that as feature points, the mouth corners possess the power for recognising faces under expression variations. Also partial neutralisation of the face models would be a practical and reasonable solution replacing the neutralisation of the whole face models. This point led our study of recognising faces in the presence of expressions towards independence on the set of feature points and partial neutralisation.

Chapter 6 Face Recognition in the Presence of Facial Expressions

6.1 Introduction

It is a challenge to recognition 3D faces purely based on geometry information because facial expressions can cause severe global geometry variations, resulting in degrading the recognition rates or computation complexity. The idea of extracting and using the T shape profiles in the expression-invariant regions, as well as the neutralization of the whole face models, which are presented in last chapter, has inspired us to develop a 3D face recognition method in the presence of facial expressions. This method simplifies the process and reduces the computational time by working on a minimum feature set.

Benefiting from the initial work in last chapter, we present a novel and comparatively computational fast method for recognising faces under expression variations. In our method, the main goal is to determine the set of intrinsic geometric descriptors representing face models which allow for fast computation. This is solved by combining two sets of descriptors: distance-based contour shape features; and distanced-based geometric descriptors. Once these intrinsic geometric descriptors are determined, we employ regression analysis models to learn the relationship between these geometric descriptors under various expressions. The learned relationship can predict the geometric descriptors of neutral faces, which are used for matching faces under expression variations. Finally, the effect of incorporating the curvature-based method using T shape profiles will be analysed.

6.2 Problem Domains and Objectives

There are six significant expressions, as shown in Fig. 1-5, which make an adverse effect on face recognition. The adverse influence of face expression on face recognition is listed by Bronstein et al [143] and needs to be solved no matter what dimensions face representation is being used (2D or 3D). However, its nonlinear nature and a lack of an associated mathematical model make the problem of face expression hard to deal with. There is no doubt that some progress has been made to solve this problem existing in 3D face recognition, which is mentioned in the Chapter 2 literature review, but there are still some challenges remaining at this stage. For instance, Bronstein et al [14, 141] assume facial scans are isometric surfaces, which are not stretched by expressions so as to produce an expression invariant facial surface representation with an assumption that mouth is closed in expressions for recognising faces. However, there is one constraint in that they only considered frontal face scans and assumed the mouth to be closed in all expressions, which is not considered realistic.

Their attempts to remove the effect of face expressions have left unresolved some issues. One of the issues with these works is that there is less reliable invariants when faces carry heavy expressions. In addition, another issue is how to optimise the combination of small rigid facial regions for matching in order to reduce the effect of expressions. Using rigid facial regions can improve the performance on a database with expression variations [144-145]. The selection of rigid regions, however, is based on the optimal extraction and combination. Another issue is computational cost. In general, more information trained in 3D face data leads to more computational cost and time. Some algorithms can work on the verification process with a time cost of about 10 seconds on

a normal PC [145], whereas efficient face matching with less computational cost is still a problem when dealing with a large gallery with thousands of faces. In addition, modelling relations between expressions and the neutral by expression-variant features and combining with expression-invariant features still remains a research question. Furthermore, our previous investigations on finding the effects of the T shape profiles and neutralisation of the mouth regions provide motivation of further studies on partial neutralisation of the minimum feature sets.

6.3 Extraction of Shape Features

Facial feature extraction is important in many face-related applications [146]. Our 3D feature is a set of expression-invariants and expression-variants representations. This is achieved by analysing the facial region's sensitivity to the expressions and representing by a set of geometric descriptors. To eliminate the computational time from the preprocessing step, such as face alignment and normalisation, we introduce a distance-based feature to avoid the preprocessing.

6.3.1 Selection of Feature Points

Having considered computational time, we intentionally discard the texture information in our proposed method, in a similar way to the other chapters. Hence, the resulting performance is completely reliant on the features extracted from the shape of the image. The shape feature analysis based on the triangle meshes of faces, reflecting the facial skin wave, represents the intrinsic facial surface structure associated with the specific facial expressions. Motivated by this idea, we propose a set of novel distance-based

geometric descriptors based on Euclidean and geodesic distances. Instead of focusing on the entire face we investigate face models by segmenting into two regions: the top face region, as shown in Fig. 6-1 (a), including eyes, eyebrows and nose; and the low region, as shown in Fig. 6-1 (b), including the mouth only. The top region is used because it is comparatively insensitive to expression variations [4]. More specifically, the nose region suffers less from the effect of expression variations. However, the nose region alone is not sufficiently discriminatory for the purpose of face recognition because it represents only a small fraction of the face. Thus, we introduced more information, such as eyebrows and eyes, to be used to perform face recognition under expression variations. In not only relying on the expression-invariant region, we also utilise expression-variant regions, found in the low region. Due to the significant change of the mouth region from laugh to neutral, we consider the low region as being sensitive to expression variations [57].

(a)   (b)
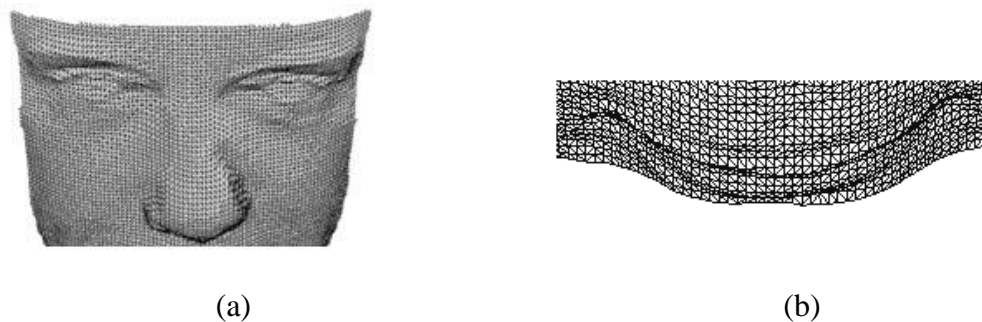
Fig. 6-1. Illustration of expression-sensitive and expression-insensitive regions on a sample subject (a) the upper face: expression-insensitive region (b) the lower face: expression-sensitive region.

Based on the analysis of the expression-variant and expression-invariant regions, there are a few concerns about selecting the feature points.

- Selecting meaningful and significant positions as feature points, such as eye corners and top of the eyebrows, and the most distinctive position, the nose tip, is one concern. By taking this into consideration, accuracy of the extracted features can be improved.

- For the insensitive region, another concern is that feature points are chosen to ensure minimum variations under change of expressions. For example, compared to the eye regions, the cheek region produces visible variations caused by expressions. Thus, we avoid locating feature points in the cheek region.

- For the expression-variant region, distinct positions along the outer mouth contour are taken into consideration rather than the areas including undesirable feature points, such as the chin regions.

- Due to the data missing in the dark region resulting from scanning, the inner contours such as mouths when laughing, we exclude those areas when selecting feature points.

- We determine the number of feature points by analysing the face representation efficiency and computation requirements. More features make face representation more accurate; however, they cause more computational time. Thus, choosing the number of feature points is based on the requirement that fewer features represent faces efficiently.

Thus, taking advantage of 83 feature points on annotated face models in the BU3D-FE database [147] we use, twelve significant positions are selected as a set of feature points. More specifically, they are top of the eyebrow, top of the upper eyelid, lowest point of the lower eyelid, the outer eye corner, the inner eye corner, the nose tip, the left and right edges of nose wings for insensitive regions; and mouth corners, mid-upper and

mid-lower lips in sensitive regions, as shown in Fig. 6-2. The explanation and illustration of the set of distance-based features is shown in Table 6-1 and Fig. 6-3 respectively.
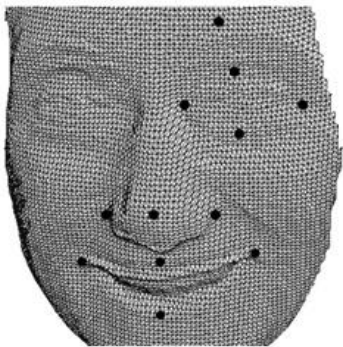
Fig. 6-2. Localisation of twelve landmarks
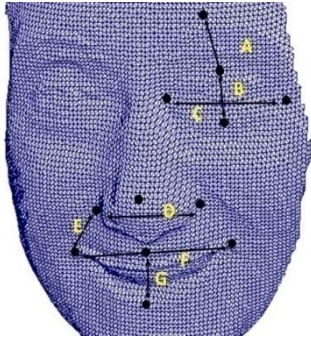
Fig. 6-3. Illustration of labelled distance-based features

Table 6-1. Seven distance-based features definition

Distance index	Distance name	Distance definition
A	Eyebrow height	Distance between uppermost eyebrow and mid-upper eyelid
B	Eye height	Distance between mid-upper eyelid and mid-lower eyelid
C	Eye width	Distance between outer eye corner and inner eye corner
D	Nose width	Distance between left edge and right edge of nose wings
E	Lip stretching	Distance between nose tip and left lip corner
F	Mouth opening	Distance between left lip corner and

		right lip corner
G	Mouth height	Distance between mid-upper lip and mid-lower lip

Not only is this set of features utilised in our method, but also contour shape features are considered, as shown in Fig. 6-4. The contour shape features describe face elements, such as contour shape of eyebrows, eyes, nose and mouth. We select a set of control points from annotated face models in the database to be placed on the contours. Specifically, the contour shape features are represented by the vector:

$$x = (x_1, y_1, z_1, x_2, y_2, z_2, \dots, x_n y_n z_n) \qquad (6.1)$$

where x_i, y_i and z_i are coordinates of control points.
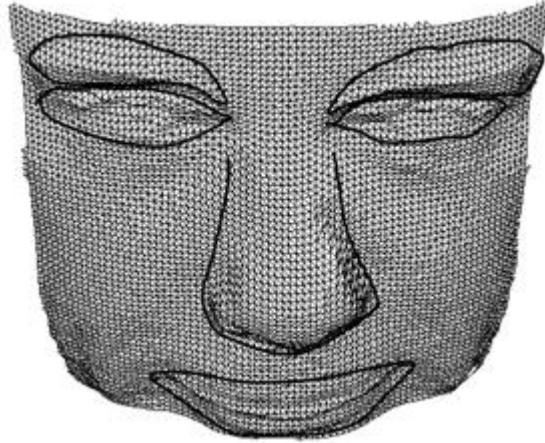
Fig. 6-4. Illustration of six contours

6.3.2 Geometric Descriptors

In this chapter, we utilise two geometric descriptors, namely geodesic distances and Euclidean distances, to represent the facial models by describing the set of distance-based features and contours. The geometric descriptors are independent of the

chosen coordinate system.

We can observe that not all the distance vectors are invariant to expression variations. For example, the mouth opening (G) in Fig. 6-3 shows a change of a distance vector caused by an open mouth, when the face of the same individual changes from neutral to a laugh expression. However, there are some certain distance vectors that remain stable under expression variations, for example, the eye width (C) in Fig. 6-3. Thus, for the distance-based features, as we mentioned, we consider A, B, C and D distances in the top region as expression-invariants since they are insensitive under expression variations, whereas E, F and G are considered as expression-variants. We utilise Euclidean distances as the geometric descriptor to represent the set of distance-based features.

Euclidean distance

The distance between point *p* and point *q* in Euclidean n-space is

$$d_{e(p,q)} = \sqrt{\sum_{i=1}^{n} |p_i - q_i|^2} \qquad (6.2)$$

where n is the dimension of Euclidean space. Specifically in this case, the Euclidean distance between points *p* and *q* in three dimensional Euclidean spaces is

$$d_{e(p,q)} = \sqrt{(p_1 - q_1)^2 + (p_2 - q_2)^2 + (p_3 - q_3)^2} \qquad (6.3)$$

The face model in the database comprises a triangulated mesh, which is discretely defined to be a set of connected point clouds. The geodesic distance computation of triangle meshes is initialised by one or more isolated points on the mesh and the

distance is propagated from them. More specifically, the geodesic distance of discrete meshes is considered as a finite set of Euclidean distances between pair-wise involved vertices. Thus, another geometric descriptor, geodesic distance, is utilised in our feature sets. Geodesic distance is capable of representing the contour shape features on the discrete meshes. Similarly, the selected contour features contain expression-invariants and expression-variants. The eye contour and the mouth contour are sensitive to expression variations. However, the eyebrow contour and the nose contour comparatively remain stable during expression variations.

Geodesic distance

On a triangle mesh, the geodesic distance with respect to a point turns out to be a piecewise function, where in each segment the distance is given by the Euclidean distance function. Thus the geodesic distance computation is initialised by one or more isolated points on the mesh and the distance is propagated from them.

$$d_{g(p,q)} = \sum_{i=1}^{n} d_{e(p_i,q_i)} \tag{6.4}$$

where $d_{g(p,q)}$ is geodesic distance of a contour, $d_{e(p_i,q_i)}$ is the Euclidean distance between two points and *n* is the number of control points of each contour.

6.3.3 Normalisation

Depending on the different facial feature extraction methods, the slight influence of face sizes and different scales of the faces can be eliminated, either by normalisation or by preprocessing before the recognition process. Thus, in addition to the geometric descriptors derived from the face models, we also consider defining two distance-based

features to avoid the face alignment process and the normalisation process.

<center>(a)   (b)</center>
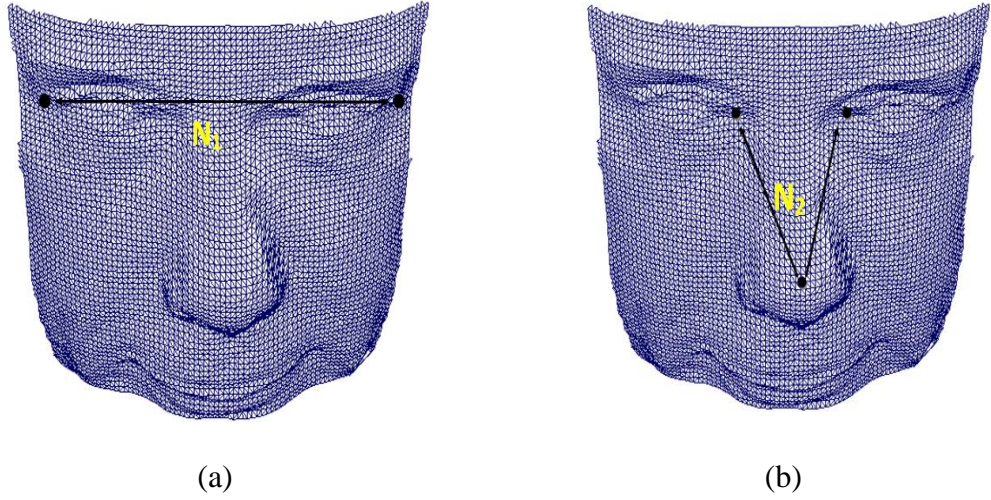
Fig. 6-5. Illustration of two distances for normalisation of two feature sets (a) for distance-based feature set (b) for the contour shape feature set.

We introduce a distance-based feature for normalising the set of seven distance-based features, which is considered as a stable expression-invariant feature, as shown in Fig. 6-5 (a). In order to be consistent with the geometric descriptor used for the features, we utilise Euclidean distance to represent the feature, named N_1. Thus seven normalised Euclidean distances are derived by the ratios of seven Euclidean distances to $N1$. Similarly, since geodesic distances are not scale-invariant, the next step is to normalise each geodesic distance by another distance-based feature [61], the eyes-to-nose distance, as shown in Fig. 6-5 (b), i.e. N_2, sum of geodesic distances between the nose tip and the two inner eye corners. This guarantees invariance with respect to scaling and facial sizes under expression variations. Thus, for the set of contour shape features, this stable expression-invariant feature. $N2$ is represented by geodesic distance descriptor to ensure its consistency with the descriptor for the contour shape features. Deriving six normalised geodesic distances is accomplished by the ratios of the six geodesic distances to $N2$.

Thus, the geometric descriptors for the whole set of features are comprised of two sets of ratios. Meanwhile, the attributes of the ratio-based geometric descriptors that are unique to each face model are investigated and proved before carrying out the next step. Compared to the commonly used descriptors in [46, 143], our geometric descriptors benefit from fast computation due to their simplicity. In the next section, we adopt regression models to learn the relationship between pair-wise expressions based on the combination of these thirteen ratio-based geometric descriptors.

6.4 Regression Analysis Model

The regression analysis model is utilised for analysing the variables and modelling the relationship between them. Recently, regression analysis has been imported and applied in the face recognition area [148-149]. In this chapter, we evaluate two types of regression model: partial least square regression and multiple linear regressions. Specifically, we employ them to learn the correlation between pair-wise expressions and predict the 3D face neutral shape information for dealing with the problem of matching faces under expression variations.

6.4.1 Partial Least Square Regression

In this section, we will introduce a commonly used regression model that will be used to train and predict the feature set when the face models are neutral. Owing to the multiple dimensions of the involved variables, i.e. the total number of the ratio-based geometric descriptors, we will use a subspace regression model based on latent variables, named

partial least square (PLS) [150].

X refers to a vector with the independent variables (predictors) and Y refers to a related vector of the dependent variables (responses).

$$X = TP + E, \qquad\qquad\qquad (6.5)$$

$$Y = UQ + F, \qquad\qquad\qquad (6.6)$$

$$U = BT + \varepsilon, \qquad\qquad\qquad (6.7)$$

X is a matrix of predictors and Y is a matrix of responses. E and F are the error terms. There is a linear relation between T and U given by a set of coefficients B. A number of variants of PLS exist for estimating the T, P and Q.

The goal of PLS is to predict Y from X using a common structure of reduced dimensionality. For this purpose, PLS introduces some latent variables:

$$\{T_i\} = T_1, ..., T_k, \qquad\qquad\qquad (6.8)$$

$$\{U_i\} = U_1, ..., U_k, \qquad\qquad\qquad (6.9)$$

T and U preserve the most relevant information of the interaction model between X and Y.

6.4.2 Multi-linear Regression

To compare with the performance of PLS, we utilise the multiple linear analysis regression (MLR) [151] method to model and learn the relationship between neutral and non-neutral facial geometric descriptors and performed recognition rate. A regression model relates Y to a function of X and β.

$$Y \approx f(X, \beta) \qquad\qquad\qquad (6.10)$$

Given a data set $\{y_i, x_{i1}, \ldots, x_{ip}\}_{i=1}^{n}$ of n statistical units, a linear regression model assumes that the relationship between the dependent variable y_i and the p-vector of regressors x_i is approximately linear. This approximate relationship is modelled through a term ε_i — an unobserved random variable that adds noise to the linear relationship between the dependent variables and responses. Thus, in detail, the model is of the form:

$$y_i = \beta_1 x_{i1} + \cdots + \beta_p x_{ip} + \varepsilon_i = x_i' \beta + \varepsilon_i, \quad i = 1, \ldots, n \tag{6.11}$$

where x_i' denotes the transpose, so that $x_i'\beta$ is the inner product between vector x_i and β. Commonly these n equations are integrated together and written in vector form as:

$$y = X\beta + \varepsilon \tag{6.12}$$

where:

$$y = \begin{pmatrix} y_1 \\ y_2 \\ \vdots \\ y_n \end{pmatrix}, \quad X = \begin{pmatrix} x_1' \\ x_2' \\ \vdots \\ x_n' \end{pmatrix} = \begin{pmatrix} x_{11} & \cdots & x_{1p} \\ x_{21} & & x_{2p} \\ \vdots & \ddots & \vdots \\ x_{n1} & \cdots & x_{np} \end{pmatrix}, \quad \beta = \begin{pmatrix} \beta_1 \\ \vdots \\ \beta_p \end{pmatrix}, \quad \varepsilon = \begin{pmatrix} \varepsilon_1 \\ \varepsilon_2 \\ \vdots \\ \varepsilon_n \end{pmatrix}$$

Multi linear regression is based on linear regression but dealing with multiple X and Y.

6.5 Experiments and Results

6.5.1 Comparison of Regression Models

We have established a set of ratio-based geometric descriptors of face models that serves as input to the regression analysis model for simulating the relation between non-neutral and neutral faces. Relying on the ratios-based geometric descriptors, the effects of head rotation, translation and different scales can be eliminated, even without

face alignment and normalisation in the preprocessing stage. Our proposed method is carried out on the BU3D-FE database [147] which is comprised of 100 subjects. In order to evaluate the two regression models, we set up a framework allowing for investigating improvement of expression-variants. To enhance the significance of the regression models, a Neural Network (NN) approach is employed for comparison. The comparison results are listed in Table 6-2.

Table 6-2 Comparison of multiple regression models

Laugh matching to neutral	PLS	NN	MLR
Expression-invariants(4)	71.63%	72.12%	65.53%
Expression-variants(3)	55.12%	54.66%	61.78%
Combination(7)	64.78%	60.73%	69.01%

From Table 6-2, we can observe that PLS, NN and MLR improve the rates by introducing expression-variants; however, PLS somehow places more emphasis on the expression-invariants in comparison to variants and also achieve almost the highest result. Although only improvement is achieved in the MRL case, it performs fairly low results based on different feature sets. Another conclusion is that employing variants indeed enhances the significance of expression-invariants. To further investigate the optimised performance of PLS, we set up another experiment allowing for PLS modelling multiple relationships between four intensities of six expressions and neutral, and vice versa. The results are shown in Fig. 6-6 and Fig. 6-7, respectively.
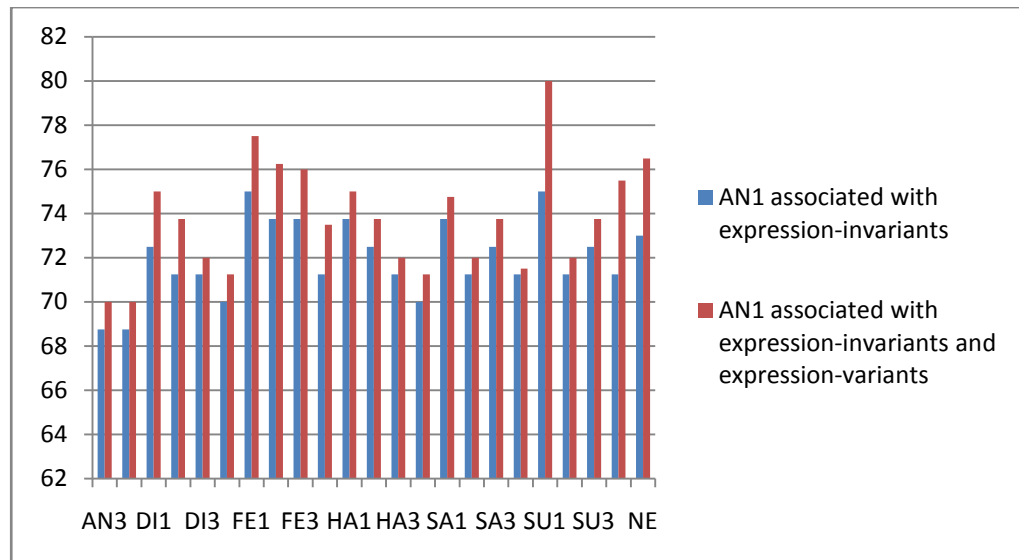
Fig. 6-6. Illustration of the improvement with additional expression-variants employed under intensity 1 of angry expression.
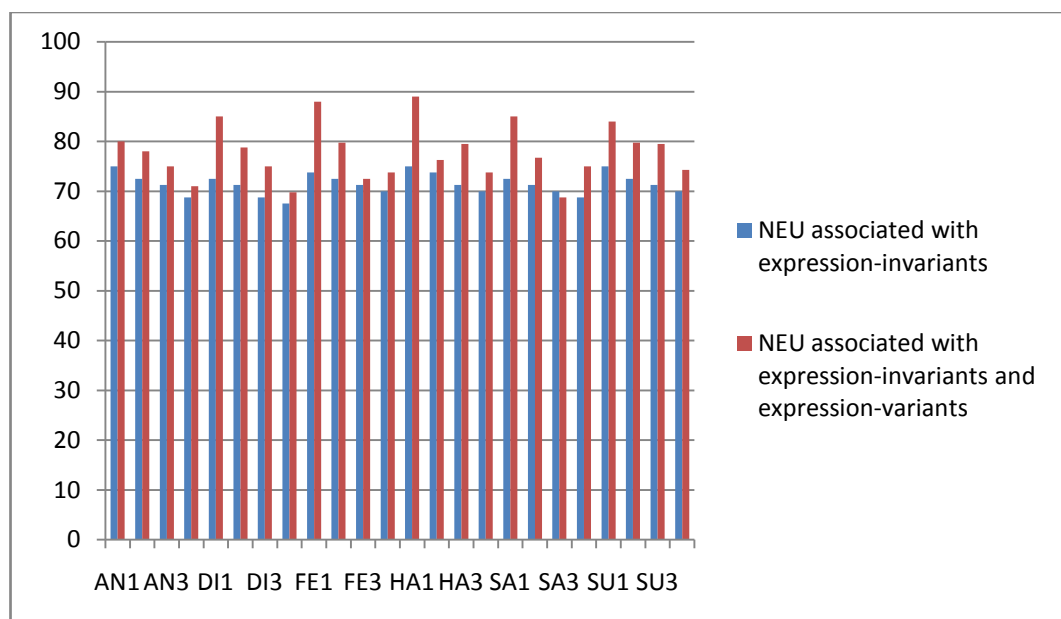
Fig. 6-7. Illustration of the improvement with additional expression-variants employed under neutral.

Fig. 6-6 shows the results of modelling intensity 1 angry to other expressions and neutral. The blue bars present the rate of expression-invariants and the red bars present

the accuracy rate of the combination of expression-variants and expression-invariants. The improvement varies in four intensities. However, on average the results further confirm the power of the expression-variants. In Fig. 6-7, the diagram shows the results of modelling neutral to six other random intensity expressions. The blue bars present the accuracy rate of expression-invariants and the red bars present the accuracy rate of the combination. The recognition experiments and results will be carried out and described in the following based on the method using PLS for modelling relationships and using the combination of ratio-based expression-variants and expression-invariants as the feature sets.

6.5.2 Classification of Multiple Expressions to Neutral Expression

In this section, we present the experimental results for recognising faces under expression variations. In particular, the experiment is implemented on the BU-3DFE database with 100 subjects.

In the experiments, we divide these 100 subjects into two sets: the training set with 80 subjects; and the testing set with 20 subjects. The experiments ensure that any subject used for training does not appear in the testing set because random partition is based on the subjects rather than the individual expressions. Four intensities of each expression are ensured to be involved in this experiment. For each iteration, the PLS regression analysis model is reset and retrained from the initial state.

Table 6-3. Recognition rate using PLS regression analysis model

Expression with intensity	Neutral face recognition rate (%)		Expression with intensity	Neutral face recognition rate (%)
Happy01	89		Angry01	85
Happy02	75		Angry02	73.75
Happy03	70		Angry03	70
Happy04	70		Angry04	68.75
Disgust01	88		Fear01	89
Disgust02	73.75		Fear02	76.25
Disgust03	72.5		Fear03	72.5
Disgust04	73.75		Fear04	73.75
Sad01	85		Surprise01	84
Sad02	73.75		Surprise02	73.75
Sad03	68.75		Surprise03	72.5
Sad04	70		Surprise04	71.25
Neutral	90.3%			

In Table 6-3, we report the recognition rate of matching six expressions with four intensities to neutral. The promising recognition accuracy is achieved even without the texture information. Happy and fear expressions achieve the highest accuracy rate of 89%, however, sad, angry, disgust and fear perform less accurately than the other three expressions. This is because happy and surprise expressions are comparatively clean and simple; their measurement allows for simplicity; some noises are produced when other expressions occur. As expected, the accentuated intensity of expressions achieves

the lowest recognition rate and the recognition rate ascends along with a descending intensity. However, as we can see, the facial expressions have significantly degraded the performance of the face recognition in the absence of expression variations since the neutral face recognition accuracy rate achieves the highest at 90.3%.

6.5.3 Comparison with Other Methods

The final recognition rates of our proposed 3D face recognition method under expressions will be listed and discussed. Some researchers have developed and achieved their results of face recognition under expressions. Although our results are not the best, we further discuss the feature sets, database, speed and the size of face models of our method in comparison with the current existing 3D face recognition methods, as shown in Table 6-4. The highest accuracy rate of 97% is generated by Alyuz et al. [94] using the nose, the forehead, the eyes and the central face, which covers the whole face with overlaps. In their work, face registration and face alignment are employed. These techniques cost computational time, although they play important roles in recognition rates. The point sets in the determined regions and the curvature related to the corresponding regions are used for dissimilarity calculation. The accuracy rate of 81.7% is achieved by Gervei et al. [152] using a least feature set with 40 dimensions. Compared to other methods, our proposed method use a minimum feature set to achieve a promising accuracy rate.

The effect of incorporating the curvature descriptors of the T shape profiles is next analysed. In last chapter, the curvature-based method is evaluated on its performance independently. It has been proved that the proposed method is promising in dealing with

expressions. Thus, we combine the distance-based feature sets with the curvature descriptors of the T shape profiles for face recognition under expressions. The results are listed in Table 6-4. We notice that the recognition rates are slightly higher with the curvature descriptors of the T shape profiles. Based on the results, it is observed that the use of the T shape profiles in the expression-invariant regions makes it possible to improve recognition performance.

The design criteria of the methods are based on the accuracy rate and speed (computational time). Regarding to various circumstances face recognition methods apply, there is no simple answer to the question of which method would fit best. In addition, the value of methods varies significantly with each application requirements and circumstances. Based on the design criteria, in some cases, fast processors are facilitated for face recognition techniques and the recognition rate can be considered as the top priority. The computational time can be sacrificed due to fast processors for high accuracy rate. However, the accuracy rate could be trade off for the fast computation if the face recognition techniques are installed on a portable or wireless device. Therefore, in some circumstances, accuracy rate and speed can be trade off. In summary, our proposed methods are suitable for the cases essentially requiring fast computation.

Table 6-4. Our method of face recognition under expressions in comparison with other existing methods

Authors	Database	Feature sets	Recognition rate	Speed	Vertices
Alyuz [94]	Bosphorus	Eye, nose, central face, forehead	97.28%	N/A	35,000
Smeets [95]	BU-3DFE	Whole face and nose region based on distances	94.5%	N/A	8000
Li [126]	FRGC v2.0	Whole face deformation model	91.9%	N/A	4500 after resample
Our proposed method	BU-3DFE	59 features	91.1%	N/A	8000
Our proposed method	BU-3DFE	14 features	90.3%	N/A	8000
Wang [96]	FRGC v2.0	Whole face	89.7%	403ms	8000
Our proposed method	GavabDB	59 features	89.6%	N/A	6000 after cropping face
Our proposed method	GavabDB	14 features	89.47%	N/A	6000 after cropping face
Chang [57]	Collective database of 546 subjects	Overlapping regions around the nose	83.5%	N/A	
Mahoor [6]	GavabDB	Contour lines	82%	1.275s on a PC Intel Core Duo 1.86 Ghz processor	13,000
Gervei [152]	GavabDB	Whole face through PCA down to 40 dimension	81.7%	4.62s	13,000

6.6 Conclusion

Based on the previous investigation on finding the acts of the curvature-based method using the T shape profiles in dealing with expressions and neutralisation of the face models, we proposed a method for 3D face recognition in the presence of expression variations. Instead of constructing a feature framework for expression-invariants, we introduced a feature set of combining the expression-invariant region with the expression-variant region. The key was to prove that expression-variants optimise the performance of independent expression-invariants. We selected two intrinsic geometric descriptors to efficiently represent the set of features due to their fast computation. By the combined feature sets, we achieved an accuracy rate of 90% of face recognition in the presence of expression variations. It validated the effectiveness of our proposed method with respect to the regression model. We further investigated on the combination of the curvature-based T profiles and this proposed method. The experimental results found out that the curvature-based method using the T shape profiles possibly boost the recognition performance.

Chapter 7 Conclusions and Future Work

7.1 Conclusions

In an overview, this thesis explored state-of-the-art face recognition techniques both on 2D and 3D. In particular, the techniques of gender classification based on 2D images have been discussed. Significant progresses on 2D face recognition methods have been made and applied in some commercial applications due to their mature techniques. However, researchers have moved towards 3D face recognition over the past few decades in order to overcome the inherent problems of 2D face recognition, which are pose, illumination and expression variations. Indeed, utilising 3D facial models can resolve the problems of pose and illumination variations due to the nature of the 3D facial models. However, the inherent problem of expression variations remains. Based on 3D facial models, various current techniques for face recognition in the presence of expression variations and gender classification have been investigated and discussed.

In this research work, we intentionally discarded the texture information and focused on the geometry face models for one main reason: the texture information requires complex computation. The contributory components of this research work are summarised as follows:

- Design a limited feature framework for characterising the 3D geometry face models using a T shape feature set and evaluate its performance in dealing with neutral face recognition and face recognition under expressions (Chapter 3 and Chapter 5);
- Decrease the search range in the gallery by deploying a novel gender classification (Chapter 4);

- Construct a correlation model between expression and neutral faces to deal with face recognition in the presence of expression variations (Chapter 6);

- Develop a extended method of recognising faces under expression variations incorporating the curvature-based method using the T shape profiles (Chapter 3)

7.1.1 Characterising Faces

The initial part of our contribution is to characterise the 3D face models using curvature. We construct a profile-base feature set, regarded as a T shape to characterise face models efficiently. The T shape profiles are considered as a minimum feature set, which is robust to the neutral face recognition and non-neutral face recognition.

7.1.2 Gender Classification

In addition, in order to improve the performance of the proposed system we deployed a gender classifier. The current 3D gender classification techniques intended to utilise a large number of facial information to achieve good performance. It is worth noting that the major portion of the current gender classification techniques verified the optimal classifier SVM by comparison with other classification methods. However, combining with either face appearance models or grey level images significantly caused more computational time. This encouraged us to develop a novel method of 3D gender classification by using a minimum feature set. In addition, by using ratio as a measurement to normalise the feature sets in order to avoid the preprocessing stage and the face alignment (registration), which some systems relied on. Thus, by taking these strategies into consideration, we built a novel gender classifier based on the surgery

researches of discriminative features between females and males.

7.1.3 Matching Non-neutral to Neutral Faces

One of the fundamental face recognition techniques in the presence of expression variations was based on a deformable model which generates a non-neutral model with a neutral model in order to match non-neutral faces to neutral faces. One of the issues pointed out by the researcher was reducing the computational cost. Rather than taking a large number of features into account, we intended to use the limited feature set representing contour information and face structure information. We built a novel framework of learning the correlation between various expressions and neutral with the limited feature set. Thus, there were two main advantages of our proposed method: training the correlations between expressions and neutral provide the flexibility of extending the feature sets; using the minimum feature set extracted from the facial structure information and the contour information explicitly to represent face models. Furthermore, incorporation of the curvature-based T shape profiles leads to better performance.

7.2 Future Work

This thesis has addressed some fundamental problems existing in the 3D face recognition area and achieved good performance. However, there are still some plans for future work to enhance the system performance: More accurate and efficient techniques for the feature extraction in characterising face models and gender classification; the comprehensive geometric descriptors representing the face models;

and the improvement of integral face recognition.

7.2.1 Feature Extraction

It has been pointed out that the initial feature points (five landmarks, as shown in Fig. 3-9 (b)) used for determining the T shape profiles in characterising faces were located manually; likewise the feature points (the landmarks to determine the sub-regions, as shown in Fig. 4-5) for extracting sub-regions in gender classification. This becomes a barrier to the applications in real life as the full automation is regarded as a key feature of 3D face recognition applications, even though some systems would leave a gap for human intervention in the cases of errors or unexpected system confusions.

In addition, the proposed integrated system has been particularly designed for the long-distance, mobile, wireless and portable devices in certain circumstances. It is essential for these applications to require the acceptable recognition rate at the low computational time. Therefore, the framework for the minimum feature set has been developed. For the purpose of recognising faces under expression variations, a framework for the feature set was built with flexibility in that it allows for the incorporation of additional geometric descriptors. The advantage of this strategy is that the users can adapt additional feature sets when needed for improving the recognition rate regardless of the computational time in some cases. Thus further investigation for improving the system performance could involve taking more prominent features into account.

There is no doubt that the noises and spikes on the face models produced from the

scanning process have an influence on the recognition rate. The system would not successfully recognise faces or handle the face models with noises and spikes. In particular, a limitation in our gender classification method is the employed multiple sub-regions may be affected by the noises from a scanner. Therefore, another achievable task in the future work is to refine the face models by removing the noises and spikes for our gender classifier.

7.2.2 The Geometric Descriptors Representing Faces

In the face recognition under expression variations, we applied two types of geometric descriptors for face models representation, namely Euclidean distance and geodesic distance. However, there are two main requirements needed to be investigated for improving the recognition rate. One is employing more geometric descriptors to represent the natural structure of the face model, for example area, curvature and normals. Normals are used to determine the surface orientation when face registration is deployed. By introducing a set of weights to those geometric descriptors, the framework will be able to manipulate the weights and render them reliable for the task. The other one is to define the feature set to a particular expression in order to obtain the corresponding natures of each expression. These possible improvements are considered as the tasks in the future work for the purpose of strengthening the power of the framework.

References

[1]   P. C. Cattin, "Biometric Authentication System Using Human Gait ", Swiss Federal Institute of Technology, Zurich, 2002.

[2]   A. F. Abate, M. Nappi, D. Riccio, and G. Sabatino, "2D and 3D Face Recognition: A Survey," *Pattern Recognition Letters,* vol. 28, pp. 1885-1906, 2007.

[3]   A.B. Moreno and A.Sanchez, "GavabDB: A 3D Face Database," in *Proceedings 2nd COST Workshop on Biometrics on the Internet: Fundamentals, Advances and Applications*, 2004, pp. 77-82.

[4]   L. Yin, X. Wei, Y. Sun, J. Wang, and M. J. Rosato, "A 3D Facial Expression Database For Facial Behavior Research," presented at the International Conference on Automatic Face and Gesture Recognition, 2006.

[5]   A. B. Moreno, A. Sanchez, J. Velez, and J. Diaz, "Face Recognition Using 3D Local Geometrical Features: PCA vs. SVM," in *In the Proceedings of the 4th International Symposium on Image and Signal Processing and Analysis*, 2005, pp. 185-190.

[6]   M. H. Mahoor and M. Abdel-Mottaleb, "3D Face Recognition Based on 3D Ridge Lines in Range Data," presented at the IEEE International Conference on Image Processing, 2007.

[7]   C. Li and O. Barreto, "Profile-Based 3D Face Registration and Recognition," *Lecture notes in computer science,* vol. 3506, pp. 478-488, 2005.

[8]   J.Y. Lapreste Cartoux, J.T. Richetin, M. , "Face authentification or recognition by profile extraction from range images," in *Workshop on Interpretation of 3D Scenes*, 1989, p. 194.

[9]   Y. Li, Y. Shen, and G. Zhang, "An Efficient 3D Face Recognition Method Using

Geometric Features," presented at the International Workshop on Intelligent Systems and Applications, 2010.

[10]   V. Bruce and A. Young, "In the Eye of the Beholder," *The Science of Face Perception,* 1998.

[11]   M. Castrillon-Santana and Q. C. Vuong, "An Analysis of Automatic Gender Classification," presented at the Iberoamerican conference on Progress in pattern recognition, image analysis and applications 2007.

[12]   P. Ekman, "Facial Expression," in *Nonverbal Behavior and Communication*, S. F. A. Siegman, Ed., ed: Lawrence Erlbaum Association, 1977.

[13]   C. Beumier and M. Acheroy, "Automatic 3D Face Authentication," *Image and Vision Computing,* vol. 18, p. 7, 2000.

[14]   A.M. Bronstein, M.M. Bronstein, and R. Kimmel, "Three-dimensional Face Recognition," *International Journal of Computer Vision,* vol. 64, p. 26, 2005.

[15]   "ISO/IEC 14496-2:1999, Information technology -Coding of audio-visual objects " in *Part 2:Visual*, ed: International Organization for Standardization, 1999.

[16]   C. Chua, F. Han, and Y. Ho, "3D Human Face Recognition Using Point Signature," presented at the IEEE International Conference on Automatic Face and Gesture Recognition, 2000.

[17]   A. B. Moreno, A. Sanchez, J. F. Velez, and F. J. Diaz, "Face Recognition Using 3D Surface-extracted Descriptors," presented at the Irish Machine Vision and Image Processing Conference, 2003.

[18]   K. I. Chang, K. W. Bowyer, and P. J. Flynn, "Multi-modal 2D and 3D Biometrics for Face Recognition," in *Proceeding of IEEE workshop on Analysis and modeling of faces and gestures*, 2003, p. 8.

[19]   C. Xu, Y. Wang, T. Tan, and L. Quan, "Automatic 3D Face Recognition Combining Global Geometric Features with Local Shape Variation Information," presented at the International Conference on Automated Face and Gesture Recognition, 2004.

[20]   W. Zhao, R. Chellappa, P. J. Phillips, and A. Rosenfeld, "Face Recognition: A Literature Survey," *ACM Computing Surveys,* vol. 35, p. 60, 2003.

[21]   K. W. Bowyer, K. Chang, and P. Flynn, "A Survey of Approaches and Challenges in 3D and Multi-modal 3D + 2D Face Recognition " *Computer Vision and Image Understanding,* vol. 101, p. 15, 2005.

[22]   S. Z. Li, *Encyclopedia of Biometrics*, 2009.

[23]   C. C. Tappert, M. Villani, and S. Cha, "Keystroke Biometric Identification and Authentication on Long-Text Input," in *Behavioral Biometrics for Human Identification: Intelligent Applications*, X. G. L. Wang, Ed., ed.

[24]   Chin-Seng Chua Yingjie Wang, Yeong-Khing Ho. , "Facial Appearance Detection and Face Recognition from 2D and 3D Images," *Pattern Recognition Letters* vol. 23, pp. 1191-1202, 2001.

[25]   S. Li and A. Jain, *Handbook of Face Recognition*, 2005.

[26]   A. P. Pentland M. A. Turk, "Face recognition using eigenfaces," in *IEEE Computer Society Conference on Computer Vision and Pattern Recognition* 1991, pp. 586-591.

[27]   P. N. Belhumeur, J. P. Hespanha, and D. J. Kriegman, "Eigenfaces vs. Fisherfaces: Recognition Using Class Specific Linear Projection," *IEEE Transactions on Pattern Analysis and Machine Intelligence,* vol. 19, pp. 711-720, 1997.

[28]   R. Brunelli and T. Poggio, "Face Recognition: Feature versus Templates," *IEEE*

Transaction on Pattern Analysis and Machine Intelligence, vol. 15, pp. 1042 - 1052 1993.

[29]   A. Pentland, B. Moghaddam, and T. Starner, "View-based and Modular Eigenspaces for Face Recognition," presented at the IEEE Computer Society Conference on Computer Vision and Pattern Recognition, 1994.

[30]   P. C. Yuen and J. H. Lai, "Independent Component Analysis of Face Images," presented at the Lecture Notes in Computer Science, 2000.

[31]   C. Liu and H. Wechsler, "Comparative Assessment of Independent Component Analysis (ICA) for Face Recognition," presented at the International Conference on Audio and Video Based Biometric Person Authentication, Washington D.C., 1999.

[32]   M. S. Bartlett, J. R. Movellan, and T. J. Sejnowski, "Face Recognition by Independent Component Analysis," *IEEE Transactions on Neural Networks,* vol. 13, pp. 1450-1464, 2002.

[33]   A. Hyvarinen, "Fast and Robust Fixed-point Algorithms for Independent Component Analysis," *IEEE Transactions on Neural Networks,* vol. 10, pp. 626-634, 1999.

[34]   T. Kanade, "Picture Processing System by Computer Complex and Recognition of Human Faces," PhD, Kyoto University, 1973.

[35]   L. Wiskott, J. M. Fellous, N. Kuiger, and C. von der Malsburg, "Face Recognition by Elastic Bunch Graph Matching," *IEEE Transactions on Pattern Analysis and Machine Intelligence,* vol. 19, pp. 775-779, 1997.

[36]   T. F. Cootes, G. J. Edwards, and C. J. Taylor, "Active Appearance Models," presented at the European Conference on Computer Vision, 1998.

[37]   H. Lee and D. J. Kim, "Tensor-Based AAM with Continuous Variation

Estimation: Application to Variation-Robust Face Recognition," *IEEE Transactions on Pattern Analysis and Machine Intelligence,* vol. 31, 2009.

[38]   L. Alba-Castro Teijeiro-Mosquera, J.L. Gonza, "Face Recognition Across Pose with Automatic Estimation of Pose Parameters through AAM-Based Landmarking," presented at the International Conference on Pattern Recognition, 2010.

[39]   J. Chen and H. Huang, "Face Recognition Using AAM and Global Shape Features," presented at the IEEE International Conference on Robotics and Biomimetics, 2009.

[40]   P. Grother P.J. Phillips, R.J Micheals, D.M. Blackburn, E Tabassi, J.M. Bone, "FRVT 2002: Overview and Summary," 2002.

[41]   C. Xu, Y. Wang, T. Tan, and L. Quan, "Depth vs. Intensity: Which is More Important for Face Recognition?," presented at the International Conference on Pattern Recognition, 2004.

[42]   Kyong Chang and Patrick Flynn Kevin W. Bowyer, "A survey of approaches and challenges in 3D and multi-modal 3D + 2D face recognition " *Computer Vision and Image Understanding,* vol. 101, p. 15, 2005.

[43]   Nick Pears Thomas Heseltine, Jim Austin. , "3D Face Recognition Using Combinations of Surface Feature Map Subspace Components," *Image and Vision Computing* vol. 26, pp. 382-396, 2008.

[44]   Samuel Cheng Le Zou, Zixiang Xiong, Mi Lu, Kenneth R. Castleman. , "3D Face Recognition Based on Warped Example Faces," presented at the IEEE Transaction on Information Forensics and Security, 2007.

[45]   M. Mayo and E. Zhang, "3D Face Recognition Using Multiview Keypoint Matching," presented at the IEEE International Conference on Advanced Video

and Signal Based Surveillance, 2009.

[46] C. Samir, A. Srivastava, and M. Daoudi, "3D Face Recognition Using Shapes of Facial Curves," *IEEE Transactions on Pattern Analysis and Machine Intelligence,* vol. 28, pp. 1858 - 1863 2006.

[47] C. Zhang and F. Cohen, "3-D Face Structure Extraction and Recognition from Images Using 3-D Morphing and Distance Mapping," *IEEE Transactions on Image Processing,* vol. 11, pp. 1249-1259, November 2002.

[48] Y. Wang, J. Liu, and X. Tang, "Robust 3D Face Recognition by Local Shape Difference Boosting," *IEEE Transactions on Pattern Analysis and Machine Intelligence,* vol. 32, pp. 1858 - 1870 2010.

[49] G. Gordon, "Face Recognition Based on Depth and Curvature Features," in *IEEE Computer Society Conference on Computer Vision and Pattern Recognition* 1992, p. 3.

[50] P. Tosranon, A. Sanpanich, C. Bunluechokchai, and C. Pintavirooj, "Gaussian Curvature-based Geometric Invariance," presented at the International Conference on Electrical Engineering/Electronics, Computer, Telecommunications and Information Technology, 2009.

[51] T. Nagamine, T. Uemura, and I. Masuda, "3D Facial Image Analysis for Human Identification," presented at the International Conference on Pattern Recognition, 1992.

[52] J. C. Lee and E. Milios, "Matching Range Images of Human Faces," presented at the International Conference on Computer Vision, 1990.

[53] H. T. Tanaka, M. Ikeda, and H. Chiaki, "Curvature-based Face Surface Recognition Using Spherical Correlation. Principal Directions for Curved Object Recognition," presented at the IEEE International Conference on Automatic

Face and Gesture Recognition, 1998.

[54]   P. J. Besl and H. D. McKay, "A method for registration of 3-D shapes," *IEEE Transactions on Pattern Analysis and Machine Intelligence* vol. 14, pp. 239-256, 1992.

[55]   K. Fatimah, T. Mohd, and O. Khairuddin, "Face Recognition Using Local Geometrical Features - PCA with Euclidean Classifier," in *International Symposium on Information Technology*, 2008, pp. 1-6.

[56]   C. Xu, Y. Wang, T. Tan, and L. Quan, "A New Attempt to Face Recognition Using 3D Eigenfaces," presented at the Asian Conference on Computer Vision, 2004.

[57]   Kevin W. Bowyer Kyong I. Chang, Patrick J. Flynn, "Multiple nose region matching for 3D face recognition under varying facial expression," presented at the IEEE Trans. Pattern analysis and machine intelligence, 2006.

[58]   A. Mian, M. Bennamoun, and R. Owens, "Automatic 3D Face Detection, Normalization and Recognition," presented at the International Symposium on 3D Data Processing, Visualization, and Transmission, 2006.

[59]   G. Medioni and R. Waupotitsch, "Face Recognition and Modeling in 3D," presented at the IEEE International Workshop on Analysis and Modeling of Faces and Gestures, 2003.

[60]   S. Wang, Y. Wang, M. Gu, and D.Samaras, "Conformal Geometry and Its Applications on 3D Shape Matching, Recognition, and Stitching," *IEEE Transactions on Pattern Analysis and Machine Intelligence,* vol. 29, p. 1209, 2007.

[61]   S. Berretti, A. Del Bimbo, and P. Pala, "3D Face Recognition Using Isogeodesic Stripes," *IEEE Transactions on Pattern Analysis and Machine Intelligence,* vol.

32, pp. 2162-2177, 2010.

[62]   S. Feng, H. Krim, and I. A. Kogan, "3D Face Recognition using Euclidean
         Integral Invariants Signature," presented at the IEEE/SP Workshop on Statistical
         Signal Processing, 2007.

[63]   R. Malpass, "Recognition for Faces of Own and Other Race," *Journal of
         Personality and Social Psychology,* vol. 13, pp. 330-334, 1969.

[64]   J. Brigham, "Do they all look alike? The effect of race, sex, experience and
         attitudes on the ability to recognize faces," *Journal of Applied Social Psychology,*
         vol. 8, pp. 306-318, 1978.

[65]   A. Peterson A. O'Toole, K. Deffenbacher, "An other-race effect for classifying
         faces by sex," *Perception,* vol. 25, pp. 669-676, 1996.

[66]   H. Abdi, D. Valentin, B. Edelman, and A. O'Toole, "More About the Difference
         Between Men and Women: Evidence from Linear Neural Networks and the
         Principal-component Approach," *Perception,* vol. 24, pp. 539-562, 1995.

[67]   I. Biederman, "Recognition by Components: A Theory of Human Image
         Understanding," *Psychol Review,* vol. 94, pp. 115-147, 1987.

[68]   A. M. Burton, V. Bruce, and N. Dench, "What's the Difference Between Men
         and Women? Evidence from Facial Measurement," *Perception,* vol. 22, pp.
         153-176, 1993.

[69]   V. Bruce, "Sex Discrimination: How do We Tell the Difference Between Male
         and Female Faces?," *Perception,* vol. 22, pp. 131-152, 1993.

[70]   D. H. Enlow, *Handbook of Facial Growth*, 2nd ed.: W.B. Saunders Company,
         1982.

[71]   B. A. Golomb, D.T. Lawrence, and T. J. Sejnowski, "Sexnet: A Neural Network
         Identifies Sex from Human Faces," presented at the Advances in Neural

Information Processing Systems, 1991.

[72] R. Brunelli and T. Poggio, "HyperBF Networks for Gender Classification," in *Proceedings of the DARPA Image Understanding Workshop*, 1992, pp. 311-314.

[73] S. Tamura, H. Kawai, and H. Mitsumoto, "Male/female Identification from 8*6 Very Low Resolution Face Images by Neural Network," *Pattern Recognition Letters,* vol. 29, pp. 331-335, 1996.

[74] L. Wiskott and J. M. Fellous, "Face Recognition and Gender Determination," in *Proceeding of International Workshop on Face Gesture Recognition*, 1995.

[75] B. Moghaddam and M.H. Yang, "Sex with Support Vector Machines," in *Proceeding of International Conference on Automatic Face and Gesture Recognition*, 2000.

[76] L. Lu, Z. Xu, and P. Shi, "Gender Classification of Facial Images Based on Multiple Facial Regions," presented at the World Congress on Computer Science and Information EngineeringI 2009.

[77] F.Scalzo, G. Bebis, M. Nicolescu, L. Loss, and A. Tavakkoli, "Feature Fusion Hierarchies for Gender Classification," presented at the International Conference on Pattern Recognition, 2008.

[78] Z. Sun, G. Bebis, X. Yuan, and S. J. Louis, "Genetic Feature Subset Selection for Gender Classification: A Comparison Study," presented at the IEEE Workshop on Applications of Computer Vision, 2002.

[79] S. Gutta, J. R.J. Huang, P. Jonathon, and H. Wechsler, "Mixture of Experts for Classification of Gender, Ethnic Origin, and Pose of Human Faces," *IEEE Transactions on Neural Networks,* vol. 11, pp. 948-960, 2000.

[80] Y. Saatci and C. Town, "Cascaded Classification of Gender and Facial Expression Using Active Appearance Models," presented at the International

Conference on Automatic Face and Gesture Recognition 2006.

[81]   B. Moghaddam and M.H. Yang, "Learning Gender with Support Faces," *IEEE Transaction on Pattern Analysis and Machine Intelligence,* vol. 24, pp. 707-711, 2002.

[82]   D. Cai, X. He, and J. Han, "Efficient Kernel Discriminant Analysis via Spectral Regression," presented at the International Conference on Data Mining, 2007.

[83]   J. Wu, W. A. P. Smitha, and E. R. Hancocka, "Gender Classification Using Shape from Shading," *Image and Vision Computing,* vol. 28, pp. 1039-1048, 2010.

[84]   M. Nakano, F. Yasukata, and M. Fukumi, "Age and Gender Classification From Face Images Using Neural Networks," *Signal and Image Processing,* 2004.

[85]   M. Nazir, M. Ishtiaq, A. Batool, M. A. Jaffar, and A. M. Mirza, "Feature Selection for Efficient Gender Classification," presented at the International Conference on Neural Networks 2010.

[86]   F. Matta, U. Saeed, C. Mallauran, and J. L. Dugelay, "Facial Gender Recognition Using Multiple Sources of Visual Information," in *IEEE Workshop on Multimedia Signal Processing*, 2008, pp. 785-790.

[87]   O. Ozbudak, M. Kirci, Y. Cakir, and E. O. Gunes, "Effects of the Facial and Racial Features on Gender Classification," presented at the IEEE Mediterranean Electrotechnical Conference 2010.

[88]   A. O'Toole, T. Vetter, and N. F. Troje, "Sex Classification is Better with Three-dimensional Structure than with Image Intensity Information," *Perception,* vol. 26, pp. 75-84, 1997.

[89]   X. Lu, H. Chen, and A. K. Jain, "Multimodal Facial Gender and Ethnicity Identification," presented at the Lecture Notes in Computer Science, 2006.

[90]   N. P. Costen, M. Brown, and S. Akamatsu, "Sparse Models for Gender Classification," presented at the IEEE International Conference on Automatic Face and Gesture Recognition, 2004.

[91]   H. Shen, L. Ma, and Q. Zhang, "Gender Categorization Based on 3D Faces," presented at the International Conference on Advanced Computer Control, 2010.

[92]   Y. Hu, J. Yan, and P. Shi, "A Fusion-based Method for 3D Facial Gender Classification," presented at the International Conference on Computer and Automation Engineering, 2010.

[93]   B. Amberg, R. Knothe, and T. Vetter, "Expression Invariant 3D Face Recognition with a Morphable Model," presented at the IEEE International Conference on Automatic Face and Gesture Recognition, 2008.

[94]   N. Alyuz, B. Gokberk, H. Dibeklioglu, and L. Akarun, "Component-based Registration with Curvature Descriptors for Expression Insensitive 3D Face Recognition," presented at the IEEE International Conference on Automatic Face & Gesture Recognition, 2008.

[95]   T. Fabry D. Smeets, J. Hermans, D. Vandermeulen, P. Suetens, , "Fusion of an Isometric Deformation Modeling Approach Using Spectral Decomposition and a Region-Based Approach Using ICP for Expression-Invariant 3D Face Recognition," presented at the International Conference on Pattern Recognition, 2010.

[96]   Y. Wang, G. Pan, and Z. Wu, "3D Face Recognition in the Presence of Expression: A Guidance-based Constraint Deformation Approach," presented at the IEEE Conference on Computer Vision and Pattern Recognition, 2007.

[97]   I. N. Cohen, A. Sebe, L. Garg, S. Chen, and T. S. Huang, "Facial Expression Recognition from Video Sequences: Temporal and Static Modeling," *Computer*

Vision and Image Understanding, vol. 91, pp. 160-187, 2003.

[98]   L. R. Rabiner, "A tutorial on Hidden Markov Models and selected applications in speech recognition," presented at the Proceedings of the IEEE, 1989.

[99]   M. Pantic and I. Patras, "Dynamics of Facial Expression: Recognition of Facial Actions and Their Temporal Segments from Face Profile Image Sequences," *IEEE Transactions on Systems, Man, and Cybernetics,* vol. 36, pp. 433-449, 2006.

[100] M. S. Bartlett, G. Littlewort, I. Fasel, and J. R. Movellan, "Real Time Face Detection and Facial Expression Recognition: Development and Applications to Human Computer Interaction," presented at the Computer Vision and Pattern Recognition Workshop, 2003.

[101] B. Fasel and J. Luettin, "Automatic Facial Expression Analysis: A Survey," *Pattern Recognition,* vol. 36, pp. 259-275, 2003.

[102] X. Lu and A. K. Jain, "Deformation Modeling for Robust 3D Face Matching," presented at the IEEE Computer Society Conference on Computer Vision and Pattern Recognition 2006.

[103] I. A. Kakadiaris, G. Passalis, G. Toderici, M. N. Murtuza, Y. Lu, N. Karampatziakis, and T. Theoharis, "Three-Dimensional Face Recognition in the Presence of Facial Expressions: An Annotated Deformable Model Approach," *IEEE Transactions on Pattern Analysis and Machine Intelligence,* vol. 29, 2007.

[104] H. Lee and D. Kim, "Expression-invariant Face Recognition by Facial Expression Transformations " *Pattern Recognition Letters,* vol. 29, pp. 1797-1805, 2008.

[105] F. R. Al-Osaimi, M. Bennamoun, and A. Mian, "On Decomposing an Unseen 3D

Face into Neutral Face and Expression Deformations," presented at the International Conference on Advances in Biometrics, 2009.

[106] X. Li, T. Jia, and H. Zhang, "Expression-insensitive 3D Face Recognition Using Sparse Representation," presented at the IEEE Conference on Computer Vision and Pattern Recognition, 2009.

[107] R. Sala Llonch, E. Kokiopoulou, I. Tosic, and P. Frossard, "3D face recognition with sparse spherical representations," *Pattern Recognition,* vol. 43, pp. 824-834, 2010.

[108] B. Gökberk, M. O. İrfanoğlua, and L. Akaruna, "3D Shape-based Face Representation and Feature Extraction for Face Recognition," *Image and Vision Computing,* vol. 24, pp. 857-869, 2006.

[109] X. Lu, "3D Face Recognition Across Pose and Expression," PhD, Department of Computer Science and Engineering, Michigan State University, 2006.

[110] X. Li and H. Zhang, "Adapting Geometric Attributes for Expression-Invariant 3D Face Recognition," presented at the IEEE International Conference on Shape Modeling and Applications, 2007.

[111] E. Kamenskaya and G.Kukharev, "Recognition of Psychological Characteristics from Face," 2008.

[112] M. Shamsia, R. Zoroofia, C. Lucasa, M. S. Hasanabadib, and M. R. Alsharifc, "3D Nasolabial Area Measurements for Analyzing facial Surgery."

[113] E. Nkenke, "3D Measurement Technology," ed, 2005.

[114] B. Hamann, "Curvature Approximation for Triangulated Surfaces," in *Geometric modelling* ed, 1993.

[115] A. Razdan and M. Baea, "Curvature Estimation Scheme for Triangle Meshes Using Biquadratic Bezier Patches," *Computer-Aided Design,* vol. 37, pp.

1481-1491, 2005.

[116] G. Taubin, "Estimating the Tensor of Curvature of a Surface from a Polyhedra Approximation," presented at the International Conference on Computer Vision, 1995.

[117] T. Surazhsky, E. Magid, O. Soldea, G. Elber, and E. Rivlin, "A Comparison of Gaussian and Mean Curvatures Estimation Methods on Triangular Meshes," presented at the IEEE International Conference on Robotics and Automation, 2003.

[118] H. P. Moreton and C. H. Sequin, "Functional Optimization for Fair Surface Design," *ACM SIGGRAPH Computer Graphics,* vol. 26, 1992.

[119] M. Meyer, M. Desbrun, P. Schröder, and A. Barr, "Discrete Differential-geometry Operators for Triangulated 2-manifolds," *Visualization and Mathematics* vol. 3, pp. 34-57, 2002.

[120] H. Fang, "Comparison and Research of Discrete Curvatures Estimation Methods on Mesh Surface.," Master, 2005.

[121] L. Alboul and G. Echeverria, "Polyhedral Gauss maps and curvature characterisation of triangle meshes " *Lecture notes in computer science,* vol. 3604/2005, pp. 14-33, 2005.

[122] A. Bac, M. Daniel, and J. Maltret, "3D modelling and segmentation with discrete curvatures," *Journal of medical informatics and technologies,* vol. 9, pp. 13-24, 2005.

[123] V. F. Ferrario, C. Sforza, A. Colombo, J. Schmitz, and G. Serrao, "Morphometry of the Orbital Region: A Soft-Tissue Study from Adolescence to Mid-Adulthood," *Plast Reconstructive Surgery* vol. 108, pp. 285-292, 2001.

[124] X. Han, H. Ugail, and I. Palmer, "3D face recognition using symmetry profile

comparison based on mean curvature," presented at the Proceedings of the eighth informatics workshop for research students, 2007.

[125] H. Tang, Y. Sun, B. Yin, and Y. Ge, "Expression-robust 3D Face Recognition Using LBP Representation," presented at the IEEE International Conference on Multimedia and Expo, 2010.

[126] X. Li and F. Da, "3D Face Recognition by Deforming the Normal Face," presented at the International Conference on Pattern Recognition, 2010.

[127] T. Heseltine, N. Pears, and J. Austin, "3D Face Recognition Using Combinations of Surface Feature Map Subspace Components," *Image and Vision Computing* vol. 26, pp. 382-396, 2008.

[128] S. Gupta, M. K. Markeyb, J. K. Aggarwala, and A. C. Bovik, "Three Dimensional Face Recognition Based on Geodesic and Euclidean Distances," *Vision Geometry XV,SPIE,* vol. 6499, 2007.

[129] A. O'Toole, A. Peterson, and K. Deffenbacher, "An Other-race Effect for Classifying Faces by Sex," *Perception,* vol. 25, pp. 669-676, 1996.

[130] S. Gutta, H. Wechsler, and P. J. Phillips, "Gender and Ethnic Classification of Face Images," presented at the IEEE International Conference on Automatic Face and Gesture Recognition, 1998.

[131] D. K. Ousterhout. (1994, *Feminization of the Transsexual*. Available: http://www.drbecky.com/dko.html

[132] Y. Zhu, L. D. Seneviratne, and S. W. E. Earles, "A New Structure of Invariant for 3D Point Sets from a Single View " presented at the IEEE International Conference on Robotics and Automation, 1995.

[133] D. Weinshall, "Model-based Invariants for 3-D Vision," *International Journal of Computer Vision,* vol. 10, pp. 27-42, 1993.

[134] G. W. Cottrell and J. Metcalfe, "Empath:face,emotion and gender recognition using holons," *Advances in neural information processing systems,* p. 8, 1991.

[135] A. Samal, V. Subramani, and D. Marx, "Analysis of Sexual Dimorphism in Human Face," *Journal of Visual Communication and Image Representation* vol. 18, 2007.

[136] Z. Xu, L. Lu, and P. Shi, "A Hybrid Approach to Gender Classification from Face Images," 2008.

[137] L. G. Farkas, *Anthropometry of the Head and Face*. New York, 1994.

[138] J. Ostermann, "Animation of synthetic faces in MPEG-4," presented at the Computer Animation 1998.

[139] G. Arfken and H. Webern, *Mathematical Methods for Physicists*, Sixth Edition ed.: Academic Press, 2005.

[140] F. B. ter Haar and R. C. Veltkamp, "A 3D Face Matching Framework," presented at the IEEE International Conference on Shape Modeling and Applications, 2008.

[141] A. M. Bronstein, M. M. Bronstein, and R. Kimmel, "Expression-invariant 3D Face Recognition," presented at the International Conference on Audio- and Video-based Biometric Person Authentication, 2003.

[142] T. C. Faltemier, K. W. Bowyer, and P. J. Flynn, "Using a Multi-Instance Enrollment Representation to Improve 3D Face Recognition," presented at the IEEE International Conference on Biometrics: Theory, Applications, and Systems, 2007.

[143] A. M. Bronstein, M. M. Bronstein, and R. Kimmel, "Robust Expression-invariant Face Recognition from Partially Missing Data," presented at the European Conference on Computer Vision, 2006.

[144] K. I. Chang, K. W. Bowyer, and P. J. Flynn, "Multiple Nose Region Matching for 3D Face Recognition Under Varying Facial Expression," presented at the IEEE Transaction on Pattern Analysis and Machine Intelligence, 2006.

[145] T. Faltemier, K. W. Bowyer, and P. Flynn, "A Region Ensemble for 3D Face Recognition," *IEEE Transactions on   Information Forensics and Security,* vol. 3, pp. 62-73, 2008.

[146] K. Fatimah, N. Khalid, and A. Lili, "3D Face Recognition Using Multiple Features for Local Depth Information," *International Journal of Computer Science and Network Security,* vol. 9, pp. 27-32, 2009.

[147] Xiaozhou Wei Lijun Yin, Yi Sun, Jun Wang, Rosato, M.J., "A 3D Facial Expression Database For Facial Behavior Research," presented at the International Conference on Automatic Face and Gesture Recognition, 2006.

[148] X. Chai, S. Shan, X. Chen, and W. Gao, "Locally Linear Regression for Pose-Invariant Face Recognition," *IEEE Transactions on Image Processing,* vol. 16, pp. 1716-1725, 2007.

[149] I. Naseem, R. Togneri, and M. Bennamoun, "Linear Regression for Face Recognition," presented at the IEEE Transactions on Pattern Analysis and Machine Intelligence, 2010.

[150] R. D. Tobias, "An Introduction to Partial Least Squares Regression," in *SUGI Proceedings*, 1995.

[151] M. Tranmer and M. Elliot, "Multiple Linear Regression," The Cathie Marsh Centre for Census and Survey Research (CCSR)2008.

[152] O. Gervei, A. Ayatollahi, and N. Gervei, "3D face recognition using modified PCA methods," presented at the World Academy of Science, Engineering and Technology, 2010.